AN ABSTRACT OF THE DISSERTATION OF

Toby Primbs for the degree of Doctor of Philosophy in Chemistry presented on September 21, 2007.
Title: Trans-Pacific and Regional Atmospheric Transport of Anthropogenic Semivolatile Organic Compounds in the Western U.S.

APPROVED :

Staci L. Simonich

The atmospheric transport of anthropogenic semivolatile organic compounds (SOCs) from Asian sources to the Western U.S. was investigated. In addition, the SOC extraction method was optimized. Hansen solubility parameter plots were used to aid in the pressurized liquid extraction (PLE) solvent selection of air sampling media in order to minimize polymeric matrix interferences. To estimate the emissions of anthropogenic semivolatile organic compounds (SOCs) from East Asia and to identify unique SOC molecular markers in Asian air masses, air samples were collected on the island of Okinawa, Japan in Spring 2004. Elevated concentrations of hexachlorobenzene (HCB), hexachlorocyclohexanes (HCHs), dichlorodiphenyltrichloroethanes (DDTs), and particulate-phase polycyclic aromatic hydrocarbons (PAHs) were attributed to air masses from China. A large proportion of the variation in the current use pesticides, gas-phase PAHs, and polychlorinated biphenyl (PCB) concentrations was explained by meteorology. Using measured PAH, carbon monoxide (CO), and black carbon concentrations and estimated CO and black carbon emission inventories, the emission of 6 carcinogenic particulate-phase PAHs were estimated to be 1518-4179 metric tons/year for all of Asia and 778-1728 metric tons/year for only China. Atmospheric measurements

of anthropogenic SOCs were made at Mt. Bachelor Observatory (MBO), located in Oregon's Cascade Range. PAH concentrations at MBO increased with the percentage of air mass time in Asia and, in conjunction with other data, provided strong evidence that particulate-phase PAHs are emitted from Asia and undergo trans-Pacific atmospheric transport to North America. Enhanced HCB, α-HCH, and γ-HCH concentrations also occurred during trans-Pacific atmospheric transport, compared with regional (Western U.S.) air masses during similar time periods. Gas-phase PAH and fluorotelomer alcohol (FTOH) concentrations significantly increased with the percentage of air mass time in California's urban areas, while retene and PCB concentrations increased with the percentage of air mass time in Oregon and during regional fire events. Regional atmospheric transport in the Western U.S. also resulted in enhanced γ-HCH, dacthal, endosulfan, metribuzin, triallate, trifluralin, and chlorpyrifos concentrations, with episodic concentration enhancements during spring application periods. Elevated ΣPCB, Σchlordane, HCHs, HCB, and trifuralin concentrations were also associated with fires, which may be due to volatization of pesticides deposited to soils and vegetation.

TRANS-PACIFIC AND REGIONAL ATMOSPHERIC TRANSPORT OF ANTHROPOGENIC SEMIVOLATILE ORGANIC COMPOUNDS IN THE WESTERN U.S.

by
Toby Primbs

A DISSERTATION

submitted to

Oregon State University

in partial fulfillment of
the requirements for the
degree of

Doctor of Philosophy

Presented September 21, 2007
Commencement June 2008

Doctor of Philosophy dissertation of Toby Primbs presented on September 21, 2007.

APPROVED :

Major Professor, representing Chemistry

Chair of the Department of Chemistry

Dean of the Graduate School

I understand that my dissertation will become part of the permanent collection of Oregon State University libraries. My signature below authorizes release of my dissertation to any reader upon request.

Toby Primbs, Author

ACKNOWLEDGEMENTS

The author is extremely grateful to his wife Danielle and son Ivan for all of their support and understanding through all the late nights and weekends with an absent dad/husband. In addition, the author would like to thank his friends and family (Julia, Jeanne, Wayne, K.C., Stew, and Jasmine) for their encouragement and support. The author wishes to dedicate his work in memory of his father Edward R.J. Primbs who continually challenged the author to question everything and work hard. The author wishes to also thank Staci Simonich, his fellow lab mates, and his committee members (Bernd Simoneit, John Westall, Jennifer Field, and William Baird) for their investment of time and support over the years to the author, in addition to Mt. Bachelor Corporation. The author is extremely thankful to the U.S. EPA STAR fellowship program and National Science Foundation CAREER for their financial support.

CONTRIBUTION OF AUTHORS

Dr. Staci L. Simonich provided advice and support in all aspects of this dissertation. Susan Genualdi assisted in the air sampling method development Chapter 2. Dr. Akinori Takami, Dr. Shungo Kato, Dr. Shiro Hatakeyama, Dr. Yoshizumi Kajii, and Dr. Dan Jaffe provided AMS, CO, Hg^0, black carbon, and submicron aerosol analysis Chapter 3. David Schmedding assisted in the sampler installation (Chapters 4 and 5), in addition to sample collection (Chapter 3). Glenn Wilson provided guidance in instrumental use and maintenance, in addition to continued field support for the collection of samples and equipment maintenance. Arkadiusz Piekarz and Dr. Jennifer Field provided the analysis of FTOHs (Chapter 5). Dr. Carol Higginbotham provided field support and sample collection (Chapters 4 and 5).

TABLE OF CONTENTS

TABLE OF CONTENTS (Continued)

TABLE OF CONTENTS (Continued)

LIST OF FIGURES

LIST OF TABLES

TRANS-PACIFIC AND REGIONAL ATMOSPHERIC TRANSPORT OF ANTHROPOGENIC SEMIVOLATILE ORGANIC COMPOUNDS IN THE WESTERN U.S.

CHAPTER 1. INTRODUCTION

The primary goal of this research was to identify anthropogenic semivolatile organic compounds (SOCs) in Asian trans-Pacific and regional North American air masses and to use these compounds as unique molecular markers for Asian and North American emissions. Where possible, a secondary goal was to estimate the emissions of SOCs from Asian and U.S. source regions. Characterization of anthropogenic SOCs in Asian air masses took place close to the emission sources in Asia and characterization of SOCs in trans-Pacific and regional North American air masses took place at a high elevation site on the West Coast of the United States.

For more than a decade, the global atmospheric transport of anthropogenic SOCs has been shown to cause surface contamination in remote locations *(1)* such as the Artic *(2)*. Remote locations may be more sensitive to impacts from contaminants *(3)* and atmospheric transport has been shown to be a major environmental transport pathway for the transport of SOCs from source regions to remote locations *(4)*.

Atmospheric transport of air pollutants, including anthropogenic SOCs, inorganic trace gases (e.g. CO, Hg^0), and dust from Asian sources to the Pacific Coast of North America has been previously identified *(5-11)*. Air trajectories, combined with chemical measurements, show that transport across the Pacific Ocean can occur in as little as 5 to 10 days in the winter and spring seasons *(6,9,12)*. With the combination of observational data (e.g. satellite images of dust and smoke), direct chemical measurements in the

atmosphere, and air mass computer modeling simulations; the evidence of Asian air pollutant transport to the Pacific coast of North America is growing *(12-14)*.

Anthropogenic SOCs are emitted from a variety of activities, including fossil fuel combustion (polycyclic aromatic hydrocarbons (PAHs)), biomass burning (levoglucosan), agriculture (pesticides), urban (fluorotelomer alcohols (FTOHs)) and/or industrial activities (polychlorinated biphenyls (PCBs)). The vapor pressures of SOCs are roughly between 10^{-4} to 10^{-11} atm, allowing them to exist in the gas and/or particle phases in the atmosphere *(4)*. In addition, SOCs have a wide range of atmospheric lifetimes (hours to months) *(15)*. Due to their wide range of atmospheric lifetimes, physical-chemical properties, and their emission from a diverse array of anthropogenic sources, SOCs may be good molecular markers for differentiating between source regions of trans-Pacific air masses as well as different source types. Anthropogenic SOCs were chosen for study over biogenic SOCs because the anthropogenic emissions can be more closely tied to specific geographic locations and human activities.

SOCs may impact both the environment and human health because of their potential to bioaccumulate and because of their long half-lives in the environment. Some SOCs are carcinogenic or they may act as endocrine disruptors *(16,17)*. As Asia becomes more industrialized and populated, there will likely be an increase in the emissions of various anthropogenic SOCs. These increased emissions, coupled with their potential to undergo trans-Pacific atmospheric transport, have the potential to impact high elevation ecosystems in the Western U.S.

Xu et al. *(17)* estimated the Chinese PAH emissions to be 25,300 tons in 2003, noting the enhanced higher molecular weight PAHs due to the coking industry and coal usage.

Energy use in China has continued to increase over the past couple of decades, leading to "severe environmental deterioration *(17)*." During the past couple of decades fluctuations in PAH emissions has been tied to fluctuations in the coking industry and coal usage, and Chinese coal usage will continue to grow in the future *(17)*.

Elevated pesticide concentrations may also be associated with Asian source regions. It has been reported that India and China accounted for ~84% of the worlds use of technical hexachlorocyclohexane (HCH) *(18)*. During a global passive air sampling campaign higher concentrations of HCHs were reported in Asia compared to the Western U.S. *(19)*. Asian regional SOC profile differences have also been reported, where China was associated with enhanced hexachlorobenzene (HCB) concentrations and both China and Japan have been associated with enhanced PCB concentrations *(20)*.

Urban and agricultural areas in the Western U.S. also have the potential to emit SOCs. For example, PCBs and FTOHs have been reported to originate from urban areas in the U.S. *(21,22)*. In addition, PAH concentrations in air have been shown to correlate with human population in North America *(22,23)*. Pesticides may enter the atmosphere during application (e.g. spray drift), wind erosion of particles with sorbed pesticides, and/or volatization from previous applications *(24,25)*. In addition, North American regional pesticide emissions have been shown to undergo atmospheric transport and deposition to remote high elevation mountains in the Western U.S. *(25,26)*. During a global passive air sampling campaign higher concentrations of chlordanes and endosulfans were reported in the Western U.S. compared with Asia *(19)*.

To date, most research on trans-Pacific atmospheric transport has focused on pollutants derived from incomplete combustion such as CO. Research on the atmospheric

trans-Pacific transport of anthropogenic SOCs adds complementary information on combustion sources, as well as agricultural and industrial sources. Research on the importance of atmospheric transport of anthropogenic SOCs from Asia to the Pacific Coast of North America is just beginning *(8,9,11)*.

One of the first studies to show the trans-Pacific atmospheric transport of SOCs was conducted in Tagish Yukon, Canada between December 1992 and January 1995 by Bailey et al. *(9)*. This study involved the collection of week-long air samples and analyzing them for a variety of organochlorine SOCs *(9)*. Five-day air mass back trajectories were used to separate air masses originating from Asian source regions from Western United States source regions; the trans-Pacific atmospheric transport of SOCs from Asia was identified in the winter months, with enhanced organochlorine pesticide concentrations *(9)*. In addition, during times of the year when the air mass back trajectories showed strong influence from North American sources, it was determined that North America was a major source of hexachlorocyclohexanes (HCHs) and chlordanes *(9)*. However, given the week-long collection of the air samples and the high frequency of changes in the origin of the sampled air masses, specific source regions could not be identified.

In spring 2002, a study by Killin et al. was conducted at Cheeka Peak Observatory, located on the tip of the Olympic Peninsula of Washington State, to better understand the trans-Pacific atmospheric transport of SOCs *(11)*. This study involved the collection of sixteen 24-48 hour air samples over 2 ½ month period of time. During three trans-Pacific atmospheric transport events elevated SOC concentrations were observed, where each event was unique. During the first event, elevated trifluralin, acenaphthene, and fluorene

concentrations were reported. The second event had elevated HCB, chlorothalonil, cis-nonachlor, mirex, and retene concentrations. Whereas, the third event reported an increase in concentrations of all measured SOCs, in addition to the only measurements of triallate, endosulfan II, and endosulfan sulfate. The anthracene to phenanthrene ratio was used to identify regional diesel ship emission impacts, and these were thought to have an effect on PAH concentrations.

During a two-week period in August 2001, Harner et al. collected twelve-hour air samples for SOC analysis at both ground based sites and on an aircraft in British Columbia, Canada *(8)*. In this work, Harner et al. measured enhanced α-HCH concentrations in the mid-troposphere (~4400 meters above sea level) due to trans-Pacific atmospheric transport. However, this increase in α-HCH concentrations was not observed at the ground based sites *(8)*. Thus, higher elevation sites may be more useful in distinguishing between trans-Pacific and regional air masses.

In addition, research investigating the trans-Pacific atmospheric transport of anthropogenic SOCs has primarily focused on the West Coast of North America *(8,9,11)*. Additional information on the SOC composition of Asian air masses, in the near vicinity of Asia, is needed to assist in the proper identification of trans-Pacific air masses of Asian origin.

In the first part of this research (Chapter 2), the pressurized liquid extraction (PLE) method used to extract the SOCs from air samples was optimized and validated. To date, the use of PLE has focused on the extraction of SOCs from various solid matrices and the intentional extraction of monomers/oligomers and additives from polymers *(27,28)*. There were two major goals in the selection of solvents for the PLE of SOCs from

polymeric air sampling media: 1) to efficiently extract the SOCs from the media; and 2) to avoid co-extraction of monomers/oligomers interferants from the polymer. Hansen solubility parameters were used to select PLE solvents to minimize co-extraction of polymeric matrix interferences, and the selected solvents resulted in good recoveries of 63 commonly measured SOCs.

Chapter 3 describes the measurement of the SOC composition of Asian air masses and their outflow from China and Asia on Okinawa, Japan in spring 2004. The primary objectives of this portion of the research were to (1) identify the SOC composition of Asian air masses; (2) determine if air masses from different Asian source regions (China, Japan, the Koreas, Russia, and Ocean/Local) had unique SOC compositions; and (3) estimate the emission of PAHs from Asia.

High elevation sites in the Western U.S. are in the free troposphere more frequently than lower elevation sites and allow for more conclusive identification of trans-Pacific atmospheric transport events *(10,13,14)*. In addition, mid-latitude, Western U.S. mountains serve as local areas of convergence for SOCs *(26,29)*. The primary objectives of the research described in Chapter 4 were to: (1) measure PCBs and incomplete combustion byproducts (PAHs, levoglucosan, and 1,3,5-triphenylbenzene) in trans-Pacific and regional air masses at a remote mountain top located on the U.S. West Coast; (2) identify source regions for PAHs, PCBs, levoglucosan, 1,3,5-triphenylbenzene, and FTOHs; and (3), where possible, estimate the emissions of these SOCs from U.S. source regions.

Chapter 5 describes the measurement of the pesticide composition of Asian and regional North American air masses with the primary objectives being: (1) to identify the

current and historical use pesticide (CUP and HUP) compositions at a remote high elevation mountain, (2) to determine source regions for the CUPs and HUPs, and (3) to identify differences and similarities in pesticide profiles for Asian and Western U.S. air masses.

This research will increase our understanding of which SOCs are transported across the Pacific Ocean and from which regions in Asia. This information may be ultimately used to support a hemispheric treaty on intercontinental transport of air pollutants *(30)*.

LITERATURE CITED:

(1) Simonich, S. L.; Hites, R. A. Global distribution of persistent organochlorine compounds *Science* **1995**, *269*, 1851-1854.

(2) Hung, H.; Blanchard, P.; Halsall, C. J.; Bidleman, T. F.; Stern, G. A.; Fellin, P.; Muir, D. C. G.; Barrie, L. A.; Jantunen, L. M.; Helm, P. A.; Ma, J.; Konoplev, A. Temporal and spatial variabilities of atmospheric polychlorinated biphenyls (PCBs), organochlorine (OC) pesticides and polycyclic aromatic hydrocarbons (PAHs) in the Canadian Arctic: Results from a decade of monitoring *Sci Total Environ* **2005**, *342*, 119-144.

(3) UNEP "Regionally Based Assessment of Persistent Toxic Substances; Arctic," UNEPChemicals: Chaˆtelaine, GE, Switzerland, 2002.

(4) Bidleman, T. F. Atmospheric processes *Environ. Sci. Technol.* **1988**, *22*, 361-367.

(5) Husar, R. B.; Tratt, D. M.; Schichtel, B. A.; Falke, S. R.; Li, F.; Jaffe, D.; Gasso, S.; Gill, T.; Laulainen, N. S.; Lu, F.; Reheis, M. C.; Chun, Y.; Westphal, D.; Holben, B. N.; Gueymard, C.; McKendry, I.; Kuring, N.; Feldman, G. C.; McClain, C.; Frouin, R. J.; Merrill, J.; DuBois, D.; Vignola, F.; Murayama, T.; Nickovic, S.; Wilson, W. E.; Sassen, K.; Sugimoto, N.; Malm, W. C. Asian dust events of April 1998 *J Geophys Res-Atmos* **2001**, *106*, 18317-18330.

(6) Jaffe, D.; Anderson, T.; Covert, D.; Kotchenruther, R.; Trost, B.; Danielson, J.; Simpson, W.; Berntsen, T.; Karlsdottir, S.; Blake, D.; Harris, J.; Carmichael, G.;

Uno, I. Transport of Asian air pollution to North America *Geophys Res Lett* **1999**, *26*, 711-714.

(7) Jaffe, D.; Bertschi, I.; Jaegle, L.; Novelli, P.; Reid, J. S.; Tanimoto, H.; Vingarzan, R.; Westphal, D. L. Long-range transport of Siberian biomass burning emissions and impact on surface ozone in western North America *Geophys Res Lett* **2004**, *31*, L16106.

(8) Harner, T.; Shoeib, M.; Kozma, M.; Gobas, F. A. P. C.; Li, S. M. Hexachlorocyclohexanes and endosulfans in urban, rural, and high altitude air samples in the Fraser Valley, British Columbia: Evidence for trans-Pacific transport *Environ Sci Technol* **2005**, *39*, 724-731.

(9) Bailey, R.; Barrie, L. A.; Halsall, C. J.; Fellin, P.; Muir, D. C. G. Atmospheric organochlorine pesticides in the western Canadian Arctic: Evidence of transpacific transport *J Geophys Res-Atmos* **2000**, *105*, 11805-11811.

(10) Jaffe, D.; Prestbo, E.; Swartzendruber, P.; Weiss-Penzias, P.; Kato, S.; Takami, A.; Hatakeyama, S.; Kajii, Y. Export of atmospheric mercury from Asia *Atmospheric Environment* **2005**, *39*, 3029-3038.

(11) Killin, R. K.; Simonich, S. L.; Jaffe, D. A.; DeForest, C. L.; Wilson, G. R. Transpacific and regional atmospheric transport of anthropogenic semivolatile organic compounds to Cheeka Peak Observatory during the spring of 2002 *J Geophys Res-Atmos* **2004**, *109*, D23S15.

(12) Wilkening, K. E.; Barrie, L. A.; Engle, M. Atmospheric science - Trans-Pacific air pollution *Science* **2000**, *290*, 65-67.

(13) Weiss-Penzias, P.; Jaffe, D. A.; Swartzendruber, P.; Dennison, J. B.; Chand, D.; Hafner, W.; Prestbo, E. Observations of Asian air pollution in the free troposphere at Mount Bachelor Observatory during the spring of 2004 *J Geophys Res-Atmos* **2006**, *111*, D10304.

(14) Weiss-Penzias, P.; Jaffe, D.; Swartzendruber, P.; Hafner, W.; Chand, D.; Prestbo, E. Quantifying Asian and biomass burning sources of mercury using the Hg/CO ratio in pollution plumes observed at the Mount Bachelor observatory *Atmospheric Environment* **2007**, *41*, 4366-4379.

(15) Mackay, D.; Shiu, W. Y.; Ma, K. C. *Physical-Chemical Properties and Environmental Fate*; Chapman and Hall/CRCnetBase: Boca Raton, FL, 2000.

(16) Fox, J. E. Chemical Communication Threatened by Endocrine-Disrupting Chemicals *Environ Health Persp* **2004**, *112*, 648-653.

(17) Xu, S.; Liu, W.; Tao, S. Emission of Polycyclic Aromatic Hydrocarbons in China *Environ. Sci. Technol.* **2006**, *40*, 702-708.

(18) Li, Y. F.; M cMillan, A.; Scholtz, M. T. Global HCH Usage with 1° x 1° Longitude/Latitude Resolution *Environ Sci Technol* **1996**, *30*, 3525-3533.

(19) Pozo, K.; Harner, T.; Wania, F.; Muir, D. C. G.; Jones, K. C.; Barrie, L. A. Toward a Global Network for Persistent Organic Pollutants in Air: Results from the GAPS Study *Environ. Sci. Technol.* **2006**, *40*, 4867-4873.

(20) Jaward, T. M.; Zhang, G.; Nam, J. J.; Sweetman, A. J.; Obbard, J. P.; Kobara, Y.; Jones, K. C. Passive air sampling of polychlorinated biphenyls, organochlorine compounds, and polybrominated diphenyl ethers across Asia *Environ Sci Technol* **2005**, *39*, 8638-8645.

(21) Piekarz, A.; Primbs, T.; Field, J. A.; Barofsky, D. F.; Simonich, S. Semi-volatile Fluorinated Organic Compounds in Asian and Pacific Northwestern U.S. Air Masses *Environ. Sci. Technol.* **Submitted June 2007**.

(22) Hafner, W. D.; Hites, R. A. Potential sources pesticides, PCBs, and PAHs to the atmosphere of the Great Lakes *Environ Sci Technol* **2003**, *37*, 3764-3773.

(23) Hafner, W. D.; Carlson, D. L.; Hites, R. A. Influence of local human population on atmospheric polycyclic aromatic hydrocarbon concentrations *Environ Sci Technol* **2005**, *39*, 7374-7379.

(24) Foreman, W. T.; Majewski, M. S.; Goolsby, D. A.; Wiebe, F. W.; Coupe, R. H. Pesticides in the atmosphere of the Mississippi River Valley, part II - air *Sci Total Environ* **2000**, *248*, 213-226.

(25) LeNoir, J. S.; McConnell, L. L.; Fellers, G. M.; Cahill, T. M.; Seiber, J. N. Summertime transport of current-use pesticides from California's Central Valley to the Sierra Nevada Mountain Range, USA *Environ Toxicol Chem* **1999**, *18*, 2715-2722.

(26) Hageman, K. J.; Simonich, S. L.; Campbell, D. H.; Wilson, G. R.; Landers, D. H. Atmospheric deposition of current-use and historic-use pesticides in snow at national parks in the Western United States *Environ Sci Technol* **2006**, *40*, 3174-3180.

(27) Vandenburg, H. J.; Clifford, A. A.; Bartle, K. D.; Carlson, R. E.; Caroll, J.; Newton, I. D. A simple solvent selection method for accelerated solvent extraction of additives from polymers *The Analyst* **1999**, *124*, 1707-1710.

(28) Lou, X. W.; Janssen, H. G.; Cramers, C. A. Parameters affecting the accelerated solvent extraction of polymeric samples *Anal Chem* **1997**, *69*, 1598-1603.

(29) Daly, G. L.; Wania, F. Organic Contaminants in Mountains *Environ. Sci. Technol.* **2005**, *39*, 385-398.

(30) Holloway, T.; Fiore, A.; Hastings, M. G. Intercontinental Transport of air pollution: Will emerging science lead to a new hemispheric treaty? *Environ Sci Technol* **2003**, *37*, 4535-4542.

CHAPTER 2. SELECTION OF SOLVENT COMPOSITION FOR PRESSURIZED LIQUID EXTRACTION OF POLYMERIC SORBENTS USED IN AIR SAMPLING

Toby Primbs[1], Susan Genualdi[1], Staci Simonich[1,2*]

[1]Department of Chemistry, Oregon State University, 153 Gilbert, Corvallis Oregon, 97331
[2]Department of Environmental and Molecular Toxicology, Oregon State University, 1007 ALS, Corvallis Oregon, 97331

*Corresponding Author: Telephone, 1-541-737-9194; Fax, 1-541-737-0497; email, staci.simonich@oregonstate.edu

Abstract

Pressurized liquid extraction (PLE) was evaluated as a method for extracting semivolatile organic compounds (SOCs) from air sampling media including quartz fiber filter (QFF), polyurethane foam (PUF), and a polystyrene divinyl benzene copolymer (XAD-2). The solvents previously used for the Soxhlet extraction (e.g. dichloromethane) of polymeric sorbents such as PUF could not be used for PLE because of co-extraction of the polymeric material. Hansen solubility parameter plots were used to aid in the PLE solvent selection in order to reduce co-extraction of polyurethane, while optimizing SOC extraction. A PLE solvent composition of 75:25 hexane:acetone was chosen for the PUF and the XAD-2 copolymer was not solubilized under the PLE conditions used. The average percent recoveries over the PLE step (and percent relative standard deviations) of 63 SOCs, including polycyclic aromatic hydrocarbons (PAHs), polychlorinated biphenyls (PCBs), and organochlorine, amide, triazine, thiocarbamate, and phosphorothioate pesticides, were QFF, 76.7 (6.2), PUF, 79.3 (8.1), and XAD-2, 93.4 (2.9).

1. Introduction

Pressurized liquid extraction (PLE) is an exhaustive extraction technique that uses less solvent and time compared to traditional solvent extraction techniques such as Soxhlet *(1)*. Extraction efficiencies reported for PLE are similar to those reported for Soxhlet and supercritical fluid extraction *(2)*. PLE has been shown to be effective for the extraction of semivolatile organic compounds (SOCs) from environmental matrices; including soils, particulate matter, fly ash, sediments, and waste solids *(3-8)*.

The minimization of matrix interferences is mandatory for trace analysis. The minimization of interferences from extraction cells used in PLE has been reported *(9)*;

however, the minimization of polymeric matrix interferences from air sampling media has not. Often, PUF and XAD-2 are combined with a quartz fiber filter (QFF) in a QFF-PUF-(XAD-2)-PUF sampling train to ensure complete collection of particulate-phase SOCs (QFF) followed by gas phase SOCs (PUF and XAD-2) *(7,10)*. Because the air sampling media used for trapping gas-phase SOCs are polymers such as polyurethane foam (PUF) and polystyrene divinyl benzene (XAD-2), the selection of PLE extraction solvents is essential in order to minimize matrix interferences due to co-extraction of the monomers and oligomers.

Previous research has focused on the extraction of monomers/oligomers and/or polymeric additives from polymers. Lou et al. *(11)* used PLE to extract monomers and oligomers from nylon-6 and poly(1,4-butyleneterephthalate), showing that the PLE extraction solvent chosen and the extraction temperature were important, but that solvent selection was "largely empirical". Vandenburg et al. *(12)* proposed using Hildebrand solubility parameters to select solvents for the extraction of the polymeric additives Irganox 1010 and dioctyl phthalate from ground polypropylene (PP), polyvinyl chloride (PVC), and nylon.

Hildebrand solubility parameters are most effective for substances lacking any significant polar or hydrogen bonding capabilities, that is substances that primarily undergo dispersion type interactions. Hansen solubility parameters divide the Hildebrand solubility parameter (δ) into three components: dispersion (δ_D), permanent dipole-permanent dipole (δ_P), and hydrogen bonding (δ_H) forces (Equation 1) *(13)*. These three components take into account the similarities (or dissimilarities) of the polar and

hydrogen bonding components of organic compounds to explain the extent of interaction better *(13)*.

$$\delta^2 = \delta_D^2 + \delta_P^2 + \delta_H^2 \qquad \textbf{(1)}$$

The human and environmental safety of the organic solvents used is also an important consideration in PLE solvent selection. For example, if dichloromethane, a probable human carcinogen *(14)*, is used as a PLE solvent to clean air sampling media and any residual remains, it may be released during sample collection and result in human exposure *(15)*.

There were two major goals in the selection of solvents for the PLE of SOCs from polymeric air sampling media: 1) efficiently extract the SOCs from the media; and 2) avoid co-extraction of monomers/oligomers from the polymer. Hansen solubility parameters were used to select PLE solvents that minimized co-extraction of matrix interferences, but resulted in good recoveries of 63 commonly measured SOCs. The SOCs selected for extraction and analysis were from 9 chemical classes and their physical chemical properties (octanol-water partition coefficient, water solubility, and vapor pressure) spanned 7-10 orders of magnitude *(16)*.

2. Experimental

2.1. Chemicals

A complete list of the targeted SOCs is shown in Table 2.1. The SOC standards were obtained from the U.S. EPA repository, Chemistry Services Inc. (West Chester, PA), Restek (Bellefonte, PA), Sigma-Aldrich Corp. (St. Louis, MO), or AccuStandard (New Haven, CT). Twenty four isotopically labeled SOCs (d_{10}-fluorene, d_{10}-phenanthrene, d_{10}-pyrene, d_{12}-triphenylene, d_{12}-benzo(a)pyrene, d_{12}-benzo(ghi)perylene, d_{14}-EPTC, d_5-

atrazine, d_{10}-diazinon, d_7-malathion, d_{10}-parathion, d_8-p,p'-DDE, d_8-p,p'-DDT, d_6-methyl parathion, d_{13}-alachlor, d_{11}-acetochlor, ^{13}C-PCB 101, ^{13}C-PCB 180, d_{10}-chlorpyrifos, ^{13}C-HCB, d_6-γ-HCH, d_{14}-trifluralin, d_4-endosulfan I, and d_4-endosulfan II) were used as surrogates. Four isotopically labeled SOCs (d_{10}-acenaphthene, d_{10}-fluoranthene, d_{12}-benzo[k]fluoranthene, and ^{13}C-PCB 138) were used as internal standards. Isotopically labeled standards were obtained from CDN Isotopes (Pointe-Claire, Quebec, Canada) or Cambridge Isotopes Labs (Andover, MA). The standards were stored at 4° C until use. All solvents (hexane, dichloromethane, and acetone) were Fisher Scientific (Fairlawn, NJ) Optima Grade.

2.2. PLE Solvent Evaluation

The initial selection of solvents was based on Hansen solubility parameter plots for the polymeric media and solvents. Following this initial selection, two experiments were conducted to evaluate the suitability of the solvents for PLE. First, the polymeric media was cleaned by PLE with the solvents to evaluate co-extraction of the polymer. After selecting PLE solvent systems that did not co-extract the polymeric media, the PLE recoveries of 63 SOCs from the sampling media were measured.

In order to evaluate the potential polymeric interferences due to PLE of PUF (Tisch Environmental, Cleves, OH), three 3" x 3" PUF plugs were cleaned with an Accelerated Solvent Extractor (ASE®) 300 (Dionex, Sunnyvale, California) and 66 mL extraction cells. Sequential extractions of 100% dichloromethane, 100% acetone, 75:25 hexane:acetone, and 100% hexane were used. The ASE® parameters for the four extractions were: cell temperature 100°C, static time 5 min., solvent flush 50% of cell volume, 1 static cycle, and a N_2 purge time of 240 sec. After cleaning, one PUF plug was

extracted with 100% dichloromethane, the second with 100% hexane, and the third with 75:25 hexane:acetone using the same ASE® parameters described above except 2 static cycles were used instead of 1. To evaluate the potential interferences from XAD-2 (Supelco, Pennsylvania), approximately 50 grams of XAD-2 were cleaned by PLE (Table 2.2) in a 100 mL ASE extraction cell *(17)*. After cleaning, the XAD-2 was extracted with 50:50 hexane:acetone using the ASE parameters described in Table 2.2. The PUF and XAD-2 extracts were concentrated using a Turbovap® II (Caliper Life Sciences, Massachusetts) at 37 °C to ~600 µL and further concentrated to a final volume of ~300 µL using a micro N_2 stream concentrator.

After the selection of PLE solvents was made using Hansen solubility parameter plots and the resulting polymeric interferences were evaluated, the PLE recoveries of 63 SOCs were measured in triplicate. The QFFs (Whatman, England) were cleaned by baking at 350 °C for 12 hours *(7,10)* and the PUF and XAD-2 were cleaned using the ASE conditions described in Table 2.2. After cleaning, the air sampling media was fortified with 15 µL of 10 ng/µL solutions of the target SOCs (Table 2.1) and extracted using the PLE solvents and parameters listed in Table 2.2. The resulting PLE extracts were fortified with 15 µL of 10 ng/µL solutions of the twenty-four isotopically labeled surrogates to assess SOC recoveries over the PLE step. The extracts were concentrated to ~300 µL and fortified with 15 µL of 10 ng/µL solutions that contained the four isotopically labeled internal standards to track recoveries of the surrogates.

2.3. Instrumental Analysis

Qualitative analysis of monomeric and oligomeric interferences was conducted using gas chromatography on an Agilent 6890 (Santa Clara, CA) coupled with mass

spectrometry (Agilent 5973N MSD). A 30 m x 0.25 mm inner diameter x 0.25 μm film thickness, DB-5 column (J&W Scientific, Palo Alto, CA) was used. The GC oven temperature program was: 60 °C held for 1 min., followed by 6.0 °C/min to 300 °C and then held for 3 min., finishing with 20.0 °C/min. to 320 °C and held for 9 min. The mass spectrometer was operated in electron impact (EI) ionization mode and scanned from 35 m/z to 500 m/z.

Quantitative analysis of SOC recoveries was conducted using gas chromatography coupled with mass spectrometry (Agilent 6890 coupled with an Agilent 5973N MSD) in selective ion monitoring (SIM) mode, using either negative chemical ionization (NCI) or EI ionization modes, depending on which form of ionization gave the lowest instrumental detection limit. Details of the instruments, ions monitored, instrument limit of detections, and GC oven temperature program have been provided elsewhere *(7,16)*.

3. Results

3.1. PLE Solvent Selection

Hansen solubility parameter plots are used to graphically display the Hansen solubility parameters for various solvents and polymers. The x-axis represents the dipole-dipole component and the y-axis represents the hydrogen bonding component *(13)*. The z-axis (dispersion) is often not displayed for organic compounds because there is usually little difference between them *(13)*.

Figure 2.1 shows the Hansen solubility parameter plot of polyurethane with various organic solvents *(13)*. The solubility sphere shown in grey represents the region where a solvent is likely to dissolve polyurethane *(13)*. The closer a solvent is to the center of the circle, the more likely it is to solubilize polyurethane *(18)*. Of the organic solvents shown

in Figure 2.1, dichloromethane and 50:50 hexane:acetone are closest to polyurethane and hexane is the furthest. It should be noted that at higher temperatures, Hansen solubility parameters tend to decrease, while the solubilization sphere tends to increase *(13)*. However, Hansen notes that the parameters at higher temperatures are similar to the established values at 25°C *(13)*. The data shown in Figure 2.1 is for 25 °C, which is lower than typical PLE temperatures (~100 °C).

The GC/MS chromatograms of the PLE of PUF using 100% dichloromethane, 100% hexane, and 75:25 hexane:acetone are overlaid in Figure 2.2a for comparison in order to evaluate the resulting polymeric interferences. Figure 2.2a also shows a solvent injection of 100% dichloromethane. The chromatographic base-line signal was elevated when 100% dichloromethane was used as the PLE extraction solvent as compared to 75:25 hexane:acetone and 100% hexane.

To estimate the signal base-line increase, the chromatograms in Figure 2.2a were integrated between 15 and 30 minutes. The percent base-line increase compared to a solvent injection of dichloromethane was found to be 2800%, 1200%, and 140% for dichloromethane, 75:25 hexane:acetone, and hexane, respectively. This result is consistent with the Hansen solubility parameter plot for polyurethane (Figure 2.1).

Figure 2.2b shows the chromatogram of a 50:50 hexane:acetone XAD-2 extract compared to a solvent injection of hexane. Because XAD-2 contains cross linking, a low signal base-line is expected *(18)*. Hansen solubility parameters have not been developed for XAD-2 because it is considered non-soluble in organic solvents *(19)*. Figure 2.2b confirms the lack of XAD-2 solubilization during PLE. A Dionex technical report has

noted the formation of naphthalene during extraction of XAD-2 at elevated temperatures, thus a PLE temperature of 75°C was chosen (Table 2.2) *(17)*.

3.2. PLE Recovery of SOCs

PLE has been reported to have similar extraction efficiencies compared to Soxhlet *(5)*, supercritical fluid extraction, and microwave assisted extraction *(2)*. Table 2.1 summarizes the target SOC PLE recoveries from the three types of sampling media using the PLE parameters and solvents listed in Table 2.2. The SOCs are listed by compound class. For the PUF recovery study, the 75:25 hexane:acetone solvent system was chosen over hexane to insure the extraction of polar, current-use pesticides. For QFF, PUF, and XAD-2 the average percent recoveries (and average %RSD) were 76.7 (6.2), 79.3 (8.1), and 93.4 (2.9), respectively.

The average percent SOC recovery (and percent relative standard deviation) over the entire analytical method for the QFF, PUF, and XAD-2 were 66.3% (4.8), 76.0% (5.5), and 77.1% (3.3), respectively. These recoveries included the solvent evaporation steps and resulted in SOC recoveries that were lower than the PLE step alone. Estimated method detection limits, calculated using EPA method 8280A and assuming an average air volume of 644 m^3, ranged from 0.0001 to 100 pg/m^3, 0.001 to 114 pg/m^3, and 0.0003 to 108 pg/m^3 for the QFF, PUF, and XAD-2, respectively *(20)*.

4. Conclusions

Polymers (i.e. PUF and XAD-2) are effective sorbents for sampling gas-phase SOCs from the atmosphere and PLE is a rapid and effective cleaning and extraction method. However, the use of PLE to extract SOCs from polymeric air sampling media with organic solvents can lead to monomeric and oligomeric interferents. Hansen solubility

parameters were used to identify solvents which were compatible with polyurethane. XAD-2, a copolymer of polystyrene divinyl benzene, was not solubilized under the PLE conditions used.

PLE is an effective method for the extraction of SOCs with a wide range of physical and chemical properties. Care should be taken in PLE solvent selection when extracting SOCs from polymeric sampling materials and Hansen solubility parameters can provide useful guidance for evaluating solvents during the initial steps of method development.

5. Acknowledgements

We thank the EPA: STAR Fellowship (to T. Primbs) and National Science Foundation CAREER (ATM-0239823) for funding. This work was made possible in part by National Institute of Health (Grant # P30ES00210).

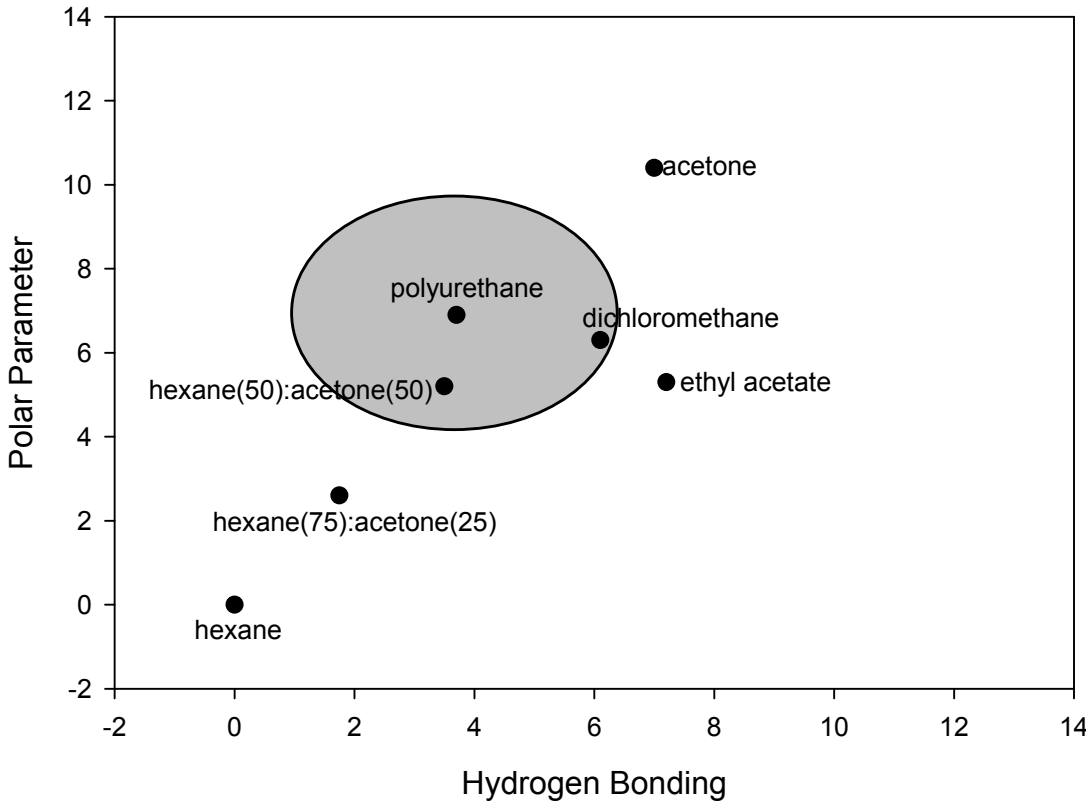

Figure 2.1: Hansen solubility parameter plot of polyurethane at 25°C *(13)*. Various solvents including, 100% acetone, 100% hexane, 100% ethyl acetate, 50:50 hexane: acetone, 75:25 hexane: acetone, and dichloromethane, are shown in the figure with respect to polyurethane.

a) PUF

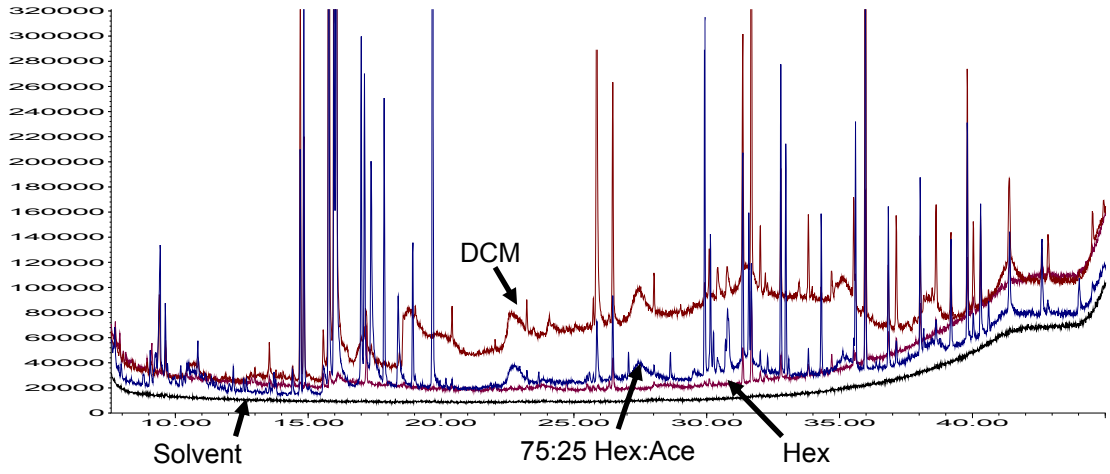

b) XAD-2

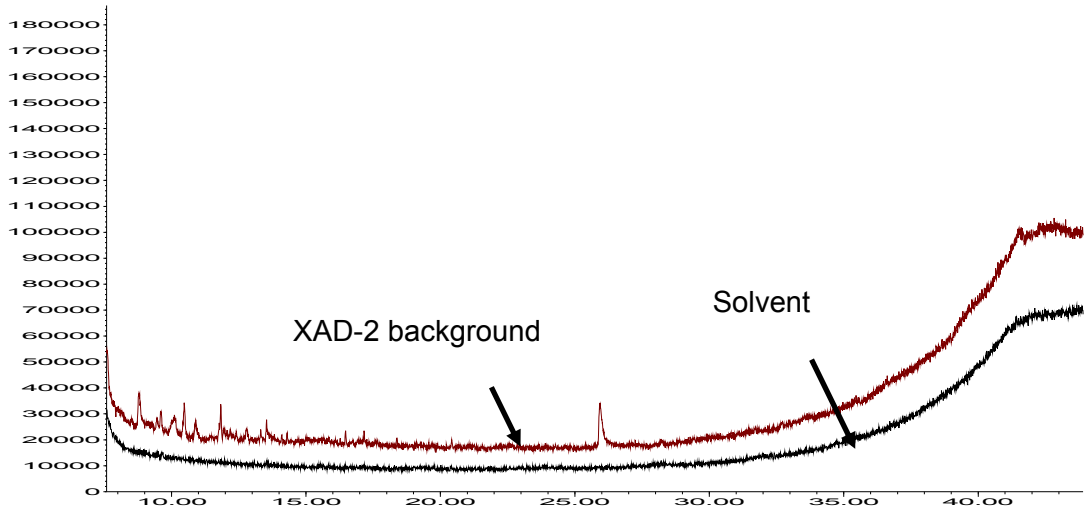

Figure 2.2: (a) GC/MS chromatogram of interferences due to co-extraction of monomers and oligomers from polyurethane foam. The figure shows the effects of three PLE solvents on PUF: dichloromethane (DCM), 100% hexane (Hex), and 75:25 hexane:acetone (Hex:Ace). Also shown for reference is a solvent injection of DCM. **(b)** GC/MS chromatogram comparing XAD-2 interferences using the PLE solvent mixture of 50:50 Hex:Ace compared to a solvent injection of Hex.

Table 2.1: Average PLE SOC recoveries (%RSD) from QFF, PUF, and XAD-2 (n=3) using the parameters and solvents listed in Table 2.2.

	QFF	PUF	XAD-2
Amide Pesticides			
Alachlor	78.7 (5.8)	81.7 (8.5)	97.0 (2.1)
Acetochlor	68.3 (5.6)	42.7 (12.6)	87.9 (3.1)
Metolachlor	84.9 (7.4)	96.1 (3.8)	102.6 (1.9)
Organochlorines Pesticides and Metabolites			
HCH, gamma	76.3 (1.2)	64.7 (1.3)	94.5 (1.1)
HCH, alpha	74.9 (2.3)	60.2 (2.2)	92.2 (0.4)
HCH, beta	83.1 (1.0)	82.0 (1.9)	89.9 (1.0)
Heptachlor	77.8 (3.8)	77.6 (3.6)	111.6 (2.6)
Heptachlor epox	72.7 (4.6)	67.2 (1.2)	122.4 (1.3)
Endrin	58.9 (6.7)	107.8 (4.3)	107.3 (2.2)
Endrin aldehyde	59.7 (15.4)	44.1 (14.7)	92.9 (1.4)
Chlordane, trans	70.6 (6.2)	49.9 (0.8)	104.1 (1.1)
Chlordane, cis	69.7 (8.4)	43.9 (1.0)	82.6 (3.7)
Nonachlor, trans	69.3 (6.6)	48.3 (1.2)	99.3 (1.6)
Nonachlor, cis	57.1 (5.7)	58.5 (1.8)	93.9 (2.5)
Chlordane, oxy	70.6 (3.3)	61.1 (1.3)	118.2 (1.4)
Aldrin	66.5 (2.9)	65.5 (3.3)	99.2 (1.3)
o,p'-DDT	77.8 (6.8)	80.6 (3.3)	94.4 (1.5)
o,p'-DDD	84.3 (6.1)	87.9 (4.2)	94.9 (1.7)
o,p'-DDE	73.2 (5.8)	83.9 (3.6)	104.2 (7.7)
p,p'-DDT	92.5 (10.7)	87.4 (2.1)	89.8 (0.4)
p,p'-DDD	84.3 (6.2)	95.7 (5.3)	106.3 (3.2)
p,p'-DDE	79.0 (3.7)	87.5 (3.2)	91.0 (1.8)
Mirex	60.4 (2.6)	76.4 (0.4)	86.5 (2.5)
Organochlorine Sulfide Pesticides			
Endosulfan I	73.3 (9.2)	60.4 (0.5)	102.0 (1.1)
Endosulfan II	73.9 (7.9)	80.1 (3.0)	97.8 (2.3)
Phosphorothioate Pesticides			
Methyl parathion	73.6 (8.1)	75.8 (2.3)	80.7 (1.4)
Malathion	69.2 (12.7)	92.3 (5.4)	74.0 (5.8)
Diazinon	79.6 (7.1)	81.0 (1.5)	81.2 (2.2)
Parathion	77.1 (8.4)	75.9 (8.4)	77.1 (3.4)
Ethion	97.6 (12.4)	113.9 (9.1)	100.4 (8.5)
Chlorpyrifos	73.6 (8.9)	90.9 (2.8)	81.8 (2.6)
Thiocarbamate Pesticides			
EPTC	79.9 (3.8)	81.4 (1.7)	83.8 (1.4)
Pebulate	91.2 (2.5)	116.9 (3.5)	88.8 (1.3)
Triallate	82.7 (5.5)	123.1 (4.2)	91.9 (2.2)
Triazine Herbicides and Metabolites			
Atrazine desisopropyl	81.5 (15.6)	94.5 (7.8)	107.7 (3.4)
Atrazine desethyl	78.9 (14.4)	93.3 (11.9)	102.7 (1.4)
Atrazine	75.1 (6.6)	89.7 (5.2)	90.2 (1.0)
Simazine	78.9 (8.4)	86.5 (6.4)	102.7 (1.3)
Miscellaneous Pesticides			
Metribuzin	97.3 (4.6)	111.6 (4.8)	90.8 (7.0)
Etridiazole	79.7 (3.6)	117.5 (7.6)	116.5 (0.7)
Dacthal	93.7 (1.7)	105.5 (2.5)	95.4 (3.7)
Trifluralin	79.5 (0.8)	80.0 (16.2)	82.6 (4.5)
Hexachlorobenzene	78.7 (2.4)	81.5 (2.4)	93.3 (1.0)
Polycyclic Aromatic Hydrocarbons			
Acenaphthene	77.1 (4.2)	77.3 (2.2)	81.2 (4.4)
Fluorene	82.9 (2.4)	78.7 (2.2)	92.1 (2.2)
Phenanthrene	81.9 (2.5	83.0 (3.6)	99.4 (2.2)
Pyrene	77.7 (3.2)	83.3 (3.9)	89.4 (2.7)
Fluoranthene	79.3 (3.9)	82.5 (3.7)	92.2 (3.0)
Chrysene + Triphenylene	75.3 (7.1)	86.0 (3.7)	87.5 (1.9)
Retene	80.5 (4.4)	93.7 (3.2)	114.2 (3.0)
Benzo(k)fluoranthene	81.9 (9.8)	84.3 (4.2)	79.6 (2.4)
Benzo(b)fluoranthene	83.4 (9.7)	83.3 (4.5)	99.2 (0.7)
Benzo(e)pyrene	84.0 (10.1)	84.7 (4.8)	101.8 (3.6)
Indeno(1,2,3-cd)pyrene	69.9 (8.9)	76.9 (4.0)	93.7 (1.4)
Dibenz(a,h)anthracene	73.3 (9.2)	81.9 (3.4)	89.9 (2.4)
Benzo(ghi)perylene	77.4 (8.9)	82.0 (4.3)	88.9 (2.5)
Polychlorinated Biphenyls			
PCB 74	79.5 (1.4)	96.9 (8.1)	93.5 (0.6)
PCB 101	82.1 (2.2)	90.4 (7.8)	88.7 (3.1)
PCB 118	95.9 (5.0)	90.7 (8.4)	70.9 (4.6)
PCB 153	73.3 (2.4)	97.8 (8.7)	103.9 (1.6)
PCB 138	78.8 (3.2)	103.4 (8.7)	95.2 (6.2)
PCB 187	76.8 (1.7)	88.6 (8.9)	91.0 (1.5)
PCB 183	78.0 (1.5)	82.0 (9.2)	91.9 (1.6)
Avg	*76.7 (6.2)*	*79.3 (8.1)*	*93.4 (2.9)*

Table 2.2: ASE® parameters and solvents used to clean XAD-2 and PUF. QFFs were cleaned by baking at 350°C for 12 hours. Additionally, ASE® parameters and solvents used for the extraction of SOCs from XAD-2, PUF, and QFF. Solvents included hexane (Hex) and acetone (Ace).

Media	Solvent	Number of Extractions	Cycles	Temp., °C	Static, min.	Flush %	Purge, sec.
Cleaning							
XAD-2	100% Ace	1	5	75	5	100	240
	25:75 Hex:Ace	1	5	75	5	100	240
	50:50 Hex:Ace	3	3	75	5	100	240
PUF	100% Ace	1	1	100	5	100	240
	75:25 Hex:Ace	1	1	100	5	100	240
	90:10 Hex:Ace	1	1	100	5	100	240
QFF	NA	NA	NA	NA	NA	NA	NA
Extraction							
XAD-2	50:50 Hex:Ace	1	3	75	5	100	240
PUF	75:25 Hex:Ace	1	2	100	5	100	240
QFF	50:50 Hex:Ace	1	3	100	5	100	240
	100% Hex	1	3	100	5	100	240

Literature Cited

(1) Richter, B. E.; Jones, B. A.; Ezzell, J. L.; Porter, N. L.; Avdalovic, N.; Pohl, C. Accelerated solvent extraction: A technique for sample preparation *Anal Chem* **1996**, *68*, 1033-1039.

(2) Camel, V. Recent extraction techniques for solid matrices-supercritical fluid extraction, pressurized fluid extraction and microwave-assisted extraction: their potential and pitfalls *Analyst* **2001**, *126*, 1182-1193.

(3) Hussen, A.; Westbom, R.; Megersa, N.; Mathiasson, L.; Bjorklund, E. Development of a pressurized liquid extraction and clean-up procedure for the determination of alpha-endosulfan, beta-endosulfan and endosulfan sulfate in aged contaminated Ethiopian soils *J Chromatogr A* **2006**, *1103*, 202-210.

(4) Ryno, M.; Rantanen, L.; Papaioannou, E.; Konstandopoulos, A. G.; Koskentalo, T.; Savela, K. Comparison of pressurized fluid extraction, Soxhlet extraction and sonication for the determination of polycyclic aromatic hydrocarbons in urban air and diesel exhaust particulate matter *J Environ Monitor* **2006**, *8*, 488-493.

(5) Bautz, H.; Polzer, J.; Stieglitz, L. Comparison of pressurised liquid extraction with Soxhlet extraction for the analysis of polychlorinated dibenzo-p-dioxins and dibenzofurans from fly ash and environmental matrices *J Chromatogr A* **1998**, *815*, 231-241.

(6) EPA *Method 3545* Washington, D.C., 1996.

(7) Primbs, T.; Simonich, S.; Schmedding, D.; Wilson, G.; Jaffe, D.; Takami, A.; Kato, S.; Hatakeyama, S.; Kajii, Y. Atmospheric Outflow of Anthropogenic Semivolatile Organic Compounds from East Asia in Spring 2004 *Environ Sci Technol* **2007**, *41*, 3551-3558.

(8) Fitzpatrick, L. J.; Zuloaga, O.; Etxebarria, N.; Dean, J. R. Environmental applications of pressurised fluid extraction *Rev Anal Chem* **2000**, *19*, 75-122.

(9) Fernandez-Gonzalez, V.; Grueiro-Noche, G.; Concha-Grana, E.; Turnes-Carou, M. I.; Muniategui-Lorenzo, S.; Lopez-Mahia, P.; Prada-Rodriguez, D. Troubleshooting with cell blanks in PLE extraction *Anal Bioanal Chem* **2005**, *383*, 174-181.

(10) Killin, R. K.; Simonich, S. L.; Jaffe, D. A.; DeForest, C. L.; Wilson, G. R. Transpacific and regional atmospheric transport of anthropogenic semivolatile organic compounds to Cheeka Peak Observatory during the spring of 2002 *J Geophys Res-Atmos* **2004**, *109*, D23S15.

(11) Lou, X. W.; Janssen, H. G.; Cramers, C. A. Parameters affecting the accelerated solvent extraction of polymeric samples *Anal Chem* **1997**, *69*, 1598-1603.

(12) Vandenburg, H. J.; Clifford, A. A.; Bartle, K. D.; Carlson, R. E.; Caroll, J.; Newton, I. D. A simple solvent selection method for accelerated solvent extraction of additives from polymers *The Analyst* **1999**, *124*, 1707-1710.

(13) Hansen, C. M. *Hansen Solubility Parameters*; CRC Press: Boca Raton, Florida, 2000.

(14) ATSDR *Methylene Chloride*; Agency for Toxic Substances and Disease Registry: http://www.atsdr.cdc.gov/tfacts14.pdf, 2001.

(15) Chuang, J. C.; Holdren, M. W. The Presence of Dichloromethane on Cleaned XAD-2 Resin: A Potential Problem and Solutions *Environ Sci Technol* **1990**, *24*, 815-818.

(16) Usenko, S.; Hageman, K. J.; Schmedding, D. W.; Wilson, G. R.; Simonich, S. L. Trace analysis of semivolatile organic compounds in large volume samples of snow, lake water, and groundwater *Environ Sci Technol* **2005**, *39*, 6006-6015.

(17) Dionex *Use of Accelerated Solvent Extraction (ASE) for Cleaning and Elution of XAD-2 Resin, Application Note 347*, 2002.

(18) Archer, W. L. *Industrial Solvents Handbook*; Marcel Dekker Inc.: New York, New York, 1996.

(19) Supelco *Personal Communication with B. Vogler, Bellefonte, Pennsylvania*, 2007.

(20) *Method 8280A, E.P.A. The analysis of polychlorinated dibenzop-dioxins and polychlorinated dibenzofurans by high-resolution gas chromatography/low resolution mass spectrometry (HRGC/LRMS).* http://www.epa.gov/epaoswer/hazwaste/test/pdfs/8280a.pdf.

CHAPTER 3. ATMOSPHERIC OUTFLOW OF ANTHROPOGENIC SEMIVOLATILE ORGANIC COMPOUNDS FROM EAST ASIA IN SPRING 2004

Toby Primbs, Staci Simonich, David Schmedding, Glenn Wilson, Dan Jaffe, Akinori Takami, Shungo Kato, Shiro Hatakeyama, and Yoshizumi Kajii

Environmental Science and Technology
PO Box 3337
Columbus, OH 43210, USA
Environmental Science and Technology.; 2007; 41; 3551-3558

Abstract

To estimate the emissions of anthropogenic semivolatile organic compounds (SOCs) from East Asia and to identify unique SOC molecular markers in Asian air masses, high volume air samples (~644 m^3 in 24 hour periods) were collected on the island of Okinawa, Japan between 22nd March and 2nd of May 2004. Contributions from different source regions (China, Japan, the Koreas, Russia, and Ocean/Local) were estimated using source region impact factors (SRIFs). Elevated concentrations of hexachlorobenzene (HCB), hexachlorocyclohexanes (HCHs), DDTs, and particulate-phase polycyclic aromatic hydrocarbons (PAHs) were attributed to air masses from China. A large proportion of the variation in the current use pesticides, gas-phase PAHs, and polychlorinated biphenyl (PCB) concentrations was explained by meteorology. Chlordanes showed a technical mixture profile and similar concentrations regardless of source region. α/γ HCH and trans/cis chlordane ratios did not vary significantly with different source regions and had regional averages of 2.5±1.0 and 1.2±0.3, respectively. Particulate-phase PAH concentrations were significantly correlated (p-value<0.05) with other incomplete combustion byproduct concentrations, including elemental mercury (Hg^0), CO, NO_x*, black carbon, submicron aerosols, and SO_2. Measured PAH, CO, and black carbon concentrations and estimated CO and black carbon emission inventories were used to calculate the emissions of 6 carcinogenic particulate-phase PAHs and these emissions were estimated to be 1518-4179 metric tons/year for Asia and 778-1728 metric tons/year for China, respectively. These results confirm that East Asian outflow contains significant emissions of carcinogenic particulate-phase PAHs.

Introduction

Atmospheric transport of air pollutants, including anthropogenic semivolatile organic compounds (SOCs) and inorganic trace gases (e.g. CO), from Asian sources to the Pacific Coast of North America has been previously identified *(1-6)*. Chemical measurements, coupled with air trajectories, have shown transport across the Pacific can occur in as little as 5 to 10 days during the winter and spring months *(1,5)*. Anthropogenic SOCs are emitted from a variety of activities including fossil fuel combustion, biomass burning, agriculture, and/or industrial activities. SOCs may exist in the gas and/or particle phase in the atmosphere and have a wide range of atmospheric lifetimes (hours to months). Due to their wide range of atmospheric lifetimes, physical-chemical properties, and their emission from a diverse array of anthropogenic sources, SOCs may be good molecular markers for differentiating source regions of trans-Pacific air masses as well as different source types.

Research investigating the trans-Pacific atmospheric transport of anthropogenic SOCs has primarily focused on the west coast of North America *(2,3,6)*. Additional information on the SOC composition of Asian air masses, in the near vicinity of Asia, is needed to assist in the proper identification of trans-Pacific air masses of Asian origin. The primary objectives of this research were to (1) identify the SOC composition of Asian air masses; (2) determine if air masses from different Asian source regions (China, Japan, the Koreas, Russia, and Ocean/Local (Okinawa, Japan)) have unique SOC compositions; and (3) to estimate the emission of PAHs from Asia. To our knowledge, this is the first research to characterize the SOC composition of Asian air masses, from

distinct source regions, in relation to trans-Pacific atmospheric transport and to estimate the emission of PAHs from Asia and China using measured concentrations.

Experimental

Chemicals:

The anthropogenic SOCs detected included *PAHs*: fluorene (FLO), anthracene (ANT), phenanthrene (PHE), fluoranthene (FLA), pyrene (PYR), retene (RET), benz[a]anthracene (BaA), chrysene/triphenylene (CT), benzo[b]fluoranthene (BbF), benzo[k]fluoranthene (BkF), benzo[e]pyrene (BeP), benzo[a]pyrene (BaP), indeno[1,2,3-cd]pyrene (IcdP), dibenz[a,h]anthracene (DahA), and benzo[ghi]perylene (BghiP); *Miscellaneous Combustion Byproducts*: 1,3,5-triphenylbenzene (TPB), and levoglucosan (Lev*)*; *PCBs*: PCB 101, PCB 118, PCB 153, PCB 138, PCB 187, and PCB 183; *Pesticides*: o,p'-DDE, p,p'-DDE, o,p'-DDT, trifluralin (Trif), hexachlorobenzene (HCB), α and γ hexachlorocyclohexane (α-HCH and γ-HCH), metribuzin (Met), heptachlor (Hept), dacthal (Dac), chlorpyrifos (Chlorp), oxy, trans, and cis chlordane (OC, TC, and CC), trans and cis nonachlor (TN and CN), endosulfan I and II (Endo I and Endo II), endosulfan sulfate (Endo S), and dieldrin (Dield). The atmospheric lifetimes of these SOCs range from hours to months. A complete list of the measured SOCs, including those not detected in these samples, the isotopically labeled surrogates and internal standards that were used for quantitation, and the origination of all standards and solvents used, has been previously reported *(7)*.

Sampling Site:

The sampling site (Hedo Station Observatory, HSO) is located on the northwest coast of the island of Okinawa, Japan (26.8N, 128.2E, 60 m a.s.l.), about 200 m from the

East China Sea (Figure 3.1). HSO is an established air monitoring site used to study the outflow of air pollution from Asia *(8-10)* and is ~800 km from the coast of China. Atmospheric transport times from China, the Koreas, and Japan to the site are ~24 to 48 hours *(8)*. Other simultaneous measurements at HSO during the sampling campaign included submicron aerosols (nephelometer), reactive gaseous mercury, particulate-phase mercury, and elemental mercury, which were conducted by the Jaffe Group (University of Washington, Seattle, WA, U.S.A) and Frontier Geosciences (Seattle, WA, U.S.A) *(10)*. Other measurements were conducted by the National Institute for Environmental Studies, Tokyo Metropolitan University, and the Acid Deposition and Oxidant Research Center, and included meteorological measurements, an Aerodyne Aerosol Mass Spectrometer (AMS), carbon monitor (to measure black carbon and organic carbon), CO, O_3, VOCs, SO_2, NO, and NO_x*. A Mo converter was used in the NO_x analyzer which also converts several NO_y species, thus NO_x* is used instead of NO_x.

Sample Collection and Extraction:

Eighteen samples (17 to 24-hours in duration) were collected for SOCs from the 22nd March 2004 to 2nd May 2004 using a modified high volume air sampler (Tisch Environmental, Cleves, OH) (Table 3.1). The sampler was located on the top of the site building and was calibrated using a standardized orifice manometer kit (Tisch Env., Cleves, OH). The sampling flow rate was recorded before and after collection of each sample. The sampling media consisted of two 20.3 x 25.4 cm quartz fiber filters (QFF) (Whatman, England), in series, for the collection of particle-phase SOCs (the first filter) and for the determination of sampling artifacts due to gas-phase sorption to the collection media itself (the second filter). Additionally, two 1½ ” x 3 ” polyurethane foam (PUF)

plugs (Tisch Env. Cleves, OH), with ~50 g XAD-2 (Supelco, Pennsylvania) resin (polystyrene divinylbenzene) in between the two plugs, was used for the collection of gas-phase SOCs (first PUF and XAD) and the determination of potential SOC break-through (second PUF). The quartz fiber filters were cleaned by heating at 350^{o}C for 12 hours. The XAD-2 and PUF plugs were cleaned using Accelerated Solvent Extraction 300 (ASE) (Dionex, California) with two sequential extractions first with dichloromethane and second ethyl acetate (100 °C, static time 5 min, flush % 100, static cycles 1, purge time 204 sec) prior to use. After cleaning, the PUF and XAD-2 were air dried in a hood for ~ 1 hour before being stored at -20° C until being deployed to the field. All of the sampling media was transported in a sealed cooler, on ice, to HSO via commercial air by OSU scientists and returned to OSU in the same manner. Seventeen of the eighteen samples were collected over a 24-hour period, while one sample was collected over a 17-hour period due to a power outage at HSO (Table 3.1).

The sampling media were packed into 34, 66, or 100 mL ASE cells (PUF, QFF, and XAD-2, respectively) spiked with 23 isotopically labeled SOCs *(7)* (15uL of a 10 ng/uL standard solution) and then extracted with ASE. The XAD-2 and quartz fiber filters were extracted with ethyl acetate, followed by a second extraction with dichloromethane. For both extractions, the ASE parameters were 100 °C, Static Time 5 min, Flush % 100, Static Cycles 1, Purge Time 240 sec. The PUF was extracted with 75:25 hexane:acetone (100 °C, static time 5 min, flush % 50, static cycles 2, purge time 240 sec.). The extracts were concentrated with a Turbovap® II (Caliper Life Sciences, Massachusetts) at 37 °C to ~600 µL, and then concentrated to ~300 µL with a micro N_2 stream concentrator. After concentration the samples were spiked with 4 isotopically

labeled SOCs (15uL of a 10 ng/uL standard solution) as internal standards. Derivatization of levoglucosan as trimethyl silyl ether has been reported elsewhere*(11)* and consisted of drying 20 μL of the sample extract under a gentle stream of N_2 and adding pyridine and BSTFA (bis-(trimethylsilyl)trifluoroacetamide) with a three hour reaction time at 70 °C.

Sample Analysis:

Samples were analyzed with gas chromatography-mass spectrometry (GC/MS) in the selective ion monitoring (SIM) mode with electron capture negative ionization (ECNI) and electron impact (EI) ionization modes *(7)*. Analysis of specific SOCs was divided between the two ionization modes based on which ionization mode resulted in the lowest instrumental detection limit *(7)*. Instrumental limits of detection ranged from 0.006 to 6.7 pg/μL *(7)*. Limits of quantification, defined as the lowest standard used in the calibration curves, ranged from 0.25 to 50 pg/μL. Estimated method detection limits, calculated using EPA method 8280A, ranged from 0.11 to 114 pg/m^3 for the GC/MS-EI and 0.0001 to 6.4 pg/m^3 for the GC/MS-ECNI *(12)*. Only signals exceeding 3 times the peak to peak noise were reported. Details of the ions monitored, instrumental limits of detection, and GC conditions are reported elsewhere *(7)*. 1,3,5-triphenylbenzene (TCI America, Florida) was measured by GC/MS-EI and SIM quantification ion m/z 306 and qualifying ions m/z 217, 289, and 228. Levoglucosan (Sigma-Aldrich, Wisconsin) was measured using quantifying ion m/z 204 and qualifying ions m/z 217, 333, and 73 by GC/MS-EI after being derivatized.

Quality Assurance Procedures:

SOC recoveries ranged from 50 to 118% over the entire analytical method. The bottom PUF plug was used to detect potential SOC breakthrough during sample

collection and the SOC concentration in the bottom PUF plug ranged from 0.06 to 22% of the total gas-phase concentration. Because SOC breakthrough during sampling was not significant, no correction was made. The second quartz fiber filter was used to investigate adsorption of gas phase SOCs to the filter media itself. Endo I, Endo II, Trif, and HCB showed occasional adsorption to the quartz fiber filters and no correction was made. Field blanks (three were collected during the campaign) consisted of installation of the sampling media in the high volume air sampler for 24 hours, with the power off. FLO, PHE, FLA, PYR, RET, Trif, Met, HCB, and Chlorp were detected in the field blanks above the quantification limit. The ratio of measured sample concentration to the average field blank concentration ranged (minimum-maximum): FLO (20-200), PHE (104-942), FLA (72-493), PYR (261-1690), RET (14-175), Trif (6-245), Met (16-51), HCB (261-775), and Chlorp (8-641). Reported SOC concentrations were field blank and surrogate recovery corrected (SOC concentrations were calculated versus the spiked isotopically labeled surrogates).

Trajectories and Data Analysis

Four-day back trajectories were calculated using NOAA's ARL HYSPLIT 4.0 model (FNL) *(13)*. For each 24 hour sample, 7 trajectories were calculated (1 every 4 hours), which included the start and stop times of the sampling period. At each 4 hour interval, three trajectories, were calculated (at 60, 250, and 500 meters a.s.l) to understand the general air mass flow in the boundary layer where the sampling site is located (elevation 60 m a.s.l.). Additionally, the model's precipitation data was included in the data output. S-PLUS version 7.0 (Insightful, Seattle, WA) was used for statistical analysis.

Results and Discussion

Back Trajectories and Source Region Impact Factors

Back trajectories were used to determine the impact of different source regions (China, Korea, Japan, Russia, and Ocean/Local) on the air masses sampled and was termed source region impact factor (SRIF). The SRIF represents the percentage of the time an air mass spent in a given source region in the four days before arriving, and being sampled at HSO. Similar methods, the amount of time trajectories spent in different regions, have been used by other researchers *(6,14)*. The higher the SRIF percentage, the more time the sampled air mass spent in a given source region. The SRIF can be used to assess transport time from source regions to HSO by comparing time spent in a given source region, to the time spent in the other source regions. Additionally, it can be used to determine if increased time spent in a given source region impacts the air concentrations of the SOCs at HSO.

$$SRIF\% = \left\{ \left[\sum_{n=1hour}^{96hour} \left(n\left(T_{sr} = 1; otherwise = 0\right)\right) \right] hours / 672 hours \right\} \times 100 \qquad \textbf{(1)}$$

Equation 1 shows the details of the calculation of the SRIF. Step 1 in the calculation of the SRIFs was to calculate the 4-day back trajectories for air masses associated with each sample. This step was done by calculating 7 trajectories for every 24 hour sample (1 every 4 hours for 24 hours, including the sample start and stop times). Step 2 was to calculate the time the trajectories spent in a given source region. This time was calculated for all source regions (China, Japan, the Koreas, Russia, and Ocean/Local (which includes the island of Okinawa)). For each trajectory, the time spent in a given source region (T_{sr}) was identified as a binary response, '1' if it was in the given source

region and '0' if it was not. This was repeated each hour for 4 days back in time (n = 1 to 96 hours). The final step was to calculate the SRIF by dividing the fraction of the total hours spent in a given source region by 672 hours (96 (the total number of hours back) × 7 (number of trajectories per sample)) and multiplying by 100.

SRIFs were calculated for three elevations 60, 250, and 500 meters a.s.l to assess boundary layer flow. There was no statistically significant difference for the SRIFs between the three elevations (p-value < 0.01) and the SRIFs at 250 meters a.s.l. were used in subsequent calculations to represent atmospheric flow above the ground level of the HYSPLIT model. Table 3.1 summarizes the site meteorology and the SRIFs for the samples collected at HSO. The 4-day back trajectories associated with the four air samples having the highest SRIFs for China, Japan, Korea, Russia, and Ocean/Local are shown in Figure 3.2.

Principal component analysis (PCA) of the SRIFs in Table 3.1 was used to further classify the samples into source regions. The PCA biplot for the first two principal components explained 90.7% of the variation in the original data (Figure 3.3). The clustering from this biplot was further used to classify the samples into four source regions, China, Ocean/Local, Japan/Korea/Russia (J/K/R), and Mixed (not falling into one of these three groups) (see Table 3.1).

Further characterization of the Ocean/Local region was conducted using Cl^- concentrations in the aerosols as an oceanic indicator to further assess if the ocean was a source or sink for SOCs in transit to HSO. None of the SOC concentrations were positively correlated with Cl^-. However, HCB, Dac, PCBs, Phe, Pyr, and Ret

concentrations were negatively correlated with Cl^- concentrations. This may indicate that the ocean is a sink and not a source for SOCs in transit to HSO.

Meteorological and Source Region Variability

Figure 3.4 shows the temporal concentrations of the major SOCs measured during the campaign. To assess the impact of meteorological conditions on the SOC atmospheric concentrations at HSO, a multivariable linear regression model was developed using the SOC concentrations and site meteorological data (Equation 2). Multivariable linear regression models have been previously used to assess the effect of meteorological conditions on SOC concentrations *(15-17)*. In equation 2, *WS* (m/s) represents the site wind speed, *Sun* (cal/(cm^2h)) is the site sun intensity, *WD* (degrees) is the average site wind direction, *ppt* (mm/h) is the precipitation summed for 4 days back in time for the back trajectory, *JD* is in Julian Days, and *T* (K) is the average site temperature. Because the sample size was relatively small (n=18) in comparison to the number of β terms (n=7) in equation 2, a best subset method (Cp-statistic) was used to find an equivalent model which only included statistically significant parameters *(18)*. Results of the best meteorological subset model for each SOC are summarized in Table 3.2 and the R^2 values ranged from 0.22 to 0.80.

$$\log(conc) = \beta_0 + \beta_1 JD + \beta_2 WS + \beta_3 Sun + \beta_4 \cos(WD) + \beta_5 \sin(WD) + \beta_6 ppt + \beta_7 1000/T \quad \textbf{(2)}$$

SOCs that existed primarily in the gas phase, operationally defined as SOCs measured in the PUF and XAD-2 fractions with <50% of their total concentration per sample measured on the QFF, were generally influenced by wind speed, temperature,

and/or Julian Day. The gas-phase SOCs included all SOCs except for TPB, Lev, BaA, BbF, BkF, BeP, BaP, IcdP, DahA, and BghiP. In general, the concentration of gas-phase SOCs decreased with increasing wind speeds at HSO or Julian Day and increased with increasing temperature at HSO. α-HCH and γ-HCH concentrations at HSO did not correlate significantly with meteorological variables.

Particulate-phase SOCs (TPB, Lev, BaA, BbF, BkF, BeP, BaP, IcdP, DahA, and BghiP), operationally defined as SOCs with >90% of their concentration measured on the QFF, were generally not influenced by meteorological variables. Of these particulate-phase SOCs only TPB, BaP, and Lev showed correlations with meteorological parameters. TPB, a marker for the combustion of plastics *(19)*, concentrations decreased with increasing wind speed at HSO. Concentrations of Lev, a marker for the combustion of biomass that originates from cellulose *(11)*, decreased with increasing temperature at HSO, possibly due to decreased burning of biomass for heating as temperatures increased throughout the spring. For unknown reasons, BaP (a particulate-phase PAH) was the only SOC to show decreased concentrations with precipitation in transit to HSO.

After determining the best meteorological subset model from equation 2 which took significant meteorological variables into account for each SOC, the differences in the source regions were investigated. This was conducted by adding the SRIF for each country to the best meteorological subset model. Equation 2 was not applied to DahA, Endo S, Hept, Met, DDTs, and Dield because of the low number of samples in which they were measured.

Combustion Byproduct Results

Figure 3.4 shows the proportion of variation (R^2) in the SOC concentrations that is explained by the best meteorological subset model and SRIF. Hatched bars indicate the proportion of variation in the SOC concentrations explained by best meteorological subset model only and the colored bars indicate the proportion of variation in the SOC concentrations explained when the SRIF is included in the model. Stars indicate the β term (slope) for the SRIF component of the model is negative, indicating decreasing SOC concentrations when the air mass came from the stated source region.

The particulate-phase PAHs; BbF, BkF, BeP, BaP, IcdP, and BghiP, showed increased concentrations when the source region was identified as China even after significant meteorological variables were taken into account (Figure 3.4). BaP was the only particulate-phase PAH to show significant correlation with meteorological parameters, while the other particulate-phase PAHs only included source region in the final model. ANT concentrations increased when Ocean/Local was identified as the source region and concentrations decreased when the source region was identified as China. This is likely due to ANT's relatively short atmospheric lifetime relative to other gas-phase PAHs *(20)*.

During the ACE-Asia campaign in 2001, Simoneit et al. *(21)* reported significant PAH concentrations (0.005 to 19.3 ng/m^3) associated with particulate matter. Xu et al. *(22)* also recently estimated an emissions inventory of PAHs for China and pointed out the relatively high proportion of higher molecular weight (particulate-phase) PAHs emitted in China as compared to the Great Lakes Region of the U.S. The major sources of these elevated concentrations of particulate-phase PAHs in China were attributed to

domestic coal and firewood combustion, as well as the coking industry *(22)*. Figure 3.6 shows the PAH profile (normalized to phenanthrene) for the China PAH emission inventory estimated by Xu et al. *(22)*, the PAH emission profile for the Great Lakes Region of the U.S. *(23)*, and the average PAH profile we measured at HSO in samples where China, Japan/Korea/Russia, and Ocean/Local were identified as the major source region. The PAH profile from Xu et al. is for all of China, while the air masses we sampled at HSO originated from central and northern China. Xu et al. points out that the provincial emission rates in China are "extremely different" *(22)*. Even with the regional differences our results confirm that significant proportions of particulate-phase PAHs are being emitted from China.

Because PAHs originate from combustion sources, a correlation with other combustion byproducts was investigated. Figure 3.7 shows the significant positive correlation (p-value <0.05) of Σparticulate-phase PAH concentration with submicron aerosol, black carbon (BC), Hg^0, CO, SO_2, and NO_x* concentrations. Gas-phase PAHs did not show a significant correlation (p-value >0.05) with NO, Hg^0, CO, SO_2, or NO_x*. A correlation between Hg^0 and CO concentrations has been previously reported for this sampling campaign and was attributed to coal combustion in China *(10)*. The significant positive correlation between particulate-phase PAHs and Hg^0, BC, and SO_2 concentrations suggests that coal combustion in China is a major source of particulate-phase PAHs.

FLA was the only gas-phase PAH that had a statistically significant correlation with the particulate-phase PAHs. Other researchers have noted enhancements in FLA concentrations as an indication of coal combustion *(24,25)*. Lev concentrations did not

show a correlation with distinct source regions (Figure 3.4), although it did show a significant correlation (p-value, 0.007) with the sum of particulate-phase PAH concentrations.

TPB has been measured in particles from solid waste incinerators and has recently been proposed as a marker for the combustion of plastics *(19)*. There are 17 municipal solid waste incinerators (MSWIs) near HSO (16 on Okinawa and 1 on the neighboring Island of Yoron). TPB concentrations were elevated at HSO in some Ocean/Local air masses (Figure 3.4) and showed a significant correlation (p-value, 0.015) with the gas-phase PAHs but not the particulate-phase PAHs. The TPB concentrations measured at HSO (0.007-0.088 ng/m^3) were lower than TPB concentrations measured in Sapporo Japan (0.06-2 ng/m^3) *(19)*.

PCB Results

PCBs were banned in Japan in 1972 *(26)* and production and use of PCBs has been banned or highly restricted since the early 1980s in China *(27)*. However, PCB sediment fluxes have increased in the Pearl River Delta area of China *(27)*. In an extensive passive air sampling campaign in the Asian region, elevated concentrations of PCBs were attributed to urban areas in both China and Japan *(28)*.

Some of the highest concentrations of PCBs were measured in air masses from the Ocean/Local region (Figure 3.4). PCB 118 and PCB 153 showed decreased concentrations when the source region was Japan/Korea/Russia (Figure 3.4). Additionally, the PCBs showed significant correlations with both gas-phase PAHs (p-value < 0.0001) and TPB (p-value, 0.028). This correlation may indicate that PCBs, gas

phase-PAHs, and TPB come from urban areas or that these SOCs are emitted from local sources, such as MSWIs *(29)*.

Concentration ratios of the PCB congeners measured in this study were investigated to determine if there was a unique PCB ratio for different source regions (Figure 3.8). The penta (PCB 101/PCB 118), hexa (PCB 153/PCB 138) and hepta (PCB 187/PCB 183) PCB ratios did not show any regional differences.

Pesticide Results

HCB, ΣHCHs, and ΣDDTs were all significantly correlated with one another (p-value<0.05) and showed elevated concentrations in air masses from China (Figure 3.4 and 5). HCB has many sources, including agricultural, industrial, and combustion sources *(30)*. Previous research in Asia using passive air samplers showed elevated concentrations of HCB in China compared to other countries in the region *(28)*. At HSO, HCB had the highest concentration of all of the organochlorine SOCs measured, with concentrations ranging from 53 to 157 pg/m^3 (Figure 3.4).

Both α- and γ-HCH showed elevated concentrations in air masses from China and α-HCH concentrations decreased in Ocean/Local air masses (Figure 3.4). Technical HCH contains α- and γ-HCH and is banned in north eastern Asian countries *(26)*. However, some stockpiles are believed to still exist *(26)*. Lindane (γ-HCH) is still being produced and used in the region *(26)*. In Korea, HCHs have been banned since 1979 *(31)*. Although technical HCH was banned in China in 1983 *(32)*, the facilities that produced technical HCH were not shut down until 2000 *(33)*. Additionally, lindane has been used in China since 1991 *(32)*. Technical HCH has been used in southeastern China and lindane has been used in northern China *(32)*.

Because technical HCH is a mixture of several isomers of HCHs, the ratio of two of the isomers (α-HCH and γ-HCH) is commonly used to help identify the source. The technical mixture ratio (α to γ-HCH) ranges between 4 and 10 *(26)*. Figure 3.8 shows the α to γ-HCH ratio of the technical mixture, compared with the measured ratio at HSO. Only the China and Japan/Korea/Russia α to γ-HCH ratios were statistically different from each other (p-value, 0.04). The sample collected on Julian days 105-106 (Japan/Korea/Russia) was an outlier in the dataset because it had an α to γ-HCH ratio of 6 and accounts for the statistical difference. The average α to γ-HCH ratio measured at HSO including all samples was 2.5 ± 1. However, excluding the Julian days 105-106 sample, the ratio was 2.3 ± 0.5.

DDT has been banned in Korea since 1973 *(31)* and was banned for all purposes in Japan in 1981 *(26)*. In China, recent research has noted higher o,p'-DDT/p,p'-DDT ratios than is expected from a technical mixture of DDT *(34)*. This has been attributed to the use of Dicofol and its contamination with o,p'-DDT *(34)*. China produces DDT for use in dicofol production and for export for use as a malaria control *(34)*. The major use of dicofol is in south and central China and applications typically occur in July and August *(35)*. At HSO, p,p'-DDT was not detected, however o,p'-DDT was measured primarily in samples associated with China (Figure 3.4). This may be due to dicofol use in China. Because the major usage of dicofol is in the summer, the o,p'-DDT concentrations measured at HSO in spring 2004 may be from revolatization or fugitive emissions from production.

CC and TC concentrations increased in Japan/Korea/Russia air masses (Figure 3.4). Chlordane is banned in Russia and Korea *(26)*. However, China and Japan still hold

exemptions for its use as a termiticide *(26)*. Chlordane is used to kill termites in Southern China *(35)* and is manufactured in eastern China *(28)*. A recent passive air sampling campaign in the Asian region showed elevated concentrations of chlordanes in Japan as compared with other countries in the region *(28)*.

TC is more susceptible to microbial degradation and photodegradation compared to CC *(6,36)*. Assuming the technical mixture TC/CC ratio in Asia is comparable to the technical mixture ratio in N. America (which has been reported to be 1.26, 1.16, and 1.01 *(6,36,37)*), a ratio less 1.0-1.26 would indicate a more aged source. At HSO, the TC/CC ratio averaged 1.2 ± 0.3, which is similar to previously reported technical mixture ratios, with no distinct source region differences (Figure 3.8). Additionally, the ratio of TC, CC, TN, and CN to the sum of chlordanes was similar to technical chlordane, with no distinct source region differences (Figure 3.8). This indicates that fresh sources of chlordane dominate the atmospheric profile in this region.

Hept, a component of chlordane and a pesticide, is primarily banned in the region *(26)*. In Korea, Hept was banned in 1979 *(31)*. Hept concentrations at HSO were 4-60 pg/m^3 and it was measured in only 6 of the 18 samples collected. Hept concentrations were significantly correlated with Σchlordane concentrations (p-value, 0.04). Heptachlor epoxide, a degradation product of Hept, was not detected in the HSO samples.

Technical endosulfan is 70% Endo I and 30% Endo II *(16)*. In Korea, endosulfan has been used since 1971 and is applied in the summer *(31)*. In China, endosulfan is also currently used *(35)*. The likely source of endosulfans during the spring 2004 sampling campaign was revolatization (temperature was a significant meteorological variable for Endo I) because the application time for endosulfan is summer. Endo I and II

concentrations did not show any major source region differences (Figure 3.4). No differences existed in the Endo I/ΣEndos and the Endo II/ΣEndos ratios between the source regions (Figure 3.8). The Endo I/Σ Endos ratio averaged 0.92 ± 0.05 and Endo II/Σ Endos ratio averaged 0.08 ± 0.04. Both ratios differed from the technical mixture ratios of 0.70 and 0.30, respectively. The difference between the technical mixture and the measured ratios may be due to different formulations or it may be due to differences in their physical or chemical properties. The vapor pressures of Endo I and Endo II are 0.0061 and 0.0032 Pa (at 25 °C), respectively *(38)*. If the major route of endosulfans to the atmosphere was revolatization, a higher Endo I/Σ Endos ratio would be expected.

Dield has not been used in China and is not currently in use in the countries in the northeastern Asian region *(26)*. In Korea, dield was banned in 1971 *(31)*. Dield was only detected in 7 of the 18 samples at HSO and a source region could not be determined.

Trif, Chlorp, and Dac are all current use pesticides that were measured at HSO. Meteorological variables explained a large proportion of the variation in Trif, Chlorp, and Dac concentrations (Figure 3.4). Met, an herbicide currently used on Okinawa, was detected in 4 of the 18 samples (Table 3.1). Wind roses, calculated from site meteorological data, showed that on the days Met was measured, strong south-easterly winds passed directly over Okinawa prior to arriving at HSO. Met has a high water solubility and a relatively short estimated atmospheric lifetime *(20)*, suggesting that on the days Met was measured at HSO, there was likely a contribution from local sources.

Emissions of SOCs from Asia

Jaffe et al. used CO inventories for Asia and China and CO and Hg^0 measurements at HSO during this sampling campaign to calculate the emission of Hg^0

from Asia *(10)*. They calculated that 1460 metric tons/year of Hg^0 are emitted from Asia *(10)*. Three assumptions were made in the estimation of Hg^0 emission: 1). only dilution of CO and Hg^0 occurs in transit to HSO and there are no chemical or physical losses; 2). there is a constant source of both CO and Hg^0; and 3). the background concentrations of CO and Hg^0 are constant *(10)*. Given the relatively short transit times to HSO from the source regions (24 to 48 hours), these assumptions are reasonable.

We used this same approach to estimate the emission of FLA, BaA, CT, BbF, BkF, BeP, BaP, IcdP, and BghiP because these PAH concentrations were significantly correlated with CO concentrations (p-value<0.05). Because the majority of these PAHs were associated with particulate matter, we also calculated the emission of these same PAHs using BC measurements from HSO and a BC inventory *(39)*. Although the PAH correlations with CO concentration were better than the correlations with BC concentration and the BC approach predicted higher PAH emissions, the emission estimates were within an order of magnitude of each other (Table 3.3). If the emission inventories for BC and CO are assumed to be equally accurate, then the emission calculations for the particulate-phase PAHs (BaA, BbF, BkF, BeP, BaP, IcdP, and BghiP) may be more accurately predicted by a particulate matter surrogate (BC). In contrast, for gas-phase PAHs such as FLA, the emission calculation based on CO would be more accurate.

The emissions of the seven carcinogenic PAHs (BaA, CHR, BbF, BkF, BaP, IcdP, and DahA) were estimated as 3460 tons in China in 2003 *(22)*. U.S. emission estimates for these same seven PAHs were reported to be 2000 and 1400 tons in 1990 and 1996, respectively *(22,40)*. The calculated emission at HSO for six of the seven carcinogenic

PAHs listed above (excluding DahA) was 1518-4179 metric tons/year for Asia and 778-1728 metric tons/year for China. DahA was only measured in 5 of the 18 samples and was not correlated with CO or BC. Our PAH emission estimates may be underestimated because the samples were collected in spring and do not reflect periods of high PAH emission (winter). Finally, o,p'-DDE, p,p'-DDE, o,p'-DDT, HCB, α-HCH, and γ-HCH concentrations were all significantly correlated (p-value<0.05) with CO concentrations, although this association was likely due to similar source regions and not similar sources.

Year-round measurements of SOCs at HSO are needed to better estimate SOC emissions and understand seasonal differences in East Asian outflow. These results confirm that East Asian outflow contains significant emissions of carcinogenic particulate-phase PAHs.

Acknowledgements

The authors thank Eric Prestbo and Frontier Geosciences (Seattle, WA), Takemitsu Arakaki of Univ. of the Ryukyus, Okinawa, Shu Tao of Peking University, Will Hafner and Phil Swartzendruber of University of Washington-Bothell, and the Acid Deposition and Oxidant Research Center, Niigata, Japan for providing SO_2, NO_x*, and NO data. We thank the EPA: STAR Fellowship (to T. Primbs) and National Science Foundation CAREER (ATM-0239823) for funding. This work was made possible in part by National Institute of Health (Grant # P30ES00210).

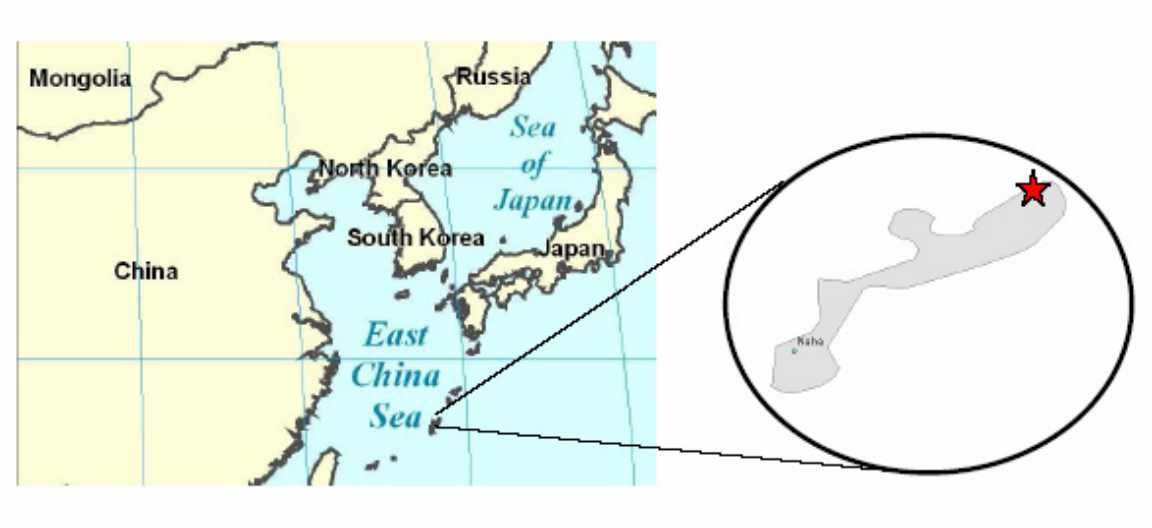

Figure 3.1: Hedo Station Observatory (HSO) is located on the northwest coast of the Island of Okinawa (red star) ~800 km east of the coast of China.

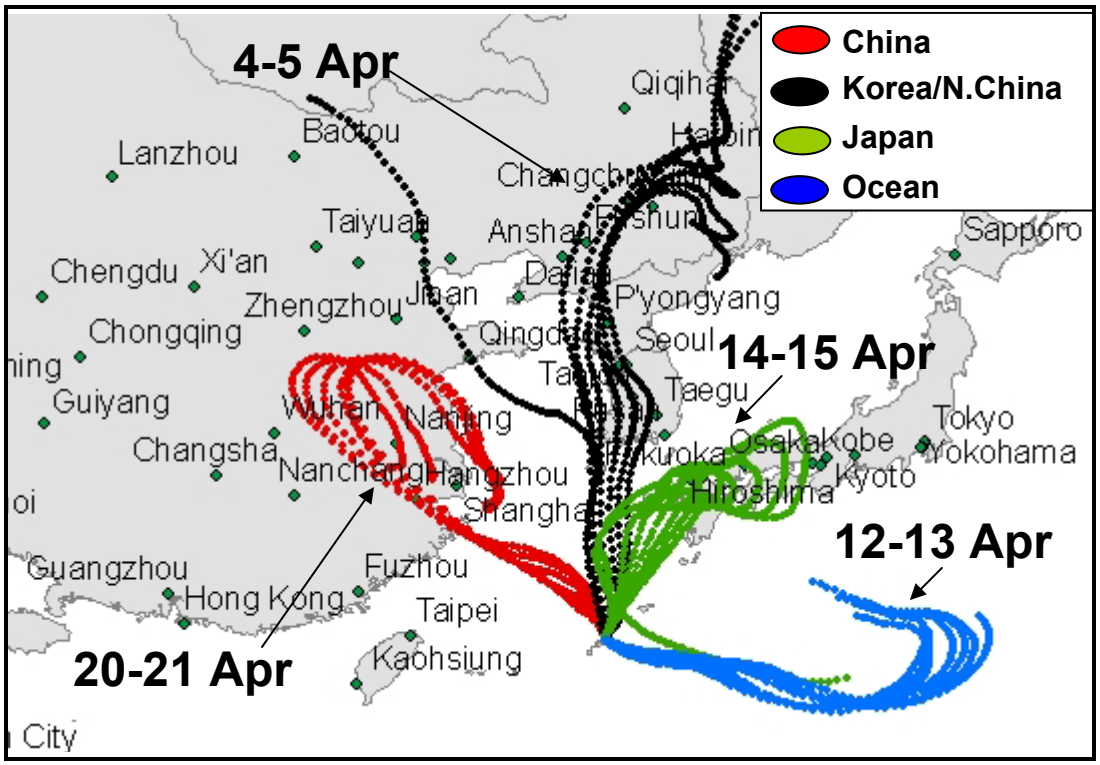

Figure 3.2: Representative 4-day back trajectories (250 meters a.s.l.) for representative air masses sampled from Japan, China, Pacific Ocean, and Korea during the six week campaign. Each dot represents 1 hour back in time. Cities with populations greater than 1 million people are labeled.

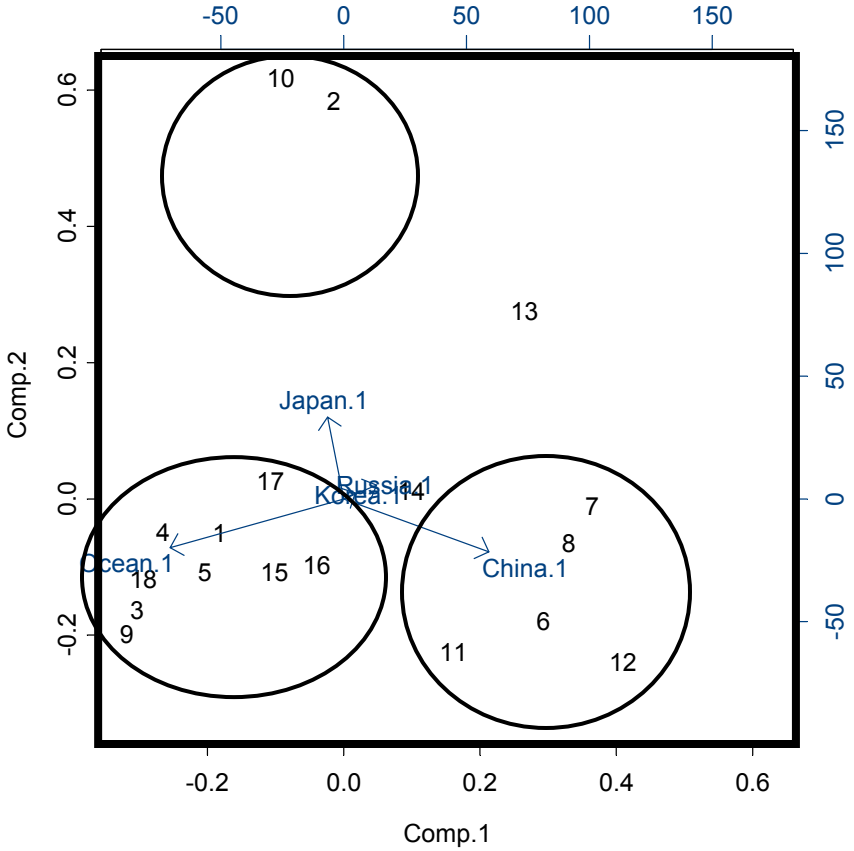

Figure 3.3: PCA biplot, using the SRIF values, used to determine source regions. The numbers correspond to sample numbers listed in Table 3.1. Ocean/Local was defined as samples 1,3,4,5,9,15,16,17 and 18; China was defined as 6,7,8,11, and 12; Japan/Korea/Russia (JKR) was defined as 2 and 10; and mixed included 13 and 14. The first two components retained 90.7% of the original variation.

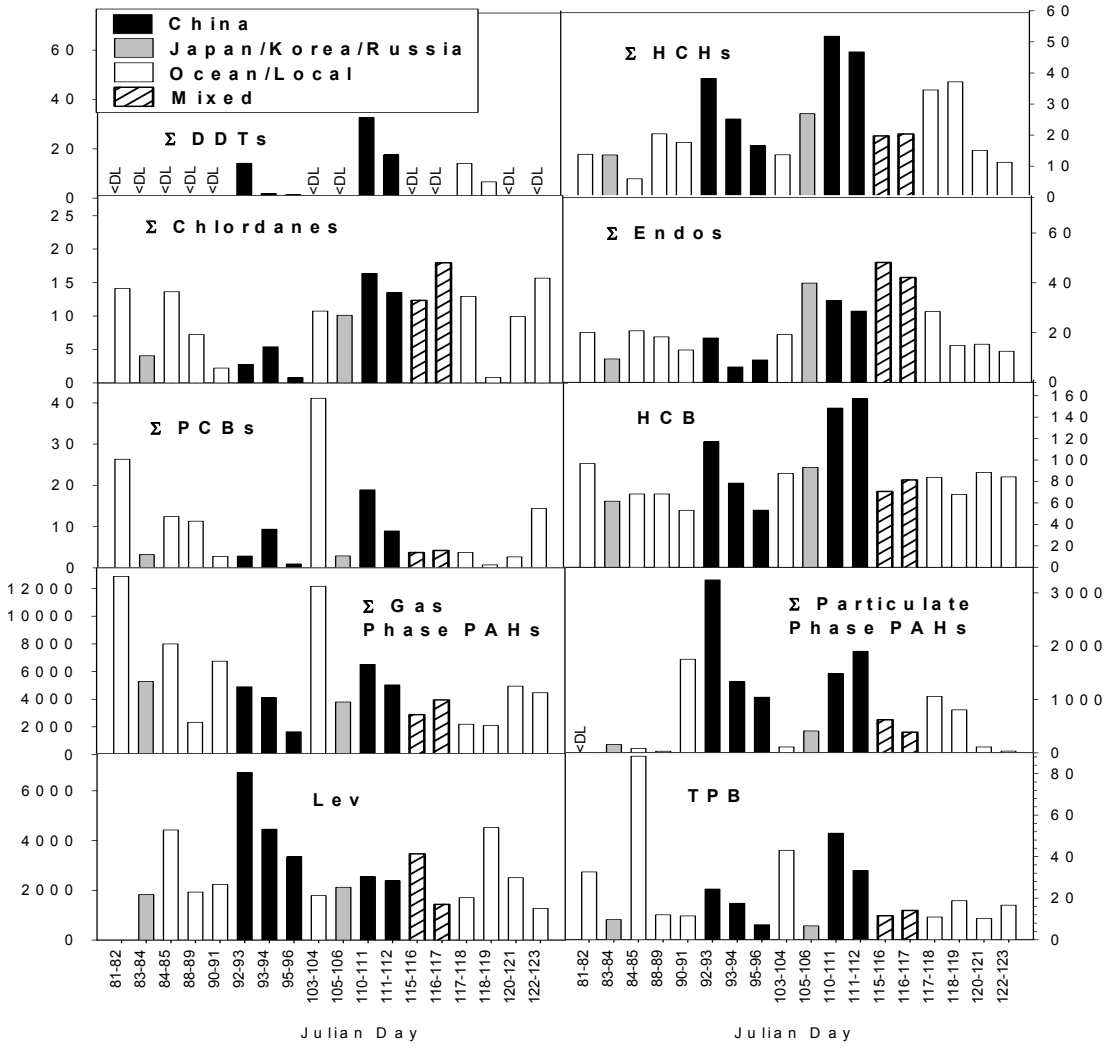

Figure 3.4: Temporal concentrations (pg/m^3) of Σchlordanes, HCB, ΣDDTs, ΣHCHs, ΣEndos, ΣPCBs, Σparticulate-phase PAHs, Σgas-phase PAHs, TPB, and Lev. Bars are labeled to indicate source region. <DL indicates below the method detection limit. Lev could not be quantified in day 81-82 sample due to interferences.

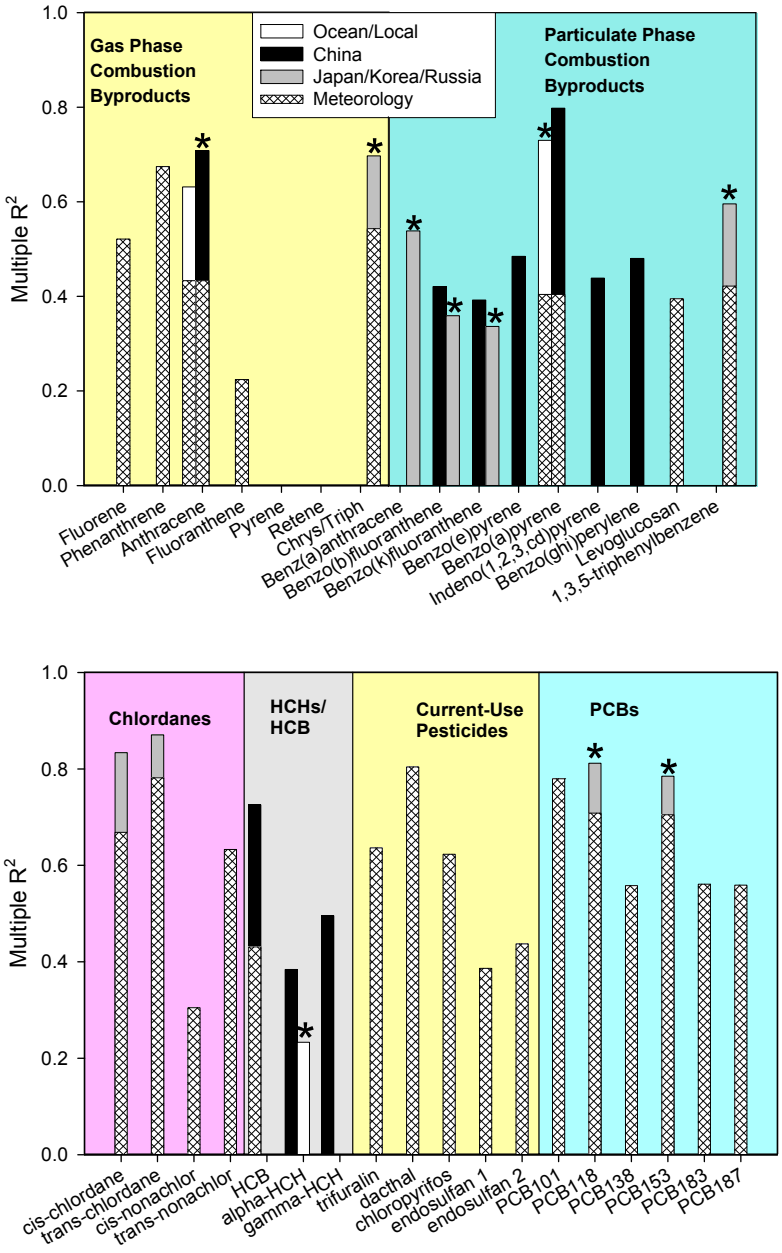

Figure 3.5: Results of multivariable linear regression model accounting for meteorological variables only (checkered) and SRIF (solid color bars). A star indicates the slope for the source term was negative, indicating decreasing SOC concentrations with increasing SRIF. Multiple bars indicate that, after accounting for meteorological variability, the SRIF was evaluated in the meteorological model separately due to multicolinearity between SRIFs.

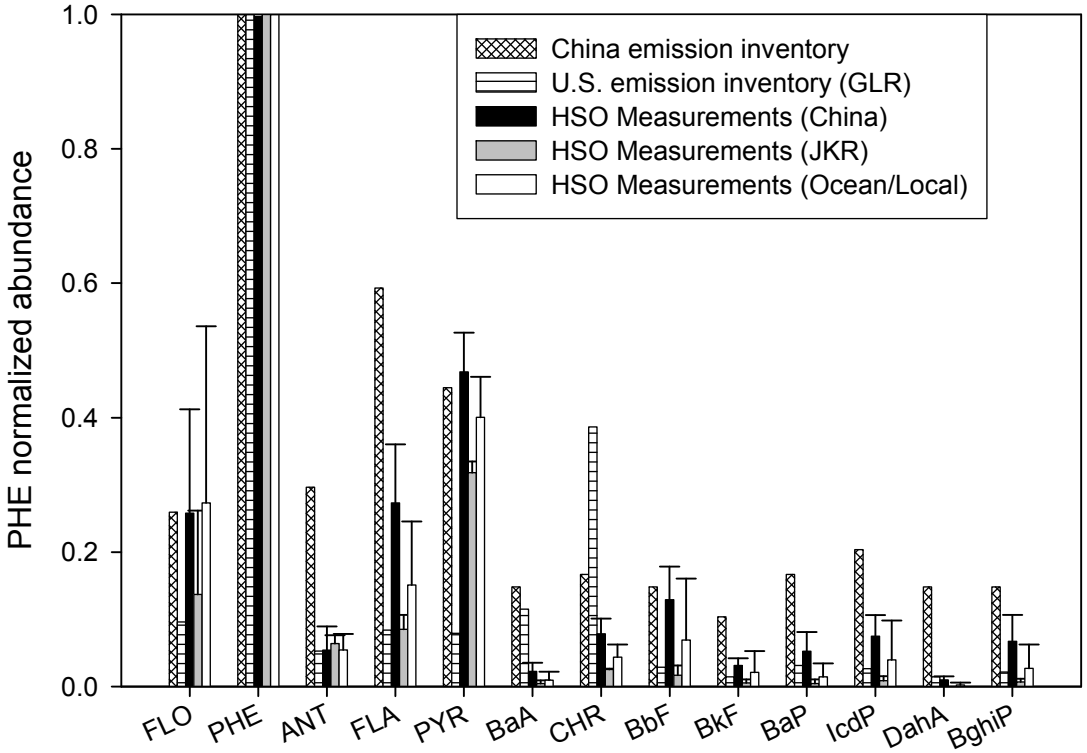

Figure 3.6: PAH profile (normalized to PHE) measured at HSO from China, Japan/Korea/Russia, and Ocean/Local source regions compared with Xu et al. PAH emission inventory for China (*20*). Also included is the profile of PAHs from the emission inventory for the Great Lakes Region, U.S. (*21*) Note that the HSO measurements for CHR also include Triphenylene, whereas the inventories represent CHR only. Additionally the Chinese inventory did not include BeP so no comparison could be made.

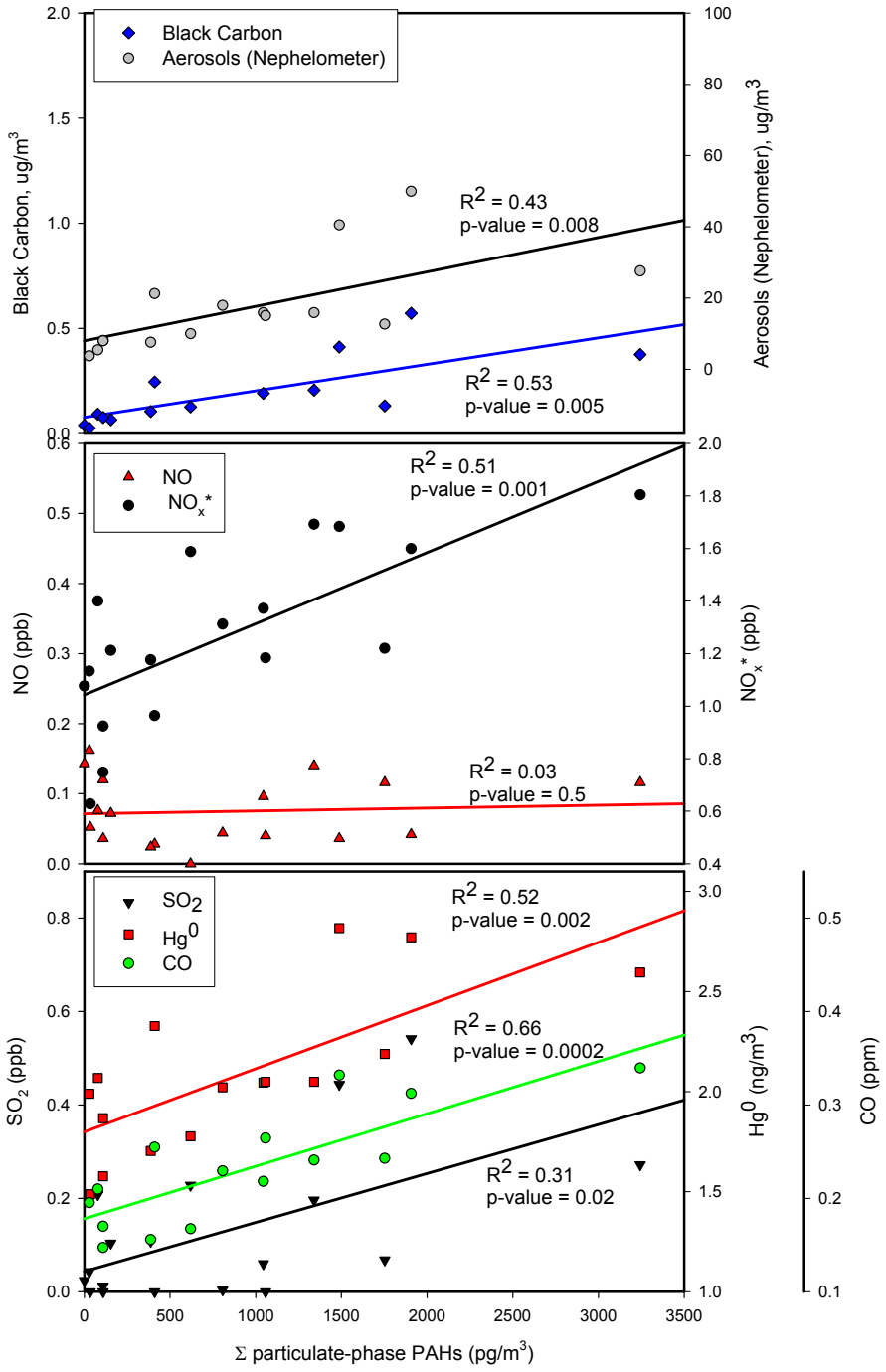

Figure 3.7: Correlation of the Σ particulate-phase PAH concentration with concurrent BC, submicron aerosols (nephelometer), SO_2, NO, NO_x*, CO and Hg^0 concentrations. The particulate-phase PAH concentrations are 24 hour averages (24 hour samples) while the concentrations of the other compounds were measured hourly but were averaged over the same 24 hour time period.

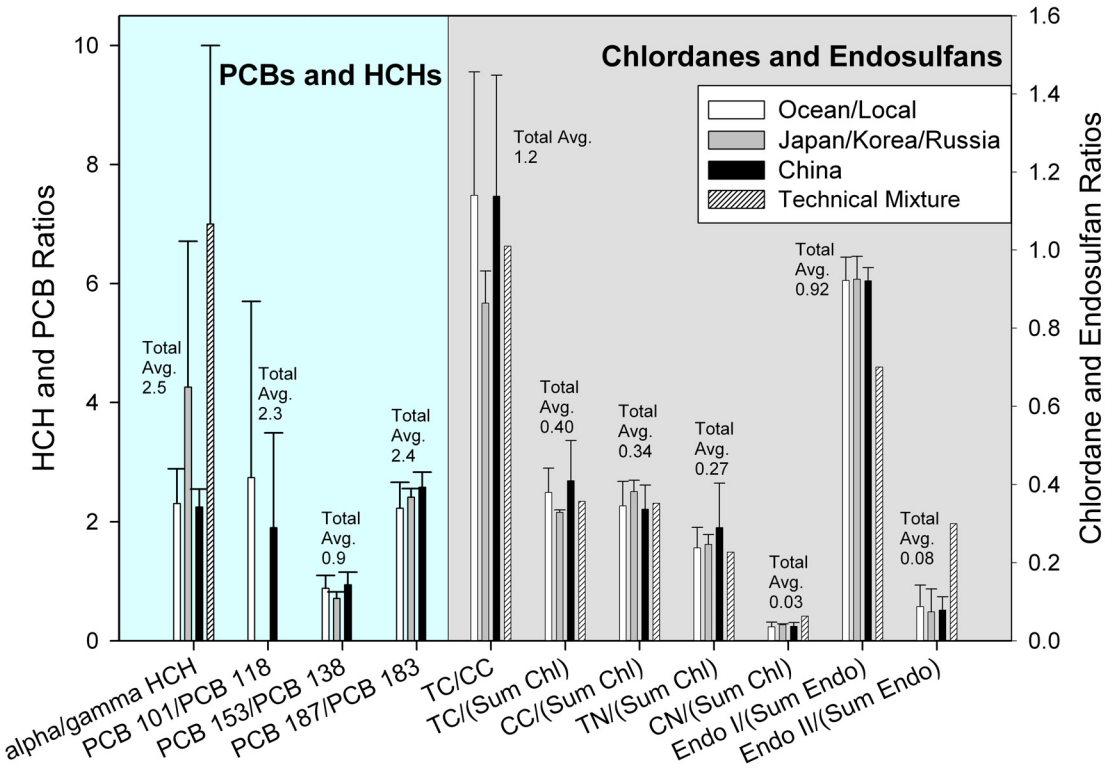

Figure 3.8: Average SOC concentration ratios and technical mixture ratios for the three source regions (China, Ocean/Local, and Japan/Korea/Russia). PCB 101 was not detected in the samples associated with the Japan/Korea/Russia source region. Total avg. is the average of all 18 samples.

Table 3.1: HSO sample and meteorological data (average ± standard deviation) for the sampled days with source region impact factors (SRIFs). PCA of the SRIFs was used to cluster the samples and designate the source regions as Ocean/Local, China, Japan/Korea/Russia (J/K/R), and Mixed (not falling into one of the other PCA categories). The sample numbers with (*) had measurable concentrations of metribuzin, a current use pesticide on Okinawa. The sum of precipitation (Σppt) was calculated using the HYSPLIT model for an air parcel in transit, 4 days back. Approximately 644 m^3 of air was sampled in the 24 hour sampling period.

Sample #	Sampled Days, GMT	Julian Day	Sampled Hours	Wind Dir., Deg.	WS, m/s	Temp., °C	Σppt., mm/hr	Ocean, SRIF%	Japan, SRIF%	Korea, SRIF%	China, SRIF%	Russia, SRIF%	Source (from PCA)
1	21-22 Mar	81-82	24	255 ± 94	4.8 ± 2.3	20.1 ± 1.7	13.3 ± 6.2	84.2	5.5	3.3	6.4	0.6	Ocean/Local
2	22-23 Mar	83-84	24	124 ± 151	4.7 ± 1.3	18.1 ± 1.1	15.6 ± 7.3	55.1	35.7	3.1	6.1	0	J/K/R
3	24-25 Mar	84-85	24	140 ± 91	2.7 ± 1.7	20.0 ± 1.0	16.3 ± 7.7	97.8	1.3	0	0.1	0.7	Ocean/Local
4	28-29 Mar	88-89	24	104 ± 11	7.7 ± 1.5	19.6 ± 1.1	13.8 ± 7.0	91.8	6.7	0.6	0.7	0.1	Ocean/Local
5	30-31 Mar	90-91	24	302 ± 92	5.9 ± 0.8	20.0 ± 0.9	2.5 ± 5.4	87.5	2.1	1.2	5.4	3.9	Ocean/Local
6	1-2 Apr	92-93	24	230 ± 137	6.5 ± 2.1	19.0 ± 1.5	3.4 ± 2.7	46.7	0	1	48.1	4.2	China
7	2-3 Apr	93-94	24	90 ± 34	4.1 ± 1.3	17.0 ± 1.5	2.7 ± 1.6	35.1	0	0	43.6	21.3	China
8	4-5 Apr	95-96	24	232 ± 157	6.7 ± 1.4	16.5 ± 1.5	0.7 ± 0.9	38.5	0	12.2	43.9	5.4	China
9*	12-13 Apr	103-104	24	139 ± 54	3.3 ± 1.7	22.1 ± 2.7	0.8 ± 1.3	100	0	0	0	0	Ocean/Local
10	14-15 Apr	105-106	24	158 ± 169	5.2 ± 1.4	22.1 ± 1.2	2.7 ± 2.4	61.6	38.4	0	0	0	J/K/R
11	19-20 Apr	110-111	24	234 ± 53	2.1 ± 0.6	21.2 ± 2.9	4.4 ± 6.0	59.7	0	0	40.3	0	China
12	20-21 Apr	111-112	24	224 ± 88	2.0 ± 0.5	22.1 ± 2.5	3.5 ± 4.5	38.8	0	0	61.2	0	China
13	24-25 Apr	115-116	24	44 ± 20	5.2 ± 2.1	20.0 ± 1.3	2.0 ± 2.8	33	2.1	13.8	19.6	31.4	Mixed
14*	25-26 Apr	116-117	24	121 ± 19	5.3 ± 1.0	21.4 ± 1.6	7.3 ± 8.4	57.7	5.2	4.8	25	7.3	Mixed
15	26-27 Apr	117-118	17	234 ± 63	6.5 ± 1.4	22.3 ± 2.5	11.7 ± 9.3	78.7	3.3	3.4	14.6	0	Ocean/Local
16	27-28 Apr	118-119	24	340 ± 15	6.5 ± 1.5	17.9 ± 1.1	10.5 ± 5.9	71.3	0	12.6	16.1	0	Ocean/Local
17*	29-30 Apr	120-121	24	130 ± 15	3.6 ± 1.0	20.7 ± 2.4	1.5 ± 1.5	75.3	5.8	2.8	8	8	Ocean/Local
18*	1-2 May	122-123	24	139 ± 25	5.2 ± 2.0	23.7 ± 1.3	1.4 ± 1.8	96	3.6	0	0	0.4	Ocean/Local

Table 3.2: Significant (p-value < 0.05) meteorological variables, shown as β values (slope), taken into account in the best meteorological subset model. Part A shows the combustion byproduct results, part B shows the PCB results, and part C shows the results for the pesticides. The Cp statistic was used to select the variables for each model, and the model with the lowest Cp-statistic was used. If the variables slope had a p-value < 0.05 it is shown below. NS means the parameter was left in the model but it had a p-value > 0.05. The best meteorological subset models shown below were determined to be equivalent to the full model (equation 2) using the Cp-statistic.

A

Comb. Prod.	JD, GMT	WS, m/s	Sun, cal/(cm^{2}h)	WD cos avg deg.	WD sin avg deg.	ppt, mm/h	1000/T, K-1	R^2
FLO	NS		-1.274			NS	-0.086	0.52
PHE	-0.026	-0.215					-0.050	0.67
ANT	-0.028							0.43
FLA		-0.146						0.22
PYR	-0.022	-0.249					-0.041	
Ret	-0.033	-0.251					-0.057	
BaA Chry/ Trip	-0.021	-0.239						0.54
BbF BkF BeP BaP I123cdP BghiP						-0.596		0.40
Lev							0.055	0.39
TPB		-0.282						0.42

B

PCBs	JD, GMT	WS, m/s	Sun, cal/(cm^{2}h)	WD cos avg deg.	WD sin avg deg.	ppt, mm/h	1000/T, K-1	R^2
PCB 101					-3.470	-1.253	-0.310	0.78
PCB 118	-0.031	-0.268					-0.064	0.71
PCB 138	-0.036	-0.255					-0.110	0.56
PCB 153	-0.034	-0.298					-0.085	0.70
PCB 183	NS	-0.304					NS	0.56
PCB 187	-0.045	-0.343					NS	0.56

(Continued)

C

Pests.	JD, GMT	WS, m/s	Sun, cal/(cm^{2}h)	WD cos avg deg.	WD sin avg deg.	ppt, mm/h	1000/T, K-1	R^2
c-chlor		-0.148				NS	-0.087	0.67
t-chlor	NS	-0.191				NS	-0.109	0.78
c-nona						NS	-0.063	0.30
t-nona	0.042	-0.192				0.358		0.63
HCB		-0.018					NS	0.43
α-HCH								
γ-HCH								
trif	0.009	0.009					0.039	0.64
dacthal	-0.064		NS				-0.136	0.80
chlorop	-0.037	-0.300					-0.082	0.62
endo 1							-0.071	0.39
endo 2			NS		0.616	0.448		0.44

Table 3.3: Calculated emissions (metric tons/year) of PAHs from Asia based on spring 2004 measurements at HSO. Emission values were calculated using CO measurements at HSO and CO inventories (left) and BC measurements at HSO and a BC inventory (right). The PAHs labeled with (*) indicates it is one of the six carcinogenic PAHs (21) summed. G represents a PAH primarily measured in the gas phase, while P represents PAHs primarily measured in the particulate phase.

Analyte	Emissions Asia (using CO)	Emissions China (using CO)	p-value	R^2	Emissions Asia (using BC)	Emissions China (using BC)	p-value	R^2
FLA (G)	684	351	0.007	0.44	2111	873	0.05	0.28
BaA* (P)	99	51	0.02	0.56	239	99	0.08	0.38
CT* (G/P)	210	107	0.04	0.29	572	237	0.2	0.13
BbF* (P)	490	251	0.0005	0.72	1456	602	0.02	0.51
BkF* (P)	117	60	0.001	0.71	332	137	0.01	0.60
BeP (P)	246	126	0.0006	0.71	797	329	0.01	0.58
BaP* (P)	289	148	0.004	0.61	683	282	0.04	0.47
IcdP* (P)	313	161	0.0002	0.70	897	371	0.009	0.51
BghiP (P)	300	154	0.001	0.61	842	348	0.03	0.41

Literature Cited

(1) Wilkening, K. E.; Barrie, L. A.; Engle, M. Atmospheric science - Trans-Pacific air pollution *Science* **2000**, *290*, 65-67.

(2) Killin, R. K.; Simonich, S. L.; Jaffe, D. A.; DeForest, C. L.; Wilson, G. R. Transpacific and regional atmospheric transport of anthropogenic semivolatile organic compounds to Cheeka Peak Observatory during the spring of 2002 *J Geophys Res-Atmos* **2004**, *109*, D23S15.

(3) Harner, T.; Shoeib, M.; Kozma, M.; Gobas, F. A. P. C.; Li, S. M. Hexachlorocyclohexanes and endosulfans in urban, rural, and high altitude air samples in the Fraser Valley, British Columbia: Evidence for trans-Pacific transport *Environ Sci Technol* **2005**, *39*, 724-731.

(4) Jaffe, D.; Bertschi, I.; Jaegle, L.; Novelli, P.; Reid, J. S.; Tanimoto, H.; Vingarzan, R.; Westphal, D. L. Long-range transport of Siberian biomass burning emissions and impact on surface ozone in western North America *Geophys Res Lett* **2004**, *31*, L16106.

(5) Jaffe, D.; Anderson, T.; Covert, D.; Kotchenruther, R.; Trost, B.; Danielson, J.; Simpson, W.; Berntsen, T.; Karlsdottir, S.; Blake, D.; Harris, J.; Carmichael, G.; Uno, I. Transport of Asian air pollution to North America *Geophys Res Lett* **1999**, *26*, 711-714.

(6) Bailey, R.; Barrie, L. A.; Halsall, C. J.; Fellin, P.; Muir, D. C. G. Atmospheric organochlorine pesticides in the western Canadian Arctic: Evidence of transpacific transport *J Geophys Res-Atmos* **2000**, *105*, 11805-11811.

(7) Usenko, S.; Hageman, K. J.; Schmedding, D. W.; Wilson, G. R.; Simonich, S. L. Trace analysis of semivolatile organic compounds in large volume samples of snow, lake water, and groundwater *Environ Sci Technol* **2005**, *39*, 6006-6015.

(8) Kato, S.; Kajii, Y.; Itokazu, R.; Hirokawa, J.; Koda, S.; Kinjo, Y. Transport of atmospheric carbon monoxide, ozone, and hydrocarbons from Chinese coast to Okinawa island in the Western Pacific during winter *Atmospheric Environment* **2004**, *38*, 2975-2981.

(9) Kanaya, Y.; Sadanaga, Y.; Nakamura, K.; Akimoto, H. Behavior of OH and HO2 radicals during the Observations at a Remote Island of Okinawa (ORION99) field campaign 1. Observation using a laser-induced fluorescence instrument *J Geophys Res-Atmos* **2001**, *106*, 24197-24208.

(10) Jaffe, D.; Prestbo, E.; Swartzendruber, P.; Weiss-Penzias, P.; Kato, S.; Takami, A.; Hatakeyama, S.; Kajii, Y. Export of atmospheric mercury from Asia *Atmospheric Environment* **2005**, *39*, 3029-3038.

(11) Simoneit, B. R. T.; Elias, V. O.; Kobayashi, M.; Kawamura, K.; Rushdi, A. I.; Medeiros, P. M.; Rogge, W. F.; Didyk, B. M. Sugars-Dominant Water-Soluble Organic Compounds in Soils and Characterization as Tracers in Atmospheric Particulate Matter *Environ Sci Technol* **2004**, *38*, 5939-5949.

(12) Method 8280A, E.P.A. The analysis of polychlorinated dibenzo-p-dioxins and polychlorinated dibenzofurans by high-resolution gas chromatography/low resolution mass spectrometry (HRGC/LRMS). http://www.epa.gov/epaoswer/hazwaste/test/pdfs/8280a.pdf

(13) Draxler, R. R.; Rolph, G. D. HYSPLIT (HYbrid Single-Particle Lagrangian Integrated Trajectory) Model access via NOAA ARL READY Website (http://www.arl.noaa.gov/ready/hysplit4.html). NOAA Air Resources Laboratory, Silver Spring, MD. **2003**.

(14) Wotawa, G.; Kroger, H.; Stohl, A. Transport of ozone towards the Alps - results from trajectory analyses and photochemical model studies *Atmospheric Environment* **2000**, *34*, 1367-1377.

(15) Hafner, W. D.; Hites, R. A. Effects of wind and air trajectory directions on atmospheric concentrations of persistent organic pollutants near the great lakes *Environ Sci Technol* **2005**, *39*, 7817-7825.

(16) Burgoyne, T. W.; Hites, R. A. Effects of Temperature and Wind Direction on the Atmospheric Concentrations of alpha-Endosulfan *Environ Sci Technol* **1993**, *27*, 910-914.

(17) Goel, A.; McConnell, L. L.; Torrents, A.; Scudlark, J. R.; Simonich, S. Spray irrigation of treated municipal wastewater as a potential source of atmospheric PBDEs *Environ Sci Technol* **2006**, *40*, 2142-2148.

(18) Ramsey, F.; Schafer, D. W. *The Statistical Sleuth*; Duxbury: Pacific Grove, CA, 2002.

(19) Simoneit, B. R. T.; Medeiros, P. M.; B.M., D. Combustion Products of Plastics as Indicators for Refuse Burning in the Atmosphere *Environ Sci Technol* **2005**, *39*, 6961-6970.

(20) EPISuite; v3.12 ed.; U.S. EPA: Washington, DC, 2000.

(21) Simoneit, B. R. T.; Kobayashi, M.; Mochida, M.; Kawamura, K.; Lee, M.; Lim, H. J.; Turpin, B. J.; Komazaki, Y. Composition and major sources of organic compounds of aerosol particulate matter sampled during the ACE-Asia campaign *J Geophys Res-Atmos* **2004**, *109*, -.

(22) Xu, S.; Liu, W.; Tao, S. Emission of Polycyclic Aromatic Hydrocarbons in China *Environ Sci Technol* **2006**, *40*, 702-708.

(23) Wu, C. Y.; Nelson, C.; Cabrera-Rivera, O.; Quan, J.; Asselmeier, D.; Baker, G.; McGeen, D. M.; McDonough, R.; Sliwinski, R.; Altenburg, R.; Velalis, T.; Judson, H.; Wong, P.; Wagemakers, J.; Moy, D. *Analysis of Air Toxics Emission Inventories for Area Sources in the Great Lakes Region*; U.S. Environmental Protection Agency: Washington, DC, 2001.

(24) Simcik, M. F.; Eisenreich, S. J.; Lioy, P. J. Source apportionment and source/sink relationships of PAHs in the coastal atmosphere of Chicago and Lake Michigan *Atmospheric Environment* **1999**, *33*, 5071-5079.

(25) Larsen, R. K.; Baker, J. E. Source apportionment of polycyclic aromatic hydrocarbons in the urban atmosphere: A comparison of three methods *Environ Sci Technol* **2003**, *37*, 1873-1881.

(26) UNEP "Regionally Based Assessment of Persistent Toxic Substances; Central and North East Asia," UNEPChemicals: Chaˆtelaine, GE, Switzerland, 2002.

(27) Mai, B. X.; Zeng, E. Y.; Luo, X. J.; Yang, Q. S.; Zhang, G.; Li, X. D.; Sheng, G. Y.; Fu, J. M. Abundances, depositional fluxes, and homologue patterns of polychlorinated biphenyls in dated sediment cores from the Pearl River Delta, China *Environ Sci Technol* **2005**, *39*, 49-56.

(28) Jaward, T. M.; Zhang, G.; Nam, J. J.; Sweetman, A. J.; Obbard, J. P.; Kobara, Y.; Jones, K. C. Passive air sampling of polychlorinated biphenyls, organochlorine compounds, and polybrominated diphenyl ethers across Asia *Environ Sci Technol* **2005**, *39*, 8638-8645.

(29) Wikstrom, E.; Persson, A.; Marklund, S. Secondary Formation of PCDDs, PCDFs, PCBs, PCBzs, PCPhs, and PAHs during MSW combustion *Organohalogen Compounds* **1998**, *36*, 65-68.

(30) Bailey, R. E. Global hexachlorobenzene emissions *Chemosphere* **2001**, *43*, 167-182.

(31) Yeo, H. G.; Choi, M.; Sunwoo, Y. Seasonal variations in atmospheric concentrations of organochlorine pesticides in urban and rural areas of Korea *Atmospheric Environment* **2004**, *38*, 4779-4788.

(32) Li, Y. F.; Cai, D. J.; Singh, A. Technical hexachlorocyclohexane use trends in China and their impact on the environment *Arch Environ Con Tox* **1998**, *35*, 688-697.

(33) Tao, S.; Xu, F. L.; Wang, X. J.; Liu, W. X.; Gong, Z. M.; Fang, J. Y.; Zhu, L. Z.; Luo, Y. M. Organochlorine pesticides in agricultural soil and vegetables from Tianjin, China *Environ Sci Technol* **2005**, *39*, 2494-2499.

(34) Qiu, X. H.; Zhu, T.; Yao, B.; Hu, J. X.; Hu, S. W. Contribution of dicofol to the current DDT pollution in China *Environ Sci Technol* **2005**, *39*, 4385-4390.

(35) Qiu, X. H.; Zhu, T.; Jing, L.; Pan, H. S.; Li, Q. L.; Miao, G. F.; Gong, J. C. Organochlorine pesticides in the air around the Taihu Lake, China *Environ Sci Technol* **2004**, *38*, 1368-1374.

(36) Hung, H.; Blanchard, P.; Halsall, C. J.; Bidleman, T. F.; Stern, G. A.; Fellin, P.; Muir, D. C. G.; Barrie, L. A.; Jantunen, L. M.; Helm, P. A.; Ma, J.; Konoplev, A. Temporal and spatial variabilities of atmospheric polychlorinated biphenyls (PCBs), organochlorine (OC) pesticides and polycyclic aromatic hydrocarbons (PAHs) in the Canadian Arctic: Results from a decade of monitoring *Sci Total Environ* **2005**, *342*, 119-144.

(37) Dearth, M. A.; Hites, R. A. Complete Analysis of Technical Chlordane Using Negative Ionization Mass Spectrometry *Environ Sci Technol* **1991**, *25*, 245-254.

(38) Mackay, D.; Shiu, W. Y.; Ma, K. C. *Physical-Chemical Properties and Environmental Fate*; Chapman and Hall/CRCnetBase: Boca Raton, FL, 2000.

(39) Streets, D. G.; Bond, T. C.; Carmichael, G. R.; Fernandes, S. D.; Fu, Q.; He, D.; Klimont, Z.; Nelson, S. M.; Tsai, N. Y.; Wang, M. Q.; Woo, J.-H.; Yarber, K. F. An inventory of gaseous and primary aerosol emissions in Asia in the year 2000 *J Geophys Res-Atmos* **2003**, *108*, 8809.

(40) "Technology Transfer Network National Air Toxics Assessment," U.S. Environmental Protection Agency, 2001.

CHAPTER 4. INFLUENCE OF ASIAN AND WESTERN U.S. URBAN AREAS AND FIRES ON THE ATMOSPHERIC TRANSPORT OF PAHS, PCBS, AND FTOHS IN THE WESTERN U.S.

Toby Primbs[1], Arkadiusz Piekarz[1], Glenn Wilson[2], David Schmedding[2], Carol Higginbotham[3], Jennifer Field[2], and Staci Simonich[1,2*]

[1]Department of Chemistry, Oregon State University, Corvallis, Oregon
[2]Department of Environmental and Molecular Toxicology, Oregon State University, Corvallis, Oregon
[3]Department of Science, Central Oregon Community College, Bend, Oregon

*Corresponding Author: Telephone, 1-541-737-9194; Fax, 1-541-737-0497; email, staci.simonich@oregonstate.edu

Abstract

Atmospheric measurements of anthropogenic semivolatile organic compounds (SOCs) were made at Mt. Bachelor Observatory (MBO) in Oregon's Cascade Range to understand the trans-Pacific and regional transport of SOCs from urban areas. High volume air sampling (~644 m^3 for 24 hour periods) of both the gas and particulate phases was conducted from the 19th of April 2004 to the 13th of May 2006 (n=69); of which NASA's INTEX-B campaign was in spring 2006 (n= 34 of 69). Air mass back trajectories were calculated and used to calculate source region impact factors (SRIFs), the percentage of time the sampled air mass resided in a given source region. Particulate-phase polycyclic aromatic hydrocarbon (PAH) concentrations at MBO increased with the percentage of air mass time in Asia and, in conjunction with other data, provided strong evidence that particulate-phase PAHs are emitted from Asia and are transported to North America. Gas-phase PAH and fluorotelomer alcohol (FTOH) concentrations significantly increased with the percentage of air mass time in California's urban areas, while retene and polychlorinated biphenyl (PCB) concentrations increased with the percentage of air mass time in Oregon and in areas impacted by regional fire events. In addition, gas-phase PAH, retene, and levoglucosan concentrations were significantly correlated (p-value < 0.001) with PCB concentrations, suggesting increased atmospheric PCB concentrations were associated with fires due to the volatilization of stored PCBs from soil and vegetation. The emissions of individual FTOHs from urban areas in the Western U.S. were estimated at 15 to 309 kg/year and the emissions of individual gas-phase PAHs were estimated at 217 to 4648 kg/year.

Introduction

The trans-Pacific atmospheric transport of some semivolatile organic compounds (SOCs) and incomplete combustion byproducts (such as CO and Hg^0) from Asian source regions to the Western U.S. has been documented *(1-6)*. In addition, the atmospheric outflow of polychlorinated biphenyls (PCBs), polycyclic aromatic hydrocarbons (PAHs), and fluorotelomer alcohols (FTOHs) from East Asia has recently been reported *(7,8)*. Coupling these outflow measurements with analogous measurements on the U.S. West Coast provides a better understanding of the trans-Pacific atmospheric transport of SOCs and the atmospheric chemistry in transit.

Anthropogenic SOCs can serve as molecular markers for Asian and North American source regions because of their specificity in source and their wide range of physical-chemical properties *(4,8)*. Combustion sources in urban areas are thought to be the dominant source of PAHs to the atmosphere in North America *(9)*. Levoglucosan, retene, and 1,3,5-triphenylbenzene have been used as specific markers for the combustion of biomass, wood, and plastics, respectively *(10-12)*. Historically, PCBs were used as plasticizers, nonflammable transformer dielectric and heat exchange fluids in industrial and urban settings, with major restrictions and prohibitions occurring in the late 1970s in Europe and the U.S. *(13)*. In addition to emissions of PCBs from historical sources, combustion processes, such as low temperature incineration, can release stored PCBs present in refuse and/or form PCBs from carbon and chlorine *(13)*. FTOHs, which are used as precursors in the synthesis of polymers, adhesives, and stain and water-resistant

products, are released to the atmosphere from commercial products and/or manufacturing *(7)*.

Previous studies investigating the trans-Pacific atmospheric transport of SOCs to the West Coast of North America have focused primarily on organochlorine pesticides *(2-4)*. However, due to the rapid industrialization of China, significant concentrations of carcinogenic PAHs, which have the potential to undergo long-range atmospheric transport, exist in Asian air masses *(8,14,15)*. To date, research on the trans-Pacific atmospheric transport of PCBs and PAHs to the West Coast of the U.S. has been limited to a site located in the marine boundary layer *(4)*.

Urban areas in the Western U.S. also have the potential to emit SOCs. For example, PCBs and FTOHs have been reported to originate from urban areas in the U.S. *(7,16)*. In addition, PAH concentrations have been shown to correlate with human population in North America *(9,16)*. Because high elevation sites in the Western U.S. are in the free troposphere more frequently than lower elevation sites, they allow for more conclusive identification of trans-Pacific atmospheric transport events *(1,5,6)*. In addition, mid-latitude, Western U.S. mountains serve as local areas of convergence for SOCs *(17,18)*.

The primary objectives of this research were to: (1) measure PCBs and incomplete combustion byproducts (PAHs, levoglucosan, and 1,3,5-triphenylbenzene) in trans-Pacific and regional air masses at a remote mountain top located on the U.S. West Coast; (2) identify source regions for PAHs, PCBs, levoglucosan, 1,3,5-triphenylbenzene,

and FTOHs; and (3), where possible, estimate the emissions of these SOCs from source regions.

Experimental

Chemicals

The semivolatile organic compounds (SOCs) detected in this study included *PAHs*: fluorene (FLO), anthracene (ANT), phenanthrene (PHE), fluoranthene (FLA), pyrene (PYR), retene (RET), benz[a]anthracene (BaA), chrysene/triphenylene (CT), benzo[b]fluoranthene (BbF), benzo[k]fluoranthene (BkF), benzo[e]pyrene (BeP), benzo[a]pyrene (BaP), indeno[1,2,3-cd]pyrene (IcdP), dibenz[a,h]anthracene (DahA), and benzo[ghi]perylene (BghiP); *Misc. Combustion Byproducts*: 1,3,5-triphenylbenzene, and levoglucosan; *PCBs*: PCB 101, PCB 118, PCB 153, PCB 138, PCB 187, and PCB 183; and *fluorotelomer alcohols*: 6:2-FTOH, 8:2-FTOH, and 10:2-FTOH. Targeted analytes not detected included: PCB 74, acenapthene, and acenapthylene. A list of isotopically labeled standards used for quantification and the extraction solvents have been previously reported *(8,19)*.

Sampling Site

The sampling site, Mt. Bachelor Observatory (MBO) (43.98°N 121.69°W, 2763 m above sea level), is located in Oregon's Cascade Range in the Pacific Northwest of the United States and is approximately 180 km east of the Pacific Ocean (Figure 4.1). MBO was established to conduct research on trans-Pacific and regional atmospheric transport *(1,5,6,20)*. The air sampling station is located on the summit of the mountain and is accessed via electrically powered ski lifts. Simultaneous measurements of submicron

aerosols (nephelometer), reactive gaseous mercury, particulate-phase mercury, elemental mercury, CO, O_3, Rn, meteorology, and water vapor at MBO were conducted by the Jaffe Group (University of Washington-Bothell) *(1,5,6,20)*.

Sample Collection and Extraction

Sixty-nine SOC air samples were collected from the 19th of April 2004 to the 13th of May 2006 at MBO using a modified high volume air sampler (Tisch Environmental, Cleves, OH) over 24 hour periods (~644 m^3); of which NASA's INTEX-B campaign was in spring 2006 (n= 34 of 69) (Figure 4.1). The sampling flow rate (~0.4 m^3/min) was recorded before and after each sample and an inline exhaust anemometer was used to ensure constant flow over the sampling period. Previously baked (12 hours at 350°C) quartz fiber filters (Whatman, England) were used to collect the particulate phase. Previously Accelerated Solvent Extraction (ASE®) 300 (Dionex, California) cleaned polyurethane foam (1½ " x 3 ")-(XAD-2)-polyurethane foam (1½ " x 3 ") sandwich (Tisch Environmental, Ohio; Supelco, Pennsylvania) were used to collect the gas-phase SOCs. Cleaning and extraction procedures have been previously reported in detail *(8)*.

The sampling media were transported to the sampling site on ice and stored in a freezer at the summit. After sampling, the used media was stored frozen and transported back to the lab on ice. Just prior to extraction, samples were brought to room temperature in sealed containers. Prior to ASE extraction QFFs, XAD-2, and PUF were fortified with 15 µL of a ~10 ng/µL isotopically labeled standard solution. ASE extraction conditions for the QFF, PUF and XAD-2 have been described elsewhere *(8,21)*. Following extraction on the ASE, samples were concentrated to 300 µL with a combination of a

Turbovap II (Caliper Life Sciences, Massachusetts) and a micro pre-purified N_2 stream concentrator. Derivatization of levoglucosan for GC analysis has been previously described in detail *(8,22)*, and consisted of drying 20 µL of the sample extract under a gentle stream of N_2, followed by addition of pyridine and BSTFA (bis-(trimethylsilyl)trifluoroacetamide) to the dried extract and a three hour reaction time at 70 °C.

Sample Analysis

Sample analysis was conducted with gas chromatographic mass spectrometry (GC/MS) in selective ion monitoring (SIM) mode with both negative chemical ionization (NCI) and electron impact (EI) ionization modes *(8,19)*. Instrumental limits of detection for PAHs and PCBs ranged from 0.01 to 0.73 pg/µL *(19)*. Limits of quantification, defined as the lowest standard used in the calibration curves, ranged from 0.25 to 50 pg/µL *(8)*. Estimated method detection limits, calculated with EPA method 8280A, ranged from 0.11 to 31 pg/m^3 for the GC/MS-EI and 0.05 to 6.4 pg/m^3 for the GC/MS-NCI *(8,23)*. Only peaks with signals three times the peak to peak noise were reported. Details of all quantifying and qualifying ions monitored have been previously reported for the fluorotelomer alcohols *(7)*, levoglucosan and 1,3,5-triphenylbenzene *(8)*, and all other targeted analytes *(19)*. All target analytes were quantified from isotopically labeled internal standards (surrogates) added prior to extraction (recovery-corrected) *(8,19)*.

Quality assurance and control for the FTOHs have been previously reported *(7)*. Recoveries of PAHs, 1,3,5-triphenylbenzene, and PCBs ranged between 49 to 114% over the entire analytical method *(21)*. Thirteen field blanks, consisting of sampling media

(QFF, XAD-2, and PUF) installed in the sampler with the motor off, were collected. Gas-phase PAHs (fluorene, phenanthrene, anthracene, fluoranthene, pyrene, and retene) and PCBs (PCB 118, PCB 153, PCB 138, PCB 187, and PCB 183) were detected in field blanks above the quantitation limit. For these SOCs, the limits of detection were defined as the average field blank concentration (n=13), plus three times the standard deviation *(3)*. SOC concentrations were blank corrected. The bottom PUF plug was used to assess if breakthrough occurred and was analyzed separately in 50% of the samples. The percentage of SOC concentration measured on the bottom PUF plug to the total gas-phase concentration ranged between 8 to 35% and no correction for breakthrough was made.

Trajectories and Data Analysis

Ten-day air mass back trajectories were calculated using NOAA's ARL HYSPLIT 4.0 model (FNL) *(24)*. Back trajectories were calculated at three elevations above model ground level (1300, 1500, and 1700 m). These three elevations were used because HYSPLIT calculates the height of MBO to be ~1400 m above model ground level *(20)*. The trajectories were calculated every three hours over the twenty-four hour sampling period (including the start and stop time) for a total of 27 trajectories per sample. Trajectories were imported into ArcGIS (ESRI, Redlands, California) for spatial representation and S-PLUS version 7.0 (Insightful, Seattle, Washington) was used for statistical analysis. Hazard mapping system (HMS) fire and smoke layers were provided by NOAA's National Geophysical Data Center and the National Environmental Satellite, Data, and Information Services *(25)*.

Results

Identification of Air Mass Source Regions

The sampling dates, site temperature, wind speed, and wind direction for the sixty-nine samples collected are listed in Table 4.1. Thirty-five air samples were initially collected over the first two year sampling period (April 2004 to March 2006) and an additional thirty-four samples were collected in spring 2006 (April-May 2006) in conjunction with Intercontinental Transport Experiment (INTEX-B) *(26)*. Access to the site was limited at times due to lift maintenance and extreme weather. The predominant wind direction on the days samples were collected was from the west-northwest and west (Figure 4.2).

To assess the influences of various source regions, back trajectories were used to calculate source region impact factors (SRIFs) *(8)*. SRIFs indicate the percentage of time an air mass has spent in a given source region as compared to the total trajectory time (ten days). Details of the calculation are reported elsewhere *(8)*. Because both urban areas and fires have the potential to result in increased PAH, PCB, and FTOH concentrations at MBO, the SRIFs were calculated in two different ways: first, by assessing the potential impact from Western North America and Asian source regions (Figure 4.1A); and second, by assessing the potential influences from urban areas of the Western U.S. (Figure 4.1B).

MBO is primarily influenced by westerly air flow, with occasional influences from Western North America, ranging from Southern California to Northern British Columbia (Figure 4.1A and 4.1B). Thus, source regions were selected from Asia and

Western North America (Figure 4.1A). The Asian source region has been previously described by Weiss-Penzias et al. and includes the area of CO concentration enhancement shown by the MOPITT (Measurements of Pollution in the Troposphere) instrument *(6)*. A large proportion of the Asian source region area is covered by China where high emissions of PAHs have been associated with biomass burning, coal combustion, and coking *(14)*.

Figure 4.1B shows the three Western U.S. urban source regions: the greater Seattle metropolitan area (urban Washington), the greater Portland metropolitan area (urban Oregon), and combined Northern and Southern California (urban California). Figure 4.1B also shows examples of back trajectories with large SRIFs in the various urban source regions (urban Washington, urban Oregon, and urban California). The source regions assessed for North American fire influences were: British Columbia, Oregon, Washington, and California (Figure 4.1A). The SRIFs for the two different approaches are shown in Figure 4.3 for all air samples.

Increased SRIFs from British Columbia and the states of Oregon and Washington occurred during late spring, summer and fall (Figure 4.3). Increased SRIFs from the state of California occurred during late winter and spring, while increased SRIFs from Asia primarily occurred during the winter and spring (Figure 4.3). Urban SRIFs were generally consistent with regional SRIFs, although there were periods where the two did not coincide. In these cases, the air mass passed over a state region but not an urban area.

Annual differences in SRIFs were present (Figure 4.3). Spring 2004 showed increased SRIFs from Asia and the states of Oregon and Washington; whereas spring

2005 showed increased SRIFs from Asia, followed by increased SRIFs from a combination of Oregon, Washington, and California. Spring 2006 showed increased SRIFs from California early on, followed by increased influences from Oregon and Washington, with some episodic events from Asia.

Temporal SOC Concentrations

Figure 4.4 shows the seasonality of Σgas-phase PAH, Σparticulate-phase PAH, ΣPCB, levoglucosan, and retene concentrations at MBO. In general, lower concentrations were measured during the winter and greater variation in concentrations occurred during the spring, summer, and fall. Recovery-corrected ΣFTOH concentrations were only measured in the spring 2006 samples *(7)*.

Gas-phase PAHs were detected in all samples with one exception, anthracene, which was detected in 62% of the samples. The Σgas-phase PAH concentrations ranged from 90 to 5970 pg/m^3 and were positively correlated with ΣFTOH (p-value, 0.0002), ΣPCB (p-value < 0.0001), retene (p-value < 0.0001), and levoglucosan concentrations (p-value 0.03). However, Σgas-phase PAHs concentrations were not correlated with Σparticulate-phase PAH concentrations. Enhancements in Σgas-phase PAH concentrations occurred during summer 2004 (11-12 July), late spring 2005 (7-8 May, 12-13 May, 27-28 May), summer 2005 (3-4 June, 15-16 June, 15-16 July, 9-10 Aug), and late spring 2006 (27-29 Apr) (Figure 4.4A). These air masses spent increased time in Oregon (Figure 4.3).

Particulate-phase PAHs were detected in ~20% of the MBO samples. The Σparticulate-phase PAH concentrations ranged from <LQ (limit of quantification) to 516

pg/m^3 and were not significantly correlated (p-value > 0.05) with levoglucosan, retene, Σgas-phase PAH, ΣFTOH, 1,3,5-triphenylbenzene, or ΣPCB concentrations. The highest concentration (516 pg/m^3) of Σparticulate-phase PAHs was measured on 25-26 April 2004 (Figure 4.4A) during a trans-Pacific atmospheric transport event from an industrial region of Asia *(1)*. This sample had the highest SRIF from Asia (17%) and an atmospheric transport time from Asia to MBO of approximately 5 to 6 days (Figure 4.3) *(1)*. During this same trans-Pacific transport event, there was no significant increase in Σgas-phase PAH concentrations likely due to the difference in the atmospheric lifetimes of particulate-phase PAHs and gas-phase PAHs. The estimated lifetimes of gas-phase PAHs are on the order of hours *(27)*, while the particulate-phase PAHs exist primarily on submicron aerosols and have lifetimes on the order of a week *(28)*.

PCBs were detected in ~50% of the MBO samples, except for PCB 101, PCB 183, and PCB 187 which were detected in only 10-20% of the samples. The ΣPCB concentrations ranged from <LQ to 19 pg/m^3 and were significantly correlated with Σgas-phase PAH (p-value < 0.0001), levoglucosan (p-value < 0.0002), and retene (p-value < 0.0001) concentrations. Enhancements in ΣPCB concentrations occurred in spring 2004 (10-11 May), summer 2004 (19-20 June, 11-12 July), spring 2005 (12-13 May, 27-28 May), summer 2005 (9-10 August), and fall 2005 (7-8 Sept) (Figure 4.4B) in air masses that spent increased time in Oregon and Washington (Figure 4.3).

8:2-FTOH and 10:2-FTOH were detected in all 34 spring 2006 samples, while 6:2-FTOH was detected in 32 of the 34 samples *(7)*. The ΣFTOH concentrations ranged from 7 to 113 pg/m^3 and were significantly (p-value, 0.0002) correlated with Σgas-phase

PAH concentrations *(7)*. Enhancements in ΣFTOH concentrations occurred in air masses that spent increased time in California, Oregon and Washington (Figure 4.4B and 3). Some of the lowest ΣFTOH concentrations occurred in trans-Pacific air masses (e.g. 23-24 Apr 2006).

Retene, 1,3,5-triphenylbenzene and levoglucosan were detected in 74%, 26%, and 67% of the samples, respectively and concentrations ranged from <LQ to 580, <LQ to 26, <LQ to 12,220 pg/m^3, respectively. Levoglucosan and retene concentrations were significantly correlated (p-value < 0.05) with ΣPCBs and Σgas-phase PAHs. The 1,3,5-triphenylbenzene concentrations were not correlated with other SOCs. Enhancements in levoglucosan and retene occurred in late spring, summer, and fall (Figure 4.4C). Enhancements in 1,3,5-triphenylbenze concentrations occurred during spring 2004 relative to other seasons and years (Figure 4.4D).

The highest concentrations of retene and levoglucosan were measured on 11-12 July 2004 and 9-10 Aug 2005, respectively (Figure 4.4C). HMS smoke and hot spot layers were imported into ArcGIS and overlaid with 10 day back trajectories to assess the potential influences of fires on these air masses (Figure 4.5). In both cases, the 10 day back trajectories passed though regions with both hot spots and smoke present. The air mass sampled on 11-12 July 2004 passed over large fires in Alaska and Canada, while the air mass sampled on 9-10 Aug 2005 passed over fires in Western Oregon. The highest concentrations of ΣPCBs were also measured in the air mass sampled on the 9-10 of Aug 2005 (Figure 4.4B). In addition, on 7-8 Sept. 2005 increased ΣPCB, retene, and PAH concentrations were measured (Figure 4.4B and 2C) and the sampled air mass passed

over fires in both Eastern and Western Oregon and Washington. Increased PCB concentrations have recently been identified in air masses associated with fires and attributed to revolatization of PCBs deposited to soils and vegetation *(29)*. These MBO measurements provide further evidence that fires volatilize stored surface deposits of PCBs from soil and vegetation.

We investigated the correlations between SOC concentrations and submicron aerosol, CO, water vapor (WV), and O_3 concentrations measured in the same air masses (Table 4.4). At MBO, subsiding air masses have been characterized as having low WV, high CO, and high O_3 concentrations *(5)*. In the 2004 to 2006 dataset, significant positive correlations ($p<0.05$) existed between Σparticulate-phase PAH and CO concentrations, as well as submicron aerosol and ΣPCB, levoglucosan and Σparticulate-phase PAH concentrations. However, significant negative correlations ($p<0.05$) existed between Σgas-phase PAH and CO concentrations. This provides further evidence that enhanced Σparticulate-phase PAH concentrations are associated with long-range transport, while enhanced Σgas-phase PAH concentration are associated with regional transport.

During the INTEX-B campaign (spring 2006), Σgas-phase PAH, ΣPCB, and ΣFTOH concentrations were significantly positively correlated ($p<0.05$) with water vapor concentration and negatively correlated with O_3 concentration. In addition, negative correlations existed between CO and Σgas-phase PAH and ΣPCB concentrations. These correlations provide further evidence that enhanced Σgas-phase PAH, ΣPCB, and ΣFTOH concentrations are associated with regional transport (Western U.S.).

Meteorological Influences

No statistically significant correlations (p-value > 0.05) existed between PAH, PCB, and FTOH concentrations and site wind speed. Only PCB 101 concentrations correlated (p-value < 0.05) with site wind direction. The Clausius-Clapeyron equation was used to assess potential temperature effects on SOC concentrations *(30)*. Of the sixty sampling days with site temperature data, only twenty-six days had average site temperatures above freezing (Figure 4.1). On these days, temperatures below 273 K were replaced with 273 K for this analysis *(31)*. Statistically significant negative correlations (p-values<0.05) between MBO site temperature (1000/T) and fluorene, phenanthrene, anthracene, fluoranthene, pyrene, retene, PCB 118, PCB 153, and PCB 138 concentrations were found (Table 4.2). The slopes of these linear regressions of SOC concentration and 1000/T were similar to slopes reported for other remote sites *(30)*. Significant positive correlation (p-value < 0.01) between site temperature and the SRIFs for rural Oregon and urban Oregon were also found, indicating increased influence from Oregon during warmer time periods (i.e. summer). Site temperature was not significantly correlated with SRIFs from other source regions.

The individual FTOH concentrations did not show statistically significant temperature dependence (p-value > 0.05). Because recovery-corrected FTOH concentrations were only measured in the spring 2006 samples, these concentrations do not represent the seasonal variation in temperature that the PAH and PCB concentrations do. In the case of the FTOHs, larger scale meteorological events, such as cyclonic systems, may play an important role in the increased concentrations observed. As cool,

dense air that is associated with cyclonic systems moves into coastal urban areas, warmer air is displaced upwards which leads to increased cloud formation (i.e. frontal lifting). The highest concentrations of ΣFTOHs, as well as increases in ΣPCB and Σgas-phase PAH concentrations (13-14 Apr 2006), corresponded in time (Figure 4.4) to increased frontal lifting in California (Figure 4.6). Other examples of SOC concentration enhancements associated with regional fronts include 4-5 Apr 2006 (California) and 20-22 April (Pacific Northwest). Enhanced Σgas-phase PAH, ΣFTOH, and ΣPCB concentrations were also measured during calm winds (e.g. 27-29 April 2006). Thus, the increased FTOH concentrations, as well as PCB and gas-phase PAH concentrations, may be associated with frontal activity over urban areas on the West Coast of the U.S.

The water vapor mixing ratio has been shown to be an effective marker for boundary layer air influences at MBO *(5)*. A statistically significant (p-value < 0.05) positive correlation was found between the spring 2006 (INTEX-B) campaign water vapor mixing ratio and gas-phase PAH (phenanthrene, fluoranthene, and pyrene), PCB (PCB 118 and PCB 153), and FTOH (6:2-FTOH and 10:2-FTOH) concentrations. Particulate-phase PAH concentrations were not correlated with the water vapor mixing ratio (p-value > 0.05). This provides further evidence that gas-phase PAH, PCB, and FTOH concentrations were elevated in Western U.S. boundary layer air, while elevated particulate-phase PAH (chrysene/triphenylene, benzo(a)anthracene, benzo(b)fluoranthene, benzo(k)fluoranthene, benzo(e)pyrene, benzo(a)pyrene, indeno(1,2,3-cd)pyrene, benzo(ghi)perylene) concentrations were associated with trans-Pacific air masses.

Asian and North American Source Regions

Pearson correlation analysis was conducted on PAH, PCB, and FTOH concentrations and SRIFs for the West Coast of North America (Oregon, Washington, California, and British Columbia) and Asia to assess the potential influence from Asian and North American source regions (Figure 4.7A). Gas-phase PAH (fluorene, phenanthrene, anthracene, fluoranthene, pyrene, and retene) and PCB (PCB 118, PCB 138, and PCB 153) concentrations were positively correlated with increased air mass time in the state of Oregon (Figure 4.7A). Increased air mass time in Washington, California, and British Columbia was not correlated (p-value > 0.05) with increased SOC concentrations (Figure 4.7A). Anthracene, a good indicator of local combustion sources due to its shorter atmospheric lifetime *(27)*, and retene, a marker for wood combustion, concentrations were correlated with increasing air mass time in Oregon (Figure 4.7A). Significant correlations (p-value<0.05) existed between anthracene concentrations and gas-phase PAH (fluorene, phenanthrene, fluoranthene, pyrene, and retene), FTOH (10:2-FTOH and 6:2-FTOH) and 1,3,5-triphenylbenzene concentrations *(7)*. The increased gas-phase PAH and PCB concentrations with increased air mass time in Oregon is likely due to urban influences, as well as biomass burning.

The particulate-phase PAH (* indicates carcinogenic) (benzo[b]fluoranthene*, benzo[e]pyrene, benzo[a]pyrene*, indeno[1,2,3-cd]pyrene*, benzo[ghi]perylene) concentrations were significantly (p-value < 0.05) positively correlated with increased air mass SRIF in Asia and were not correlated with air mass time in any North American source region (Figure 4.7A). Thus, enhanced concentrations of particulate-phase PAHs at

MBO are indicative of trans-Pacific transport. The highest concentrations of particulate-phase PAHs (Figure 4.4A) were measured during a previously documented trans-Pacific transport event on 25-26 Apr 2004 *(1)*. Concurrent measurements by our laboratory in Spring 2004 on Okinawa, Japan showed increased particulate-phase PAH concentrations in air masses from China *(8)*. In combination, these data provide strong evidence that particulate-phase PAHs are emitted from China and undergo trans-Pacific atmospheric transport to North America.

North American Urban Influences

After the influence of North American and Asian source regions on SOC concentrations at MBO was assessed, the influence from North American urban areas was evaluated. This was done using the high temporal resolution spring 2006 INTEX-B data set; which consisted of thirty-four samples collected over fifty-one days (Figure 4.1). To assess urban influences, a top boundary of 2 km a.g.l. (above model ground level) was set in the calculation of hourly trajectory points for the SRIFs to ensure boundary layer air. Sampled air masses that were primarily impacted by a single urban source region were identified by dividing the air mass time spent in one source region by the total air mass time spent in all urban source regions [Σ (urban Washington, urban Oregon, and urban California)] and multiplied by 100 (i.e. % urban impact). Figure 4.8 shows the % urban impact for each sample and several air masses did not spend any time at < 2 km a.g.l. in the defined urban areas. Next, the data for air masses impacted primarily by one urban source region (> 95%) were isolated and data for air masses with a low total urban SRIF (<1%) were not used in this interpretation.

Using this method, samples of air masses impacted primarily (>95%) by urban Oregon (n=5: 17-18 Apr, 28-29 Apr, 29-30 Apr, 30 Apr-1 May, 8-9 May) and urban California (n=5: 3-4 Apr, 4-5 Apr, 11-12 Apr, 12-13 Apr, and 22-23 Apr) were identified (Figure 4.8B). No air masses were primarily (>95%) impacted by urban Washington (Figure 4.8B). The data from these urban air masses were used to evaluate urban influences of SOCs.

Figure 4.7B shows the significant (p-value < 0.05) correlation coefficients of SOC concentration versus SRIF associated with the urban air masses. Increased time spent in urban California was associated with increased concentrations of FTOHs (6:2-FTOH, 8:2-FTOH, and 10:2-FTOH) and gas-phase PAHs (fluorene, phenanthrene, fluoranthene, and pyrene). The sampled air masses primarily influenced by urban California occurred during periods when fires did not have a significant impact on gas-phase PAH concentrations. Increased time spent in urban Washington was associated with increasing concentrations of 6:2-FTOH and 10:2-FTOH. Particulate-phase PAH and PCB concentrations were measured in too few samples from each urban group to assess their Western U.S. urban impact.

Source Profiles

To further understand the possible PAH and PCB sources to MBO, the measured profiles were compared to source profiles. Figure 4.9 shows the phenanthrene normalized PAH profile for a PAH emission inventory for China *(32)*, the PAH emission profile for the Great Lakes Region of the U.S. *(33)*, the average PAH profile measured in Los Angeles (L.A.), California *(34)*, and the average PAH profile measured at Hedo Station

Observatory (HSO), Okinawa, Japan *(8)*, compared with the average PAH profile for MBO samples with measurable particulate-phase PAH concentrations (trans-Pacific transport) and without measurable particulate-phase PAH concentrations (nontrans-Pacific transport). Elevated particulate-phase PAH concentrations relative to gas-phase PAH concentrations were identified in the Chinese inventory, measurements of Asian air masses on Okinawa, Japan, and measurements at MBO (Figure 4.9). The PAH emission profile for the Great Lakes Region of the U.S., as well as the measurements near L.A., California, indicate lower relative particulate-phase PAH concentrations in U.S. air masses compared to both Asian and MBO air masses. Principal component analysis confirms this interpretation (see supporting information). This provides additional evidence that the high proportion of particulate-phase PAHs in MBO air masses is due to Asian emissions and trans-Pacific atmospheric transport.

Principal component analysis (PCA) was used to identify potential PAH sources (Figure 4.10). The first biplot contained both gas and particulate phase PAHs: measured at MBO; measured near Asia (HSO) *(8)*; and measured near L.A., California *(34)*. Benzo[e]pyrene was not measured in the Southern California study and it was left out of the PCA analysis. Figure 4.10A shows the two main groups formed from the gas and particulate phase PAHs. One group contained the Asian PAH profile (HSO) and the PAH profile at MBO. The second group contained the measurements from L.A., California. The Asian and MBO samples were enhanced in particulate-phase PAHs, while the measurements in southern California were enhanced in gas-phase PAHs.

The second PCA biplot shows the particulate-phase PAHs only: measured at MBO, measured at HSO *(8)*, and measured in Southern California *(34)*. Two major groups were identified (Figure 4.10B). One group consisted of particulate-phase PAHs in the Southern California urban area *(34)*, while the second group clustered together the Asian particulate-phase PAHs *(8)* and the measurements at MBO. The major source of particulate-phase PAHs in the Southern California urban area were attributed to gasoline emissions *(34)*, whereas the elevated particulate-phase PAHs in the Asian region were attributed to biomass, coal, and coking emissions *(8,14)*. This provides further evidence that MBO is impacted by trans-Pacific atmospheric transport of particulate-phase PAHs from China.

Some of the targeted PCBs (PCB 101, PCB 183, and PCB 187) were only detected in 10-20% of the samples, where as PCB 118, PCB 138, and PCB 153 were detected in ~50% of the samples. Samples containing all three most frequently detected PCBs (PCB 118, PCB 138, and PCB 153) were compared to the PCB profile at Okinawa, Japan (HSO), incinerator flue gas sources of PCBs, Kanechlor, and Aroclor profiles *(8,13,35)*. Aroclor and Kanechlor were the two PCB mixtures primarily used in the U.S. and Japan *(13)*. This comparison was made by looking at the percent composition of the most detected PCBs. Figure 4.11 shows the measurements at MBO and HSO were similar to combustion sources, Aroclor 1254 and Kanechlor 500. Aroclor 1254 and Kanechlor 500 have a similar chlorine content *(13)*.

Estimated Urban Emission Rates

SRIFs were used to assess air mass transport time from source regions to a receptor site; a larger SRIF indicates an air mass spent more time in the source region and less time in transit to MBO *(8)*. Using the slopes of the regressions of SOC concentrations versus SRIF and the area of the urban source regions, annual emissions of SOCs from Western U.S. urban areas were estimated. This assumes that the urban SOC emissions are constant and there are no significant physical or chemical losses of the SOCs in transit to MBO. Because atmospheric transport times from Western U.S. urban source regions to MBO are on the order of hours to ~1 day and PAHs, PCBs, and FTOHs are continually emitted to the atmosphere, these assumptions are reasonable.

To do this, the slope of the SOC concentration versus the SRIF was calculated for statistically significant (p-value < 0.05) correlations (pg/(SRIF*m^3)). Next, the number of hours the air mass spent in the source region was back calculated by taking the slope of the regression and dividing it by 6480 hours (10 day back trajectories, at 3 elevations, and at 9 time intervals over a 24 hour sample), converting the slope into the concentration enhancement due to a single cubic meter of air from an urban region (pg/(hour*m^3)). This value was then multiplied by the total volume of the urban air column (m^3) to yield the SOC emissions (kg/year). Per person emissions were calculated by dividing the emissions by the population of each urban area. It should be noted that trajectories are associated with a large uncertainty and are not absolute calculations *(36)*. Representation of boundary layer flow can further increase the trajectory uncertainty due to turbulence

(36). The relative standard deviation of the slope parameter was used to assess the error associated with the emission estimates, and it ranged between ~10-50%.

Figure 4.3 shows the estimated 2006 emissions of FTOHs and gas-phase PAHs from Western U.S. urban areas. PCB emission could not be estimated because of the limited number of detections. Emissions of individual FTOHs from the Western U.S. urban areas ranged from 15 to 309 kg/year. From 2000 to 2002, FTOH production in North America was 2-2.6 million kg/year *(37)*. Estimated per person emission rates of FTOHs were within an order of magnitude for urban Washington (2-21 mg/(year*person)) and urban California (2-7 mg/(year*person)) (Figure 4.3). Estimated emissions of individual gas-phase PAHs ranged from 217 to 4648 kg/year and 6 to 138 mg/(year*person) (Figure 4.3). In 1996, U.S. emissions of gas-phase PAHs (fluorene, phenanthrene, fluoranthene, and pyrene) were 4020 tons *(33)*. Because the atmospheric lifetimes of FTOHs are much longer (~50-80 days) than gas-phase PAHs (hours to days), the FTOH emission estimates are likely more accurate *(7,38)*.

Acknowledgements

The authors would like to thank Dan Jaffe, Paul Hutter, Nat Bingham, Eugen Helmbrecht, James B. Dennison, Isaac Bertschi, Peter Weiss-Penzias, Phil Swartzendruber, Danielle Primbs, and Jessica Murray. Mt. Bachelor Corporation, especially the lift maintenance crew. Will Hafner for the development of a Visual Basic trajectory analysis program. The research described in this paper has been funded in part by the United States Environmental Protection Agency (EPA) under the Science to Achieve Results (STAR) Graduate Fellowship Program to Toby Primbs EPA has not

officially endorsed this publication and the views expressed herein may not reflect the views of the EPA. We would also like thank National Science Foundation CAREER (ATM-0239823) for funding. This work was made possible in part by National Institute of Health (Grant # P30ES00210).

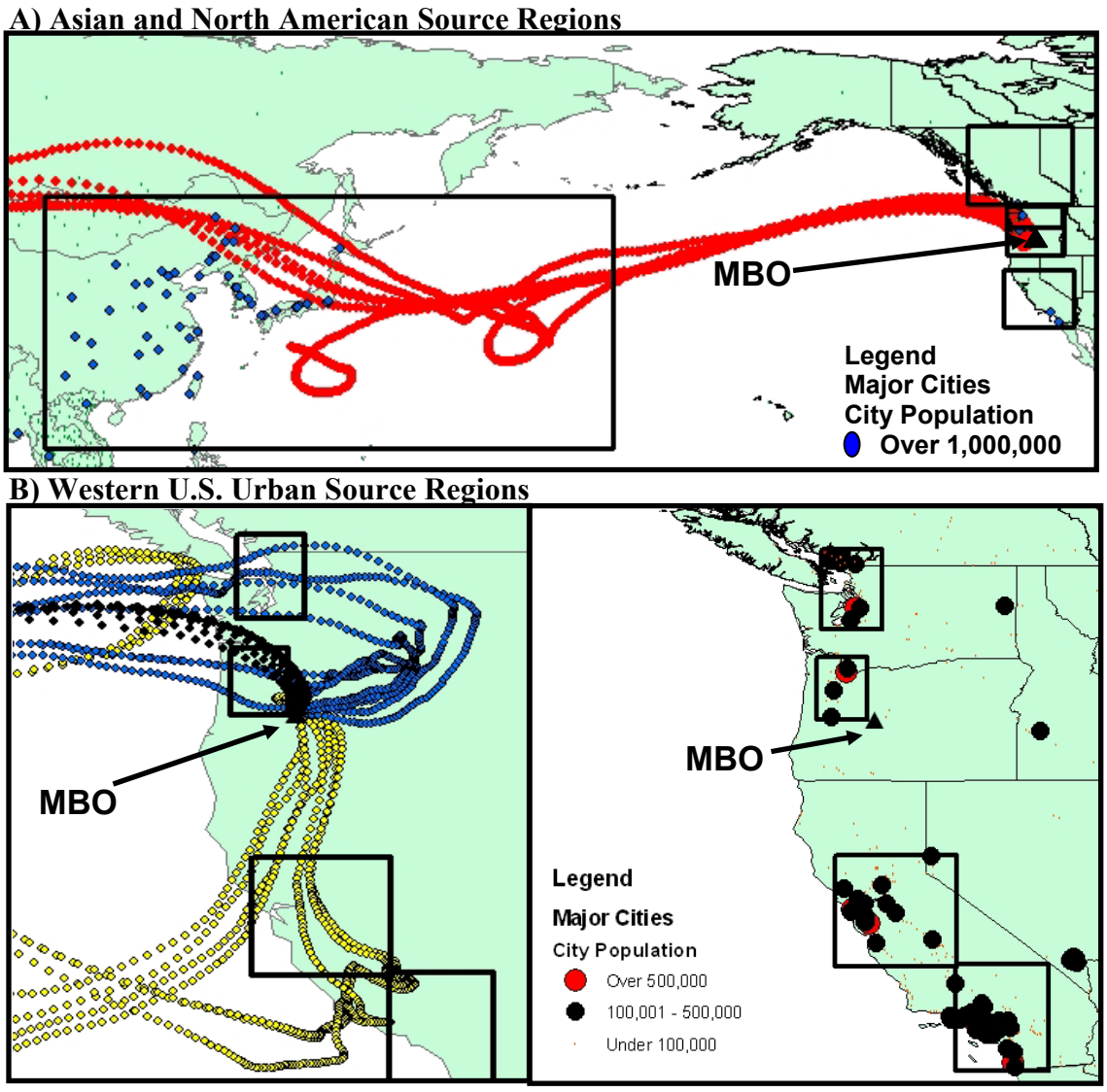

Figure 4.1: A) MBO (black triangle at 43.98°N 121.69°W, 2.7 km a.s.l.) is located in Oregon's Cascade Range. Source regions (boxes) used to assess Asian and North American sources, including fires. The 25-26 April 2004 10 day back trajectory is shown in red. Each trajectory point is an hourly point. **B)** Source regions (boxes) used to assess Western U.S. urban influences. Example back trajectories include: 7-8 September 2005 (blue, urban Washington State); 4-5 April 2006 (yellow, urban California); 27-28 April 2006 (black, urban Oregon).

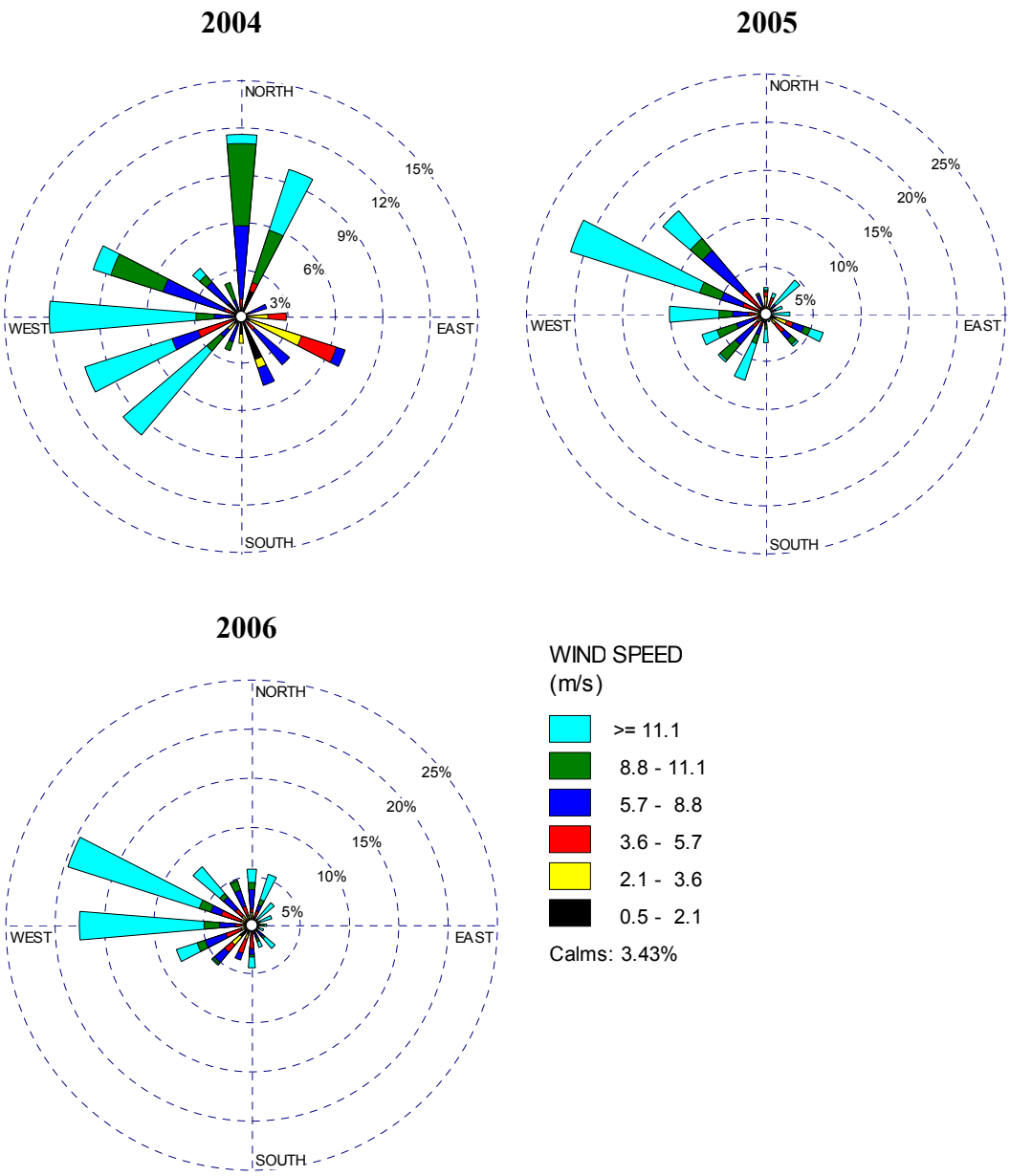

Figure 4.2: Average wind rose for 2004, 2005, and 2006 sampling days at MBO using site hourly wind speed and wind direction data.

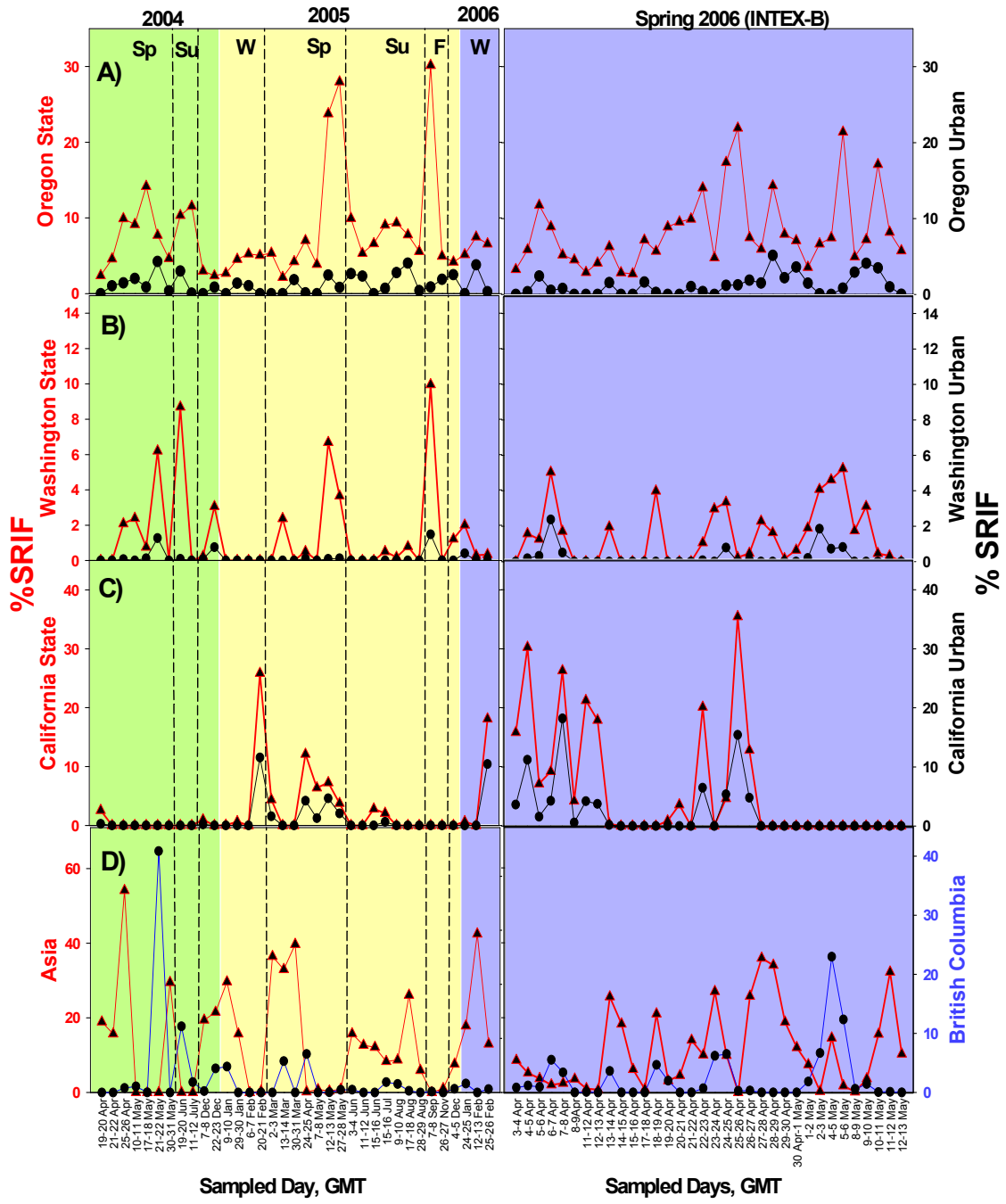

Figure 4.3: Source region impact factors (SRIFs) for: **A)** Oregon State and Urban Oregon; **B)** Washington State and Washington Urban; **C)** California State and California Urban; **D)** Asia and British Columbia. SRIFs from Asia, California State, Washington State, Oregon State, and British Columbia were used to assess Asian and Western North America influences (red and blue lines). SRIFs from California urban, Oregon urban, and Washington urban were used to assess influences from Western U.S. urban areas (black lines).

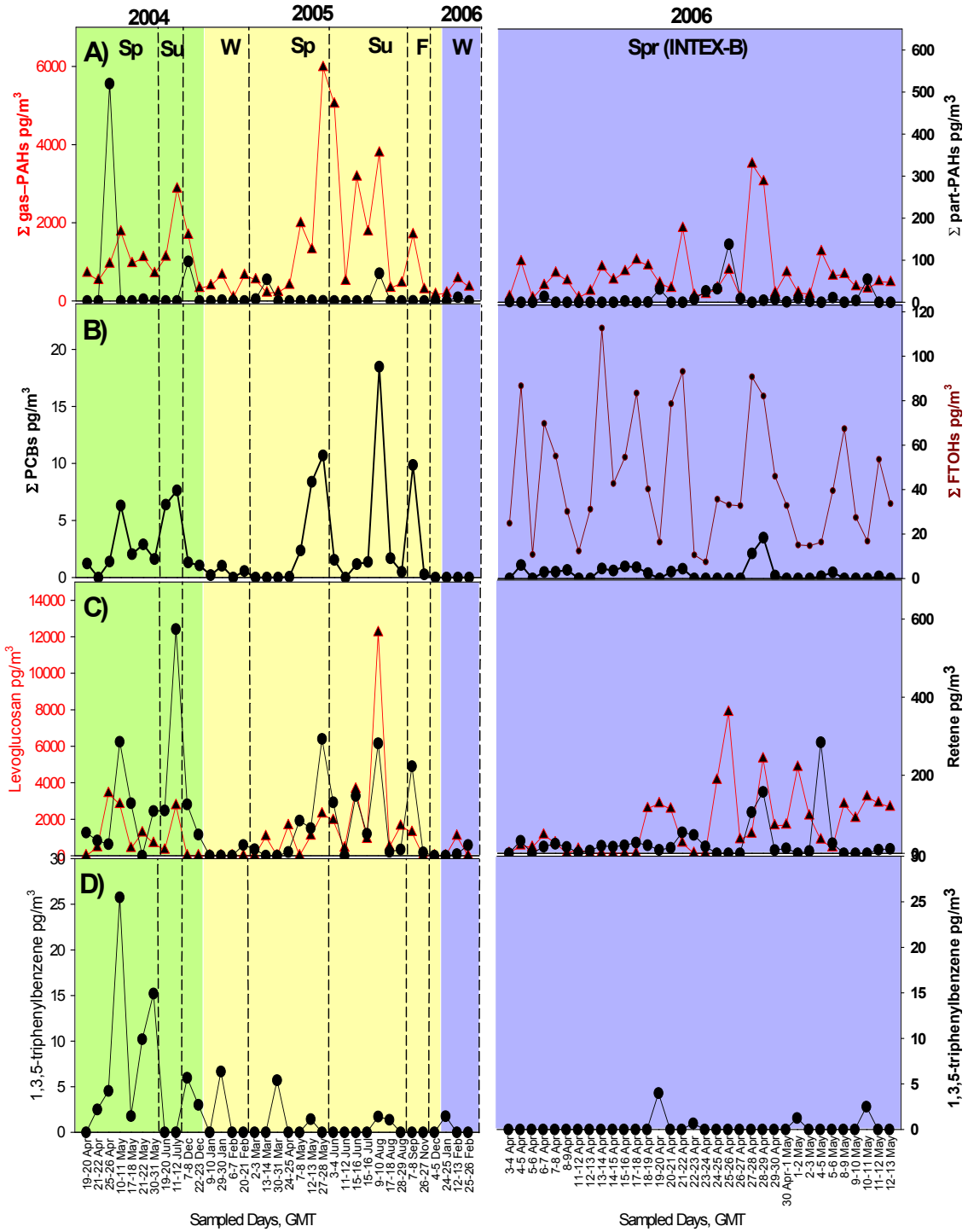

Figure 4.4: A) Σgas (red, triangles) and Σparticulate-phase PAH (black, circles). **B)** ΣPCB (black, circles) and ΣFTOH (red, circles). **C)** levoglucosan (red, triangles) and retene (black, circles) **D)** 1,3,5-triphenylbenzene (black, circles). [MBO from 2004 to 2006, Spring (Sp), Summer (Su), Fall (F), Winter (W)]. Recovery-corrected FTOH concentrations were only measured in the spring 2006 samples *(7)*.

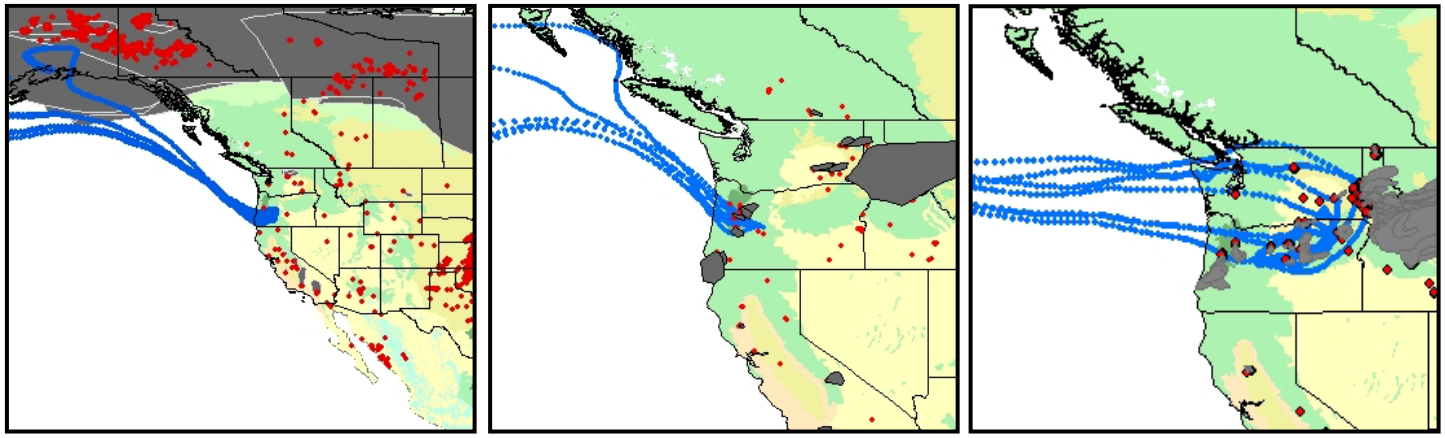

A) 11-12 July 2004 **B) 9-10 Aug 2005** **C) 7-8 Sept 2005**

Figure 4.5: HMS smoke (grey) and hotspot (red dots) layers and 10 day back trajectories (blue) for the sampling dates where retene (A) 11-12 July 2004 and levoglucosan (B) 9-10 Aug 2005 concentrations were the highest. Enhanced PCBs, retene, and PAH concentrations also occurred on (C) 7-8 Sept 2005.

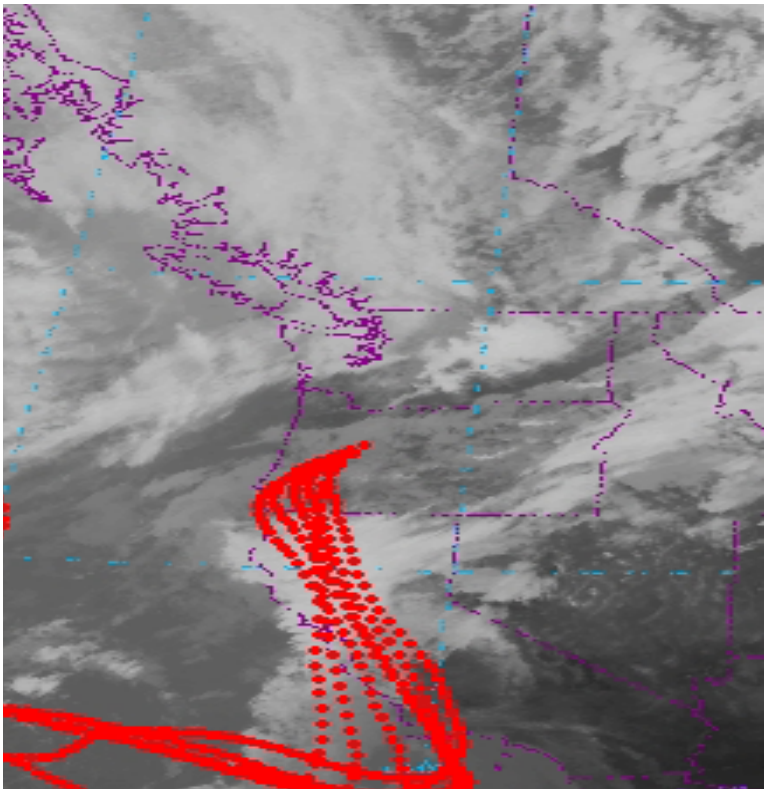

Figure 4.6: Satellite image of frontal lifting, as seen by the increased cloud formation in California associated with the highest concentrations of FTOHs (13-14 Apr 2006). The trajectories for this sample are shown in red.

A.) Asian and Western North American, 2004-2006

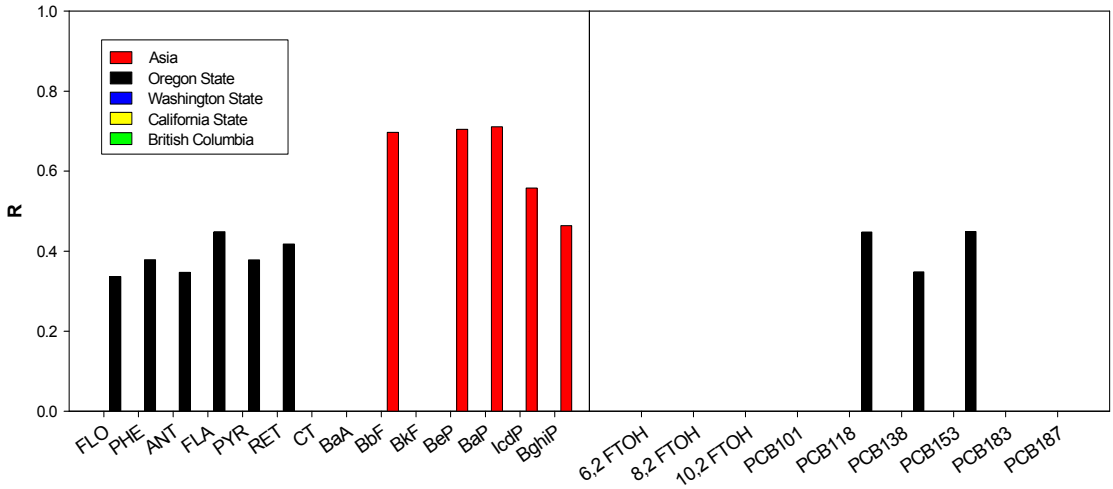

B) Western U.S. Urban Influences, Spring 2006

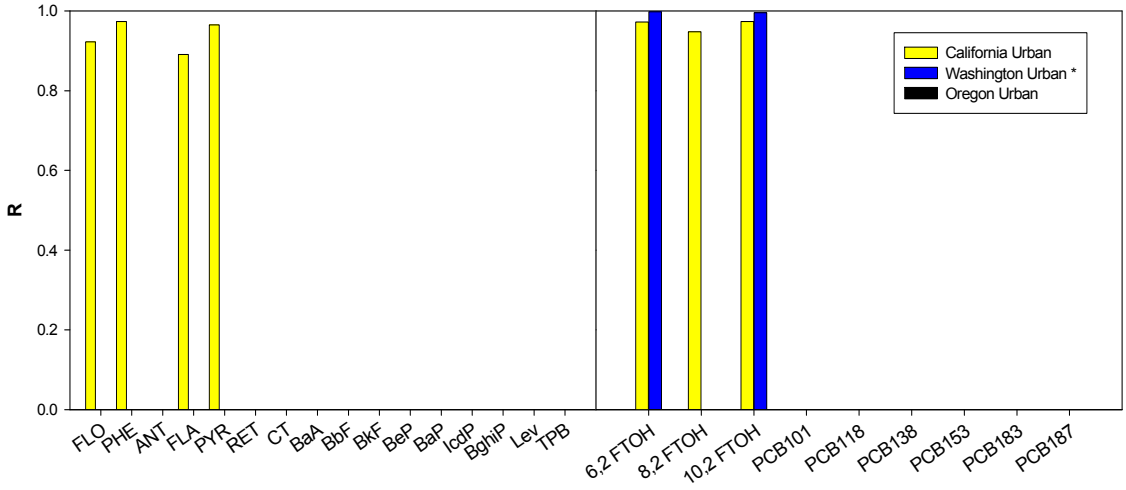

Figure 4.7: Statistically significant (p-value < 0.05) correlation coefficient (R) of SOC concentrations with SRIFs for **A)** the Oregon and Asia source regions (p-value < 0.05) for 2004-2006 samples. Washington, California, and British Columbia did not have significant correlations (p-value > 0.05) between SRIFs and concentrations. **B)** Significant (p-value < 0.05) correlation coefficient (R) for western U.S. urban area SRIFs for spring 2006 samples, where %urban impact was > 95% of total SRIF. (*) For urban Washington samples with >5% SRIF were used.

A.) Asian and Western North American, Spring 2006

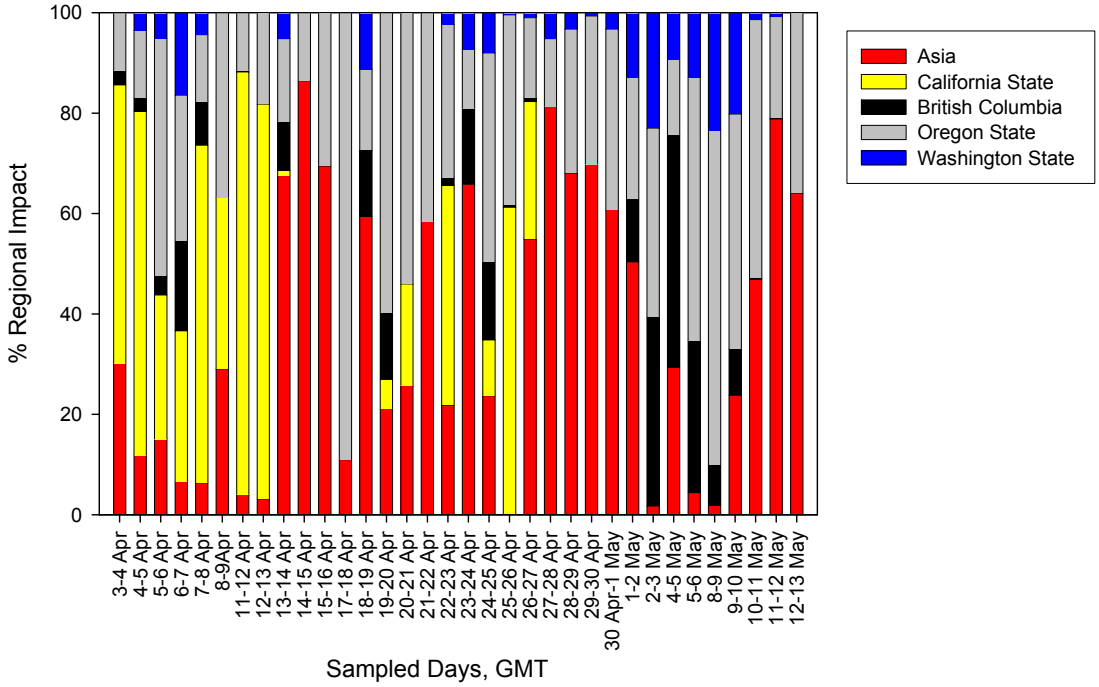

B) Western U.S. Urban Influences, Spring 2006

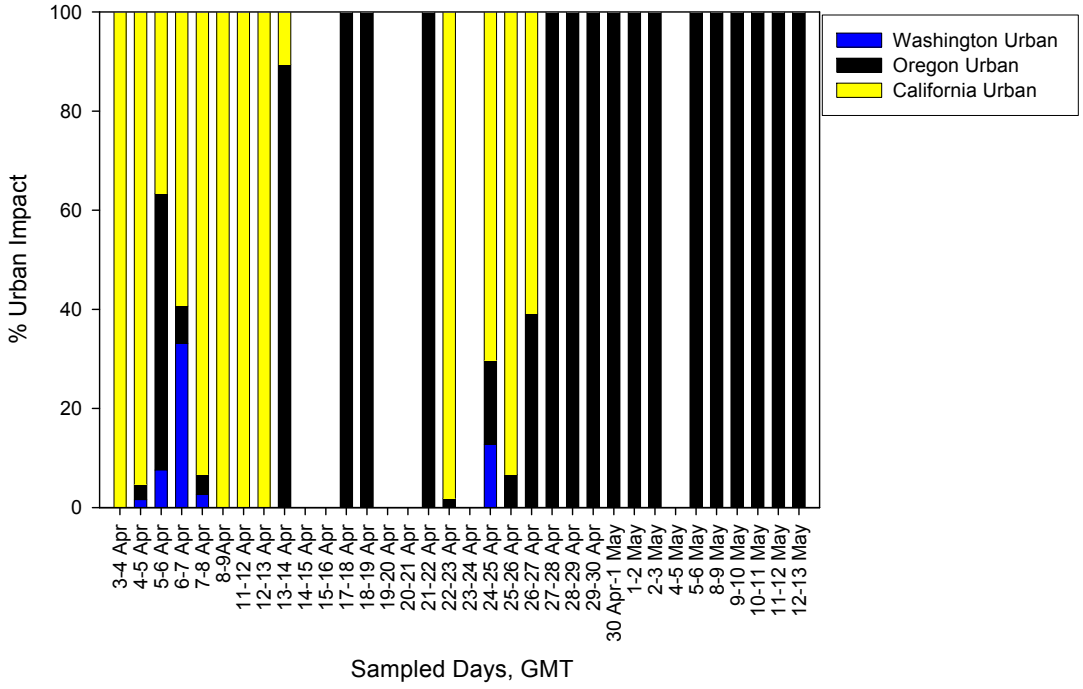

Figure 4.8: A) Asian and Western North American % impact, spring 2006 (INTEX-B). **B)** Spring 2006 % urban impact, as defined as time in the urban source region < 2km a.g.l. compared to the total time in all urban regions, < 2 km a.g.l. Samples on 15-16 Apr and 4-5 May did not have trajectories in the designated urban areas at < 2 km a.g.l.

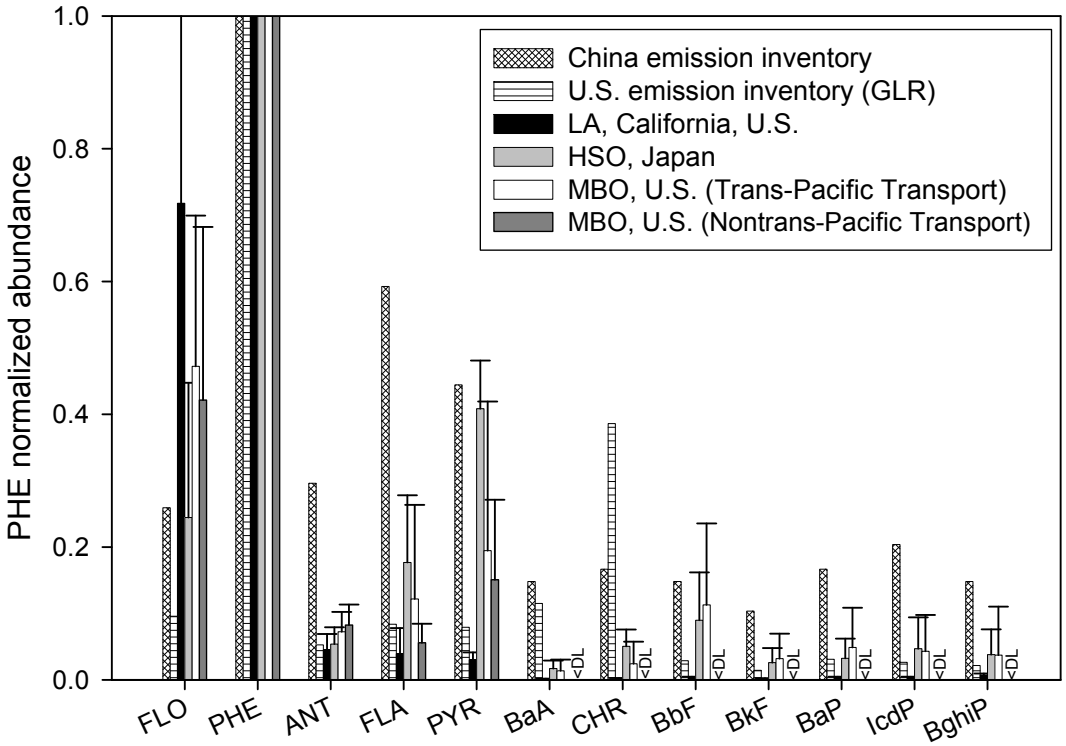

Figure 4.9: Average PAH profile (normalized to phenanthrene) for MBO samples with measurable particulate-phase PAH concentrations (trans-Pacific transport), compared to MBO samples with no measurable particulate-phase PAH concentrations (nontrans-Pacific transport), compared with Xu et al. PAH emission inventory for China (*20*), the profile of PAHs from the emission inventory for the Great Lakes Region, U.S. (*21*), the PAH profile from measurements near LA, California *(34)*, and the average PAH profile from measurements on Okinawa, Japan *(8)*. Note that the HSO and MBO measurements for CHR also include Triphenylene, whereas the inventories represent CHR only.

.

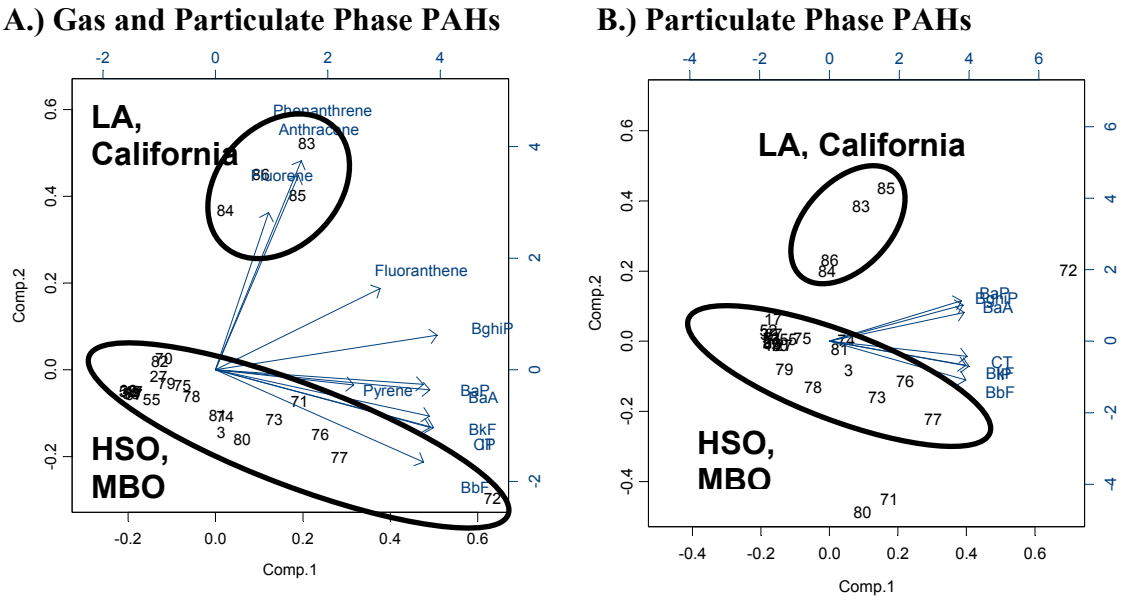

Figure 4.10: PCA biplots of PAHs measured in Asian outflow (HSO) *(8)*, at MBO, and near Los Angeles, California *(34)*. A.) PCA biplot for gas and particulate phase PAHs combined. The first two components explain 82% of the variation. B) PCA biplot for particulate-phase PAHs only. The first two components explain 95% of the variation.

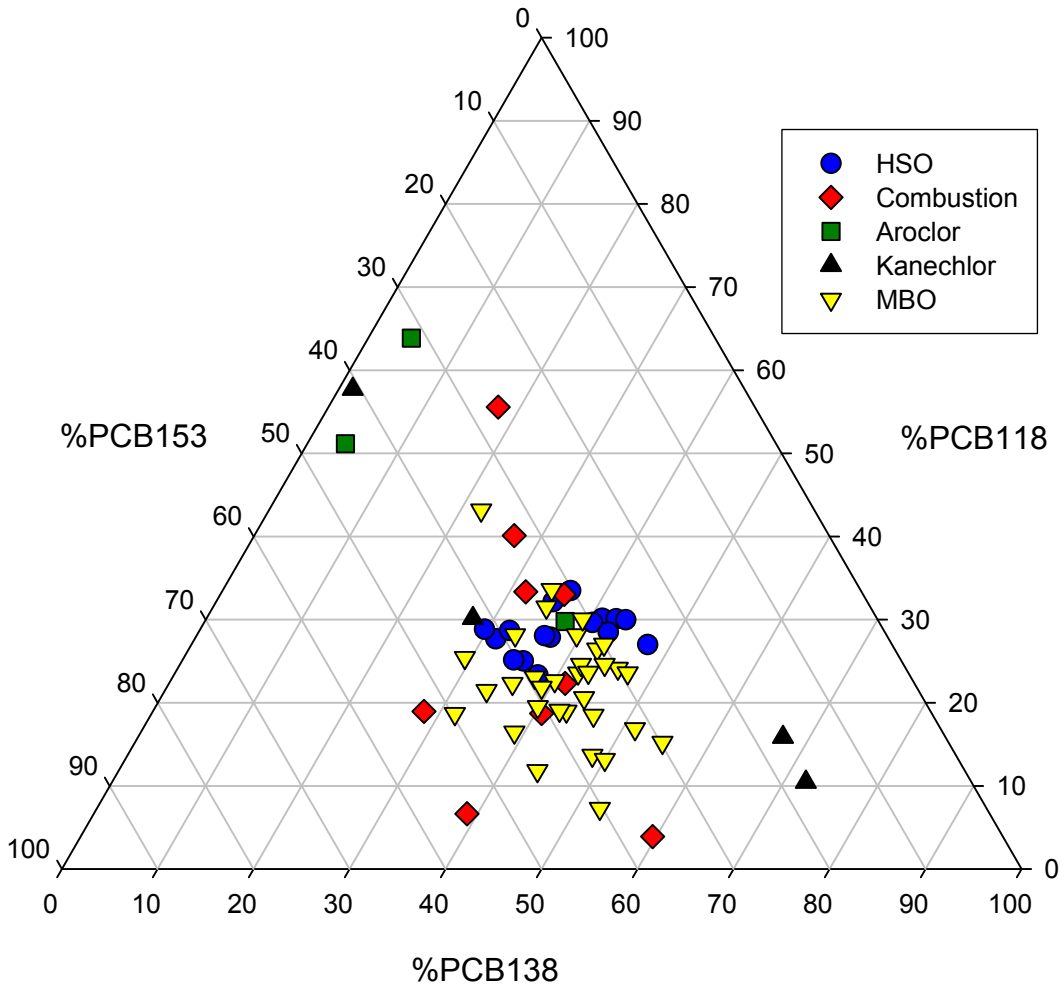

Figure 4.11: Fractional composition of measured PCBs at MBO compared with Okinawa, Japan (HSO)*(8)*, aroclor *(35)*, kanechlor, and incinerator flue gas profiles (combustion) *(13)*.

Table 4.1: Sampling days (GMT), average (±standard deviation) site temperature, wind speed (WS), and wind direction (WD). NA means data not available.

Sampled Days, GMT	Temp, °C	WS, m/s	WD, Deg.	Sampled Days, GMT	Temp, °C	WS, m/s	WD, Deg.
2004				**Spring 2006**		**INTEX-B**	
19-20 Apr	-7.2 (1.6)	NA	NA	3-4 Apr	-6.9 ± 1.5	8.4 ± 4.3	176 ± 119
21-22 Apr	-6.9 ± 1.6	NA	NA	4-5 Apr	-4.5 ± 0.8	10.3 ± 4.3	175 ± 87
25-26 Apr	6.2 ± 2.5	3.9 ± 2.2	105 ± 39	5-6 Apr	-6.6 ± 2.9	21.3 ± 3.0	267 ± 103
10-11 May	-5.5 ± 0.9	13.4 ± 4.6	297 ± 25	6-7 Apr	-3.7 ± 1.6	13.2 ± 5.1	204 ± 59
17-18 May	-1.1 ± 2.2	5.6 ± 2.4	104 ± 84	7-8 Apr	-3.7 ± 1.9	13.7 ± 4.9	195 ± 67
21-22 May	0.6 ± 2.2	10.6 ± 3.7	281 ± 13	8-9Apr	-7.5 ± 1.8	12.7 ± 5.0	248 ± 38
30-31 May	-2.3 ± 1.8	19.0 ± 4.4	236 ± 3.5	11-12 Apr	-5.0 ± 0.6	4.6 ± 3.0	225 ± 81
19-20 Jun	5.3 ± 2.4	2.7 ± 2.4	244 ± 44	12-13 Apr	NA	12.3 ± 8.6	250 ± 62
11-12 July	7.1 ± 3.5	1.2 ± 1.5	167 ± 120	13-14 Apr	NA	23.6 ± 5.6	266 ± 13
7-8 Dec	-8.7 ± 0.6	NA	164 ± 126	14-15 Apr	NA	18.1 ± 10.5	204 ± 81
22-23 Dec	-5.6 ± 1.1	10.3 ± 1.8	82 ± 138	15-16 Apr	NA	6.0 ± 3.4	254 ± 58
2005				17-18 Apr	-8.8 ± 1.9	8.2 ± 6.4	236 ± 91
9-10 Jan	-11.8 ± 1.1	NA	NA	18-19 Apr	-4.3 ± 1.1	4.6 ± 2.7	198 ± 25
29-30 Jan	-6.3 ± 3.4	7.9 ± 5.8	285 ± 49	19-20 Apr	-0.8 ± 1.0	5.1 ± 1.4	205 ± 35
6-7 Feb	-10.1 ± 1.4	12.4 ± 3.1	284 ± 22	20-21 Apr	0.5 ± 3.2	9.7 ± 6.0	246 ± 35
20-21 Feb	-5.6 ± 0.7	4.1 ± 4.0	204 ± 73	21-22 Apr	-2.3 ± 2.7	10.5 ± 6.7	193 ± 137
2-3 Mar	-4.7 ± 3.0	8.3 ± 4.3	265 ± 57	22-23 Apr	-6.4 ± 2.3	23.9 ± 3.1	37.5 ± 7.1
13-14 Mar	-5.9 ± 2.0	20.8 ± 3.1	58 ± 21	23-24 Apr	-2.5 ± 2.8	11.8 ± 5.3	87 ± 123
30-31 Mar	-9.0 ± 2.8	NA	NA	24-25 Apr	-1.1 ± 3.1	8.1 ± 3.8	291 ± 28
24-25 Apr	-2.2 ± 1.7	5.4 ± 2.3	192 ± 80	25-26 Apr	1.8 ± 3.1	8.1 ± 5.6	267 ± 29
7-8 May	-1.5 ± 2.3	10.2 ± 3.2	222 ± 18	26-27 Apr	2.0 ± 1.4	11.2 ± 3.3	281 ± 106
12-13 May	3.3 ± 1.8	7.7 ± 3.0	252 ± 34	27-28 Apr	6.9 ± 2.8	3.8 ± 1.6	157 ± 137
27-28 May	8.1 ± 1.4	12.0 ± 3.4	142 ± 57	28-29 Apr	8.4 ± 3.7	3.4 ± 2.9	232 ± 82
3-4 Jun	3.7 ± 2.1	6.7 ± 2.8	259 ± 55	29-30 Apr	0.4 ± 4.5	17.3 ± 11.2	300 ± 52
11-12 Jun	-1.3 ± 4.0	12.6 ± 6.5	306 ± 66	30 Apr-1 May	0.5 ± 4.3	11.2 ± 5.9	273 ± 51
15-16 Jun	2.7 ± 2.5	13.2 ± 6.5	207 ± 22	1-2 May	-2.0 ± 2.7	7.0 ± 2.2	181 ± 166
15-16 Jul	12.5 ± 2.4	20.3 ± 4.3	291 ± 4	2-3 May	2.2 ± 2.7	3.4 ± 2.8	161 ± 110
9-10 Aug	13.0 ± 3.5	8.9 ± 3.6	304 ± 12	4-5 May	1.3 ± 1.9	8.2 ± 5.9	191 ± 103
17-18 Aug	8.7 ± 3.0	5.9 ± 4.9	227 ± 93	5-6 May	1.0 ± 3.0	17.2 ± 2.7	287 ± 8
28-29 Aug	3.7 ± 4.9	15.4 ± 5.3	282 ± 23	8-9 May	-1.6 ± 2.0	5.1 ± 2.3	257 ± 134
7-8 Sep	13.7 ± 3.1	3.0 ± 1.4	64 ± 67	9-10 May	4.8 ± 2.8	3.3 ± 2.7	266 ± 88
26-27 Nov	NA	NA	NA	10-11 May	5.8 ± 2.0	5.4 ± 5.4	232 ± 41
4-5 Dec	NA	NA	NA	11-12 May	-0.3 ± 3.7	20.6 ± 3.8	290 ± 5
2006				12-13 May	0.8 ± 0.8	12.8 ± 3.9	256 ± 14
24-25 Jan	NA	NA	NA				
12-13 Feb	NA	NA	NA				
25-26 Feb	NA	NA	NA				

Table 4.2: Correlation between individual PAH, PCB, and FTOH concentrations and temperature (1000/T) at MBO. NS means p-value > 0.05, not significant.

Analyte	Slope	p-value	R^2
FLO	-3.2 ± 0.9	0.0006	0.18
PHE	-5.2 ± 1.2	< 0.0001	0.25
ANT	-3.8 ± 1.4	0.008	0.19
FLA	-6.0 ± 1.0	< 0.0001	0.41
PYR	-6.9 ± 1.4	< 0.0001	0.3
RET	-5.8 ± 1.5	0.0004	0.26
6:2-FtOH	NS	0.2	0.06
8:2-FtOH	NS	0.8	0.002
10:2-FtOH	NS	0.2	0.06
PCB101	NS	0.6	0.11
PCB118	-4.0 ± 0.9	< 0.0001	0.36
PCB153	-5.1 ± 1.1	< 0.0001	0.39
PCB138	-3.6 ± 1.0	0.002	0.31
PCB187	NS	0.8	0.003
PCB183	NS	0.5	0.11

Table 4.3: 2006 emissions of FTOHs and gas-phase PAHs from urban areas in the Western U.S. (Washington (WA) and California (CA). NS means not significant (p-value > 0.05). Urban Oregon SRIFs were not significantly correlated with SOCs. NA means not available and that the analyte was detected in fewer than two samples from the urban source region.

Analyte	CA Urban Emissions (kg/year)	CA Urban Emissions (mg/(year* person))	p-value	R^2	WA Urban Emissions (kg/year)	WA Urban Emissions (mg/(year* person))	p-value	R^2
6:2-FTOH	71	2	0.005	0.95	15	2	0.03	1.00
8:2-FTOH	309	9	0.01	0.90	NS	NS	0.2	0.87
10:2-FTOH	233	7	0.005	0.95	138	21	0.04	1.00
FLO	1546	46	0.03	0.85	NS	NS	0.7	0.23
PHE	4648	138	0.005	0.95	NS	NS	0.3	0.74
ANT	*NA*	*NA*	*NA*	*NA*	*NA*	*NA*	*NA*	*NA*
FLA	217	6	0.04	0.79	NS	NS	0.7	0.08
PYR	662	20	0.04	0.93	*NA*	*NA*	*NA*	*NA*

Table 4.4: Correlation coefficients (R) (p-value < 0.05) between SOCs and submicron aerosols, CO, water vapor (WV), and O_3 concentrations. **A)** 2004-2006 data and **B)** spring 2006 data only. NS (not significant, p-value > 0.05), p-value > 0.05. NA (not available), recovery-corrected data for FTOHs was only available in the Spring 2006 data set.

A) 2004-2006

	Submicron Aerosol	CO	WV	O_3
Σgas-phase PAHs	NS	-0.31	0.36	NS
Σpart-phase PAHs	0.78	0.72	NS	NS
ΣFTOHs	NA	NA	NA	NA
ΣPCBs	0.42	NS	NS	NS
Retene	NS	NS	NS	NS
Levoglucosan	0.46	NS	NS	NS
1,3,5-triphenylbenzene	NS	NS	NS	NS

B) Spring 2006 (INTEX-B)

	Submicron Aerosol	CO	WV	O_3
Σgas-phase PAHs	NS	-0.48	0.40	-0.44
Σpart-phase PAHs	0.60	NS	NS	NS
ΣFTOHs	NS	NS	0.42	-0.44
ΣPCBs	NS	-0.55	0.63	-0.73
Retene	NS	NS	NS	NS
Levoglucosan	0.46	NS	NS	NS
1,3,5-triphenylbenzene	NS	NS	NS	NS

Literature Cited

(1) Jaffe, D.; Prestbo, E.; Swartzendruber, P.; Weiss-Penzias, P.; Kato, S.; Takami, A.; Hatakeyama, S.; Kajii, Y. Export of atmospheric mercury from Asia *Atmospheric Environment* **2005**, *39*, 3029-3038.

(2) Bailey, R.; Barrie, L. A.; Halsall, C. J.; Fellin, P.; Muir, D. C. G. Atmospheric organochlorine pesticides in the western Canadian Arctic: Evidence of transpacific transport *J Geophys Res-Atmos* **2000**, *105*, 11805-11811.

(3) Harner, T.; Shoeib, M.; Kozma, M.; Gobas, F. A. P. C.; Li, S. M. Hexachlorocyclohexanes and endosulfans in urban, rural, and high altitude air samples in the Fraser Valley, British Columbia: Evidence for trans-Pacific transport *Environ Sci Technol* **2005**, *39*, 724-731.

(4) Killin, R. K.; Simonich, S. L.; Jaffe, D. A.; DeForest, C. L.; Wilson, G. R. Transpacific and regional atmospheric transport of anthropogenic semivolatile organic compounds to Cheeka Peak Observatory during the spring of 2002 *J Geophys Res-Atmos* **2004**, *109*, D23S15.

(5) Weiss-Penzias, P.; Jaffe, D. A.; Swartzendruber, P.; Dennison, J. B.; Chand, D.; Hafner, W.; Prestbo, E. Observations of Asian air pollution in the free troposphere at Mount Bachelor Observatory during the spring of 2004 *J Geophys Res-Atmos* **2006**, *111*, D10304.

(6) Weiss-Penzias, P.; Jaffe, D.; Swartzendruber, P.; Hafner, W.; Chand, D.; Prestbo, E. Quantifying Asian and biomass burning sources of mercury using the Hg/CO ratio in pollution plumes observed at the Mount Bachelor observatory *Atmospheric Environment* **2007**, *41*, 4366-4379.

(7) Piekarz, A.; Primbs, T.; Field, J. A.; Barofsky, D. F.; Simonich, S. Semi-volatile Fluorinated Organic Compounds in Asian and Pacific Northwestern U.S. Air Masses *Environ. Sci. Technol.* **Submitted June 2007**.

(8) Primbs, T.; Simonich, S.; Schmedding, D.; Wilson, G.; Jaffe, D.; Takami, A.; Kato, S.; Hatakeyama, S.; Kajii, Y. Atmospheric Outflow of Anthropogenic Semivolatile Organic Compounds from East Asia in Spring 2004 *Environ Sci Technol* **2007**, *41*, 3551-3558.

(9) Hafner, W. D.; Carlson, D. L.; Hites, R. A. Influence of local human population on atmospheric polycyclic aromatic hydrocarbon concentrations *Environ Sci Technol* **2005**, *39*, 7374-7379.

(10) Simoneit, B. R. T.; Schauer, J. J.; Nolte, C. G.; Oros, D. R.; Elias, V. O.; Fraser, M. P.; Rogge, W. F.; Cass, G. R. Levoglucosan, a tracer for cellulose in biomass burning and atmospheric particles *Atmospheric Environment* **1999**, *33*, 173-182.

(11) Ramdahl, T. Retene-a molecular marker of wood combustion in ambient air *Nature* **1983**, *306*, 580-582.

(12) Simoneit, B. R. T.; Medeiros, P. M.; B.M., D. Combustion Products of Plastics as Indicators for Refuse Burning in the Atmosphere *Environ Sci Technol* **2005**, *39*, 6961-6970.

(13) Kim, K. S.; Hirai, Y.; Kato, M.; Urano, K.; Masunaga, S. Detailed PCB congener patterns in incinerator flue gas and commercial PCB formulations (Kanechlor) *Chemosphere* **2004**, *55*, 539-553.

(14) Xu, S.; Liu, W.; Tao, S. Emission of Polycyclic Aromatic Hydrocarbons in China *Environ. Sci. Technol.* **2006**, *40*, 702-708.
(15) Simoneit, B. R. T.; Kobayashi, M.; Mochida, M.; Kawamura, K.; Lee, M.; Lim, H. J.; Turpin, B. J.; Komazaki, Y. Composition and major sources of organic compounds of aerosol particulate matter sampled during the ACE-Asia campaign *J Geophys Res-Atmos* **2004**, *109*, -.
(16) Hafner, W. D.; Hites, R. A. Potential sources pesticides, PCBs, and PAHs to the atmosphere of the Great Lakes *Environ Sci Technol* **2003**, *37*, 3764-3773.
(17) Daly, G. L.; Wania, F. Organic Contaminants in Mountains *Environ. Sci. Technol.* **2005**, *39*, 385-398.
(18) Hageman, K. J.; Simonich, S. L.; Campbell, D. H.; Wilson, G. R.; Landers, D. H. Atmospheric deposition of current-use and historic-use pesticides in snow at national parks in the Western United States *Environ Sci Technol* **2006**, *40*, 3174-3180.
(19) Usenko, S.; Hageman, K. J.; Schmedding, D. W.; Wilson, G. R.; Simonich, S. L. Trace analysis of semivolatile organic compounds in large volume samples of snow, lake water, and groundwater *Environ Sci Technol* **2005**, *39*, 6006-6015.
(20) Swartzendruber, P. C.; Jaffe, D. A.; Prestbo, E. M.; Weiss-Penzias, P.; Selin, N. E.; Park, R.; Jacob, D. J.; Strode, S.; Jaegle, L. Observations of reactive gaseous mercury in the free troposphere at the Mount Bachelor Observatory *J Geophys Res-Atmos* **2006**, *111*, -.
(21) Primbs, T.; Genualdi, S.; Simonich, S. Optimization of Solvent Composition for Pressurized Liquid Extraction of Polymeric Sorbents Used in Air Sampling *Journal of Chromatography A* **Submitted July 2007**.
(22) Medeiros, P. M.; Simoneit, B. R. T. Analysis of sugars in environmental samples by gas chromatography-mass spectrometry *Journal of Chromatography A* **2007**, *1141*, 271-278.
(23) Method 8280A, E.P.A. The analysis of polychlorinated dibenzo-p-dioxins and polychlorinated dibenzofurans by high-resolution gas chromatography/low resolution mass spectrometry (HRGC/LRMS). http://www.epa.gov/epaoswer/hazwaste/test/pdfs/8280a.pdf
(24) Draxler, R. R.; Rolph, G. D. HYSPLIT (HYbrid Single-Particle Lagrangian Integrated Trajectory) Model access via NOAA ARL READY Website (http://www.arl.noaa.gov/ready/hysplit4.html). NOAA Air Resources Laboratory, Silver Spring, MD. **2003**.
(25) McNamara, D.; Stephens, G.; Ramsay, B.; Prins, E.; Csiszar, I.; Elvidge, C.; Hobson, R.; Schmidt, C. Fire Detection and Monitoring Products at the National Oceanic and Atmospheric Administration *Photogrammetric Engineering & Remote Sensing* **2002**, *68*.
(26) Singh, H. B.; Brune, W. H.; Crawford, J. H.; Fuelberg, H.; Jacob, D. J. The Intercontinental Chemical Transport Experiment – Phase B (INTEX-B): An update (http://cloud1.arc.nasa.gov/intex-b/) **2006**.
(27) Bernhard, M. J.; Simonich, S. L. Use of a Bench-top Photchemical Reactor and Solid-phase Microextraction to Measure Semivolatile Organic Compound-Hydroxyl Radical Rate Constants *Environ Toxicol Chem* **2000**, *19*, 1705-1710.

(28) Garivait, H.; Polprasert, C.; Yoshizumi, K.; Reutergardh, L. B. Airborne polycyclic aromatic hydrocarbons (PAH) in Bangkok urban air: Part II. Level and distribution *Polycycl Aromat Comp* **2001**, *18*, 325-350.

(29) Eckhardt, S.; Breivik, K.; Manø, S.; Stohl, A. Record high peaks in PCB concentrations in the Arctic atmosphere due to long-range transport of biomass burning emissions *Atmospheric Chemistry and Physics Discussions* **2007**, *7*, 6229-6254.

(30) Wania, F. H., J-E.; Lei, Y.; Mackay D. Temperature Dependence of Atmospheric Concentrations of Semivolatile Organic Compounds *Environ. Sci. Technol.* **1998**, *32*, 1013-1021.

(31) Carlson, D. L.; Hites, R. A. Temperature dependence of atmospheric PCB concentrations *Environ Sci Technol* **2005**, *39*, 740-747.

(32) Xu, S.; Liu, W.; Tao, S. Emission of Polycyclic Aromatic Hydrocarbons in China *Environ Sci Technol* **2006**, *40*, 702-708.

(33) Wu, C. Y.; Nelson, C.; Cabrera-Rivera, O.; Quan, J.; Asselmeier, D.; Baker, G.; McGeen, D. M.; McDonough, R.; Sliwinski, R.; Altenburg, R.; Velalis, T.; Judson, H.; Wong, P.; Wagemakers, J.; Moy, D. *Analysis of Air Toxics Emission Inventories for Area Sources in the Great Lakes Region*; U.S. Environmental Protection Agency: Washington, DC, 2001.

(34) Eiguren-Fernandez, A.; Miguel, A. H.; Froines, J. R.; Thurairatnam, S.; Avol, E. L. Seasonal and Spatial Variation of Polycyclic Aromatic Hydrocarbons in Vapor-Phase and PM2.5 in Southern California Urban and Rural Communities *Aerosol Sci Tech* **2004**, *38*, 447-455.

(35) Frame, G. M.; Wagner, R. E.; Carnaha, J. C.; Brown, J. F.; May, R. J.; Smullen, L. A.; Bedard, D. L. Comprehensive, Quantitative, Congener-Specific Analyses of Eight Arochlors and Complete PCB Congener Assignments on DB-1 Capillary GC Columns *Chemosphere* **1996**, *33*, 603-623.

(36) Stohl, A. Computation, Accuracy, and Applications of Trajectories-A Review and Bibliography *Atmospheric Environment* **1998**, *32*, 947-966.

(37) Stock, N. L.; Lau, F. K.; Ellis, D. A.; Martin, J. W.; Muir, D. C. G.; Maybury, S. A. Perfluorinated Telomer Alcohols and Sulfonamides in the North American Troposphere *Environ Sci Technol* **2004**, *38*, 991-996.

(38) Ellis, D. A.; Martin, J. W.; Mabury, S. A.; Hurley, M. D.; SulbaekAndersen, M. P.; Wallington, T. J. Atmospheric Lifetime of Fluorotelomer Alcohols *Environ. Sci. Technol.* **2003**, *37*, 3816-3820.

CHAPTER 5. INFLUENCE OF ASIAN AND WESTERN U.S. AGRICULTURAL AREAS AND FIRES ON THE ATMOSPHERIC TRANSPORT OF PESTICIDES IN THE WESTERN U.S.

Toby Primbs[1], Glenn Wilson[2], David Schmedding[2], Carol Higginbotham[4], and Staci Simonich[1,2*]

[1]Department of Chemistry, Oregon State University, Corvallis, Oregon
[2]Department of Environmental and Molecular Toxicology, Oregon State University, Corvallis, Oregon
[3]University of Washington-Bothell, Bothell, WA
[4]Department of Science, Central Oregon Community College, Bend, Oregon

*Corresponding Author: Telephone, 1-541-737-9194; Fax, 1-541-737-0497; email, staci.simonich@oregonstate.edu

Abstract

Historic and current use pesticides (HUPs and CUPs), with respect to the United States, were identified in trans-Pacific and regional air masses at Mt. Bachelor Observatory (MBO), a remote high elevation mountain in the Western U.S., during the sampling period of April 2004 to May 2006 (n=69), including NASA's INTEX-B campaign (Spring 2006). Enhanced HUP (hexachlorobenzene (HCB), α-hexachlorocyclohexane (α-HCH)) and γ-HCH concentrations occurred during trans-Pacific atmospheric transport. Regional atmospheric transport resulted in enhanced CUP concentrations (γ-HCH, dacthal, endosulfan, metribuzin, triallate, trifluralin, and chlorpyrifos), with episodic concentration enhancements during spring application periods. Endosulfan I, γ-HCH, and dacthal concentrations were significantly positively correlated (p-value < 0.05) with increased air mass time in regional agricultural areas in the Western U.S., while enhanced Σchlordane, HCH, HCB, and trifuralin concentrations were associated with fires due to volatization of pesticides deposited to soils and vegetation. Trans-chlordane/cis-chlordane and α-HCH/γ-HCH ratios were significantly different in "aged" free tropospheric air masses (0.87 ± 0.05 and 5.2 ± 0.8, respectively), regional boundary layer air masses (1.4 ± 0.1 and 2.9 ± 0.3, respectively), and Asian boundary layer air masses (1.2 ± 0.1 and 2.5 ± 0.2, respectively). These ratios may be used to distinguish between regional, Asian, and aged air masses.

Introduction

Evidence of trans-Pacific atmospheric transport of combustion byproducts (e.g. CO, Hg^0) and semivolatile organic compounds (SOCs), including pesticides, is growing *(1-7)* and the outflow of SOCs from Asia was recently reported *(8)*. Coupling

measurements of pesticides in trans-Pacific air masses on the West Coast of North America with measurements in Asian air masses, near source regions, may result in the identification of unique molecular markers for specific source regions based on regional pesticide use patterns.

Previous research investigating the trans-Pacific atmospheric transport of pesticides has focused on organochlorine pesticides *(2-4)*. Using aircraft measurements in the Western U.S. Harner et al. found elevated α-hexachlorocyclohexane (α-HCH) concentrations in the mid-troposphere due to trans-Pacific atmospheric transport but no enhancement at a ground based site *(3)*. In addition, Bailey et al. found increasing concentrations of HCHs with increasing air mass time in Asia *(2)*. Killin et al. reported enhancements of both current-use (e.g. chlorothalonil, trifluralin, triallate and endosulfans) and historic-use (e.g. mirex, cis-nonachlor, and HCB) pesticides in trans-Pacific transport events, although HCHs were not detected *(4)*.

Pesticides may enter the atmosphere during application (e.g. spray drift), wind erosion of particles with sorbed pesticides, and/or volatization from previous applications *(9,10)*. Once in the atmosphere, pesticides may be transported far from their use regions to remote locations such as the Arctic or high elevation ecosystems *(11,12)*. In addition, mid-latitude mountains serve as local areas of convergence for SOCs *(13)* and regional agricultural pesticide usage has been reported to have an impact on remote high elevation mountains in the Western U.S. *(10,12)*. The objectives of this research were: (1) to measure current use and historic use pesticides (CUPs and HUPs) at a remote high elevation mountain site in the Western U.S.; (2) determine the source regions for CUPs

and HUPs; and (3) identify differences and similarities in pesticide profiles of trans-Pacific and Western U.S. air masses.

Experimental

Chemicals

The pesticides and pesticide degradation products detected in this study included trifluralin, hexachlorobenzene (HCB), α- and γ-hexachlorocyclohexane (α-HCH and γ-HCH), metribuzin, dacthal, chlorpyrifos, chlorpyrifos oxon, trans and cis chlordane (TC, and CC), trans and cis nonachlor (TN and CN), endosulfan I and II, endosulfan sulfate, and dieldrin. A matrix interferant prevented the measurement of heptachlor. A complete list of targeted pesticides, including those not detected, isotopically labeled standards used for quantification, and solvents has been previously reported *(8,14)*.

Sampling Site

Figure 5.1 shows the location of Mt. Bachelor Observatory (MBO) (43.98°N 121.69°W, 2763 m above sea level) in Oregon's Cascade Range *(1,5-7,15)*. Figure 5.1 also shows the agricultural intensive areas in Western North America. Air sampling was conducted at the summit building and access to the site was limited during extreme weather and lift maintenance. Other simultaneous measurements included: submicron aerosols (nephelometer), reactive gaseous mercury, particulate-phase mercury, Hg^0, NO, NO_x, CO, O_3, Rn, meteorology, and water vapor mixing ratio (g/kg) conducted by the Jaffe group (University of Washington-Bothell) *(1,5,6,15)*. Measurements of polycyclic aromatic hydrocarbons (PAHs), polychlorinated biphenyls (PCBs), and fluorotelomer alcohols (FTOHs) during this same sampling period have been previously reported *(7,16)*.

Sample Collection, Extraction, and Analysis

Details of sample collection, extraction, and analysis are reported in Chapter 4. In brief, sixty-nine SOC air samples were collected from the 19th of April 2004 to the 13th of May 2006, of which NASA's INTEX-B campaign was in spring 2006 (n= 34 of 69), at MBO with a modified high volume air sampler (Tisch Environmental, Cleves, OH) over 24 hour periods (~644 m^3) *(7)*. The sample collection, extraction, and analysis for these samples have been reported previously *(7)*. Quartz fiber filters (Whatman, England) were used to collect the particulate-phase and polyurethane foam (PUF)-(XAD-2)-PUF sandwich (Tisch Environmental, Ohio; Supelco, Pennsylvania) was used to collect the gas-phase. ASE (Dionex, California) cleaning and extraction has been previously reported in detail *(7,8)*. Sample analysis was conducted with gas chromatographic mass spectrometry (GC/MS) in selective ion monitoring (SIM) mode with both negative chemical ionization (NCI) and electron impact (EI) ionization modes *(8,14)*. Additional information on sample collection, extraction and analysis is provided in supporting information.

Trajectories and Data Analysis

Ten-day air mass back trajectories were calculated using NOAA's ARL HYSPLIT 4.0 model (FNL) *(17)*. Back trajectories were calculated at three elevations above model ground level 1300, 1500, and 1700 m, every three hours over the twenty-four hour sampling period (including start and stop time) to determine the time spent in designated source regions (27 trajectories per sample). The trajectories were imported into ArcGIS (ESRI, Redlands, California) for spatial representation and S-PLUS version 7.0 (Insightful, Seattle, Washington) was used for statistical analysis.

Results

Identification of Air Mass Source Regions

The sampling dates, site temperature, wind speed, and wind direction for the samples collected are reported elsewhere *(7)*. Thirty-five air samples were initially collected over the first two year sampling period (April 2004 to March 2006) and an additional thirty-four samples were collected in spring 2006 (April-May 2006) in conjunction with NASA's Intercontinental Transport Experiment (INTEX-B) *(18)*. The predominant wind direction on the days sampled was from the west-northwest and west *(7)*.

Figure 5.1 shows the agricultural intensive source regions in the Western U.S. as represented by percent cropland on the county scale *(19)*. Figure 5.2 shows the 1997 estimated pesticide usage maps in kilograms per 1° x 1° cell for the CUPs (dacthal, endosulfan, trifluralin, chlorpyrifos, triallate, and metribuzin) and trajectories for samples with enhanced CUP concentrations *(20)*. Estimated 2002 agricultural pesticide usage was recently reported, however GIS data was not available for the 2002 pesticide usage estimates to compare directly air parcel transport from agricultural usage areas. In general, the 1997 usage maps are very similar to the 2002 maps for the current use pesticides discussed herein. Lindane (primarily γ-HCH), a CUP used as a seed treatment, is not represented in the usage maps. However, the state of Washington holds active labels for its use as a seed treatment *(21)*.

Agricultural intensive regions in the Western U.S. were identified based on percent cropland and pesticide usage maps and a box was made around these areas *(12,19)*. Figures 5.1B shows the agricultural source regions (solid boxes) identified to

assess regional atmospheric transport of pesticides from East Asia and the Western U.S. to MBO. The potential source regions in the Western U.S. included: Eastern Oregon/Washington, Western Oregon (Willamette Valley), and Central California. In East Asia, two source regions were identified: the first was a more agriculturally intensive area including China, Koreas, and Japan (Asia); and the second was Eastern Russia (Siberia) with less agricultural intensity (Figures 5.1A and 5.1C) *(2)*.

Source region impact factors (SRIFs), the percentage of time a back trajectory spent in a designated source region compared to the total trajectory time, were calculated with ten-day back trajectories. Details of the SRIF calculations are reported elsewhere *(7,8)*. Figure 5.3 shows the SRIFs for the different agricultural source regions. Figure 5.4 shows the impact of each individual source region divided by the total air mass time spent in all source regions [Σ (Siberia, Asia, Eastern Oregon/Washington, Western Oregon, and Central California)]. Increased air mass time in Eastern Oregon/Washington occurred primarily during the spring and fall, while increased air mass time in Central California occurred primarily in late winter and spring. Increased air mass time in the Western Oregon occurred in late spring and summer, with occasional periods of enhanced SRIFs in other seasons. Increased air mass time in Asia primarily occurred during the spring and winter, while enhanced Siberian SRIFs occurred throughout the year.

Meteorological Influences

The only pesticide that was significantly positively correlated (p-value < 0.05) with wind speed was chlorpyrifos, and none of the detected pesticides were significantly correlated (p-value > 0.05) with wind direction. Pesticide volatization during application

and/or after application from soils is a major route of pesticide entry to the atmosphere *(22)*. To assess the impacts of temperature on pesticide concentrations, the Clausius-Clapeyron equation was used *(8,23,24)* and MBO site temperatures below 273 K were replaced with 273 K *(24)*.

Table 5.1 shows the statistically significant slope parameters (p-value < 0.05) for log HCB, α-HCH, γ-HCH, trans-chlordane, cis-chlordane, trans-nonachlor, trifluralin, dacthal, and endosulfan I concentrations versus 1000/T. These slopes were similar to previous studies *(23)* and the variability in pesticide concentrations are, in part, explained by volatization.

Weiss-Penzias et al. *(5)* previously reported using the water vapor mixing ratio (WV) at MBO as a good indicator of boundary layer (wet) and free tropospheric (dry) air. During spring 2006, statistically significant positive correlations (p-value < 0.05) existed between WV and metribuzin concentrations, indicating increased metribuzin concentrations were associated with boundary layer air. Significant negative correlations existed between WV and Σendosulfan and α-HCH concentrations. Anticyclonic systems associated with subsiding air masses in the Pacific Northwest of North America often are associated with back trajectories passing over the agricultural intensive region in Eastern Oregon/Washington. An example of this is shown in Figure 5.2 (23-24 Apr 2006). Thus, in addition to increases in free tropospheric air, decreases in WV may also be indicative of impacts from Eastern Oregon/Washington. Higher concentrations of α-HCH in the mid troposphere, compared to ground based sites, have been attributed to Asian sources *(3)* and may be due to trans-Pacific transport. However endosulfan air concentrations are higher in the Pacific Northwest of North America than in Asia *(25)* and elevated

concentrations of endosulfans at MBO may be due to agricultural uses in Eastern Oregon/Washington.

Trans-Pacific and Regional Atmospheric Transport

Historic Use Pesticides

Figure 5.5 shows the temporal profile for CUPs and HUPs over the sampling period. HUPs (i.e. HCB and α-HCH) were more frequently detected than CUPs; where FOD% (frequency of detection) was HCB (100%) and α-HCH (100%) > γ-HCH (90%) > chlordanes (includes nonachlors) (~80%) > dieldrin (7%). The concentration ranges of HUPs were: HCB (18 to 94 pg/m^3); α-HCH (2 to 43 pg/m^3); trans-chlordane (<DL to 5 pg/m^3); cis-chlordane (<DL to 3 pg/m^3); trans-nonachlor (<DL to 2 pg/m^3); and dieldrin (<DL to 4 pg/m^3).

Even though Mt Bachelor Observatory (MBO) receives primarily free tropospheric air in the winter time, the concentrations of HCHs and HCB did not drop significantly in winter samples (Figure 5.5). Significant HCB and HCH concentrations exist in the the upper troposphere. For example, a sample collected on 15-16 of April 2006 and on 12-13 of May 2006 were primarily influenced by Siberia (Figure 5.3), and concentrations of CUPs and chlordanes were low to not detected, while HCB and HCH concentrations did not change significantly compared to the rest of spring 2006. The Σchlordanes showed a more pronounced enhancement in concentrations in the spring and summer compared to α-HCH and HCB.

Technical HCH was a source of γ-HCH, and it was the primary source of α-HCH to the environment. Use of technical HCH were canceled in the U.S. and Canada in 1978 and 1971, respectively *(26)*. Although technical HCH was banned in China in 1983 *(27)*,

the facilities that produced technical HCH were not shut down until 2000 *(28)*. Recent measurements of Asian air masses showed elevated concentrations of α-HCH associated with increased air mass time in China *(8)*.

The α-HCH concentrations at MBO were significantly positively correlated (p-value < 0.05) with: HCB, γ-HCH, trifluralin, Σgas-phase PAH, Σparticulate-phase PAHs, and retene concentrations (Table 5.2). The significant correlations between α-HCH concentrations and markers for Asian air masses (Σparticulate-phase PAHs), in addition to markers for regional fires (Σgas-phase PAHs and retene), suggests that both trans-Pacific atmospheric transport and fires lead to enhanced α-HCH concentrations. The highest concentrations of α-HCH were measured during a trans-Pacific transport event on 25-26 April 2004 (Figures 5.5 and 5.3). Eckhardt et al recently reported elevated HCH, DDT, and PCB concentrations associated with fires suggesting the increase was due to volatization from previously contaminated soils and vegetation *(29)*. During an Alaska/Canada fire event on 11-12 July 2004, increased concentrations of α-HCH were measured.

Water vapor mixing ratio data was available for 53 of the 69 samples and the 53 samples were divided into two groups, using the median water vapor (2.52 g/kg) as the divider. The air samples corresponding to a water vapor mixing ratio greater than the median (wet, boundary layer air) were compared to the ratio in samples corresponding to a mixing ratio less than the median (dry, free tropospheric air) using a Students t-test. A significantly higher (p-value, 0.01) α/γ HCH ratio was measured in the free tropospheric air, average ratio (±standard error) of 5.2 ± 0.8, compared to the boundary layer air, 2.9 ±

0.3. The α-HCH isomer has a 25% longer atmospheric lifetime, based on reactions with the OH radical, compared to γ-HCH *(30)*.

The average (±standard error) α/γ-HCH ratio measured near Asia in Spring 2004 was 2.5 ± 0.2. During a relatively fast (i.e. ~5-6 days) trans-Pacific atmospheric transport event from Asia to MBO (25-26 April 2004) a ratio of 1.5 was measured, which was similar to Asian measurements (Figures 5.1 and 5.6A). Shen et al reported annual average α/γ HCH ratios for multiple sites in North America *(31)*. The 7 sites in Western Canada had an average (±standard error) of 5.2 ± 0.7, with the ratio dropping significantly to 0.2 as the sites continued inland to the Canadian Prairies due to the usage of lindane (γ-HCH) as a seed treatment *(31)*.

During periods of increased air mass time over the Pacific Ocean and Siberia (e.g. 9-10 Jan 2005, 6-7 Feb 2005, 15-16 April 2006, 8-9 May 2006, and 12-13 May 2006) the α/γ ratio was also higher (Figure 5.6A). During spring 2006 the α/γ HCH ratio (5.6 ± 0.9) was similar to the α/γ HCH ratio (5.2 ± 0.8) in the upper troposphere. It appears that during periods of relatively fast (<10 days) trans-Pacific transport and/or regional transport, the ratio is lower (Figure 5.6A). Thus, a lower ratio (2.9 ± 0.3) is reflective of impacts from agricultural regions in both the U.S. and in Asia and a higher ratio (5.2 ± 0.8) is reflective of a more aged air mass with increased time over the Pacific Ocean, Arctic, and/or Siberia.

HCB sources include use as a fungicide, which was canceled in U.S. and Canada 1984 and 1972, respectively *(26)*, and as an industrial byproduct, combustion byproduct, and contaminant in pesticides (e.g. dacthal) *(32)*. The major source of HCB to the

atmosphere is thought to be volatization from past uses *(32)*. However, increasing HCB concentrations have been reported to be associated with Chinese air masses *(8)*.

Elevated concentrations of HCB at MBO occurred during late spring and summer, and when the source region was Asia (e.g. 25-26 Apr 2004) (Figures 5.5 and 5.3). HCB concentrations were significantly positively correlated (p-value < 0.05) with: α-HCH, γ-HCH, Σchlordane, trifluralin, ΣPCB, Σgas-phase PAH, Σparticulate-phase PAH, and retene concentrations, while negatively correlated with chlorpyrifos concentrations. Slightly elevated concentrations of HCB were measured in samples influenced by fires in Alaska/Canada (11-12 July 2004) and Western Oregon (9-10 August 2005) *(7)*.

Dieldrin was used as a pesticide and is a degradation product of aldrin. Dieldrin uses were limited to use as a termiticide in 1974, followed by cancellation in 1987. Dieldrin was only measured in the spring 2006 samples, on 11-12 Apr, 12-13 Apr, 29-30 Apr, 10-11 May, and 11-12 May at concentrations of ~3 pg/m^3. During 11-13 April 2006, the air mass was associated with Central California; whereas on the 29-30 Apr and 10-12 May 2006 the air masses were associated with Western Oregon (Figure 5.3).

Following a major cancellation of chlordane uses in 1983, it was limited to use for subterranean termites from 1983 to 1988 *(33)*. In a global passive air sampling study, some of the highest concentrations of chlordane were associated with California *(25)*. Increased chlordane concnetrations have also been associated with urban areas, compared to rural areas *(25,34)*.

The Σchlordane concentrations were significantly positively correlated (p-value < 0.05) with: HCB, γ-HCH, Σendosulfan, trifluralin, ΣPCB, Σgas-phase PAH, retene, and levoglucosan concentrations (Table 5.2). Enhanced chlordane concentrations were

measured in air masses that had spent considerable time in Central California; 24-25 April 2005, 7-8 May 2005, 12-13 May 2005, 27-28 May 2005, 4-5 April 2006, and 12-13 April 2006 (Figures 5.5 and 5.3). Lower chlordane concentrations were significantly associated (p-value < 0.05) with increasing air mass time in Siberia (Figure 5.7). The chlordane concentrations were lower in trans-Pacific air masses and in aged air masses that had spent significant time in Siberia or the Pacific Ocean (Figure 5.3).

The highest Σchlordane concentrations were measured during the 9-10 of Aug 2005 regional fire event and elevated concentrations on 11-12 of July 2004 were associated with fires in Alaska/Canada. The statistically significant correlation between Σchlordane concentrations and Σgas-phase PAH, levoglucosan, and retene concentrations provide further evidence that fires result in volatization of chlordanes stored in soils and vegetation.

A significantly higher (p-value, 0.02) trans-chlordane/cis-chlordane (TC/CC) ratio was measured in boundary layer air (1.39 ± 0.1), compared to free tropospheric air (0.87 ± 0.05), using median water vapor mixing ratio as a border. The technical chlordane used in North America has been reported to have a TC/CC ratio of 1.0-1.26 *(2,11,35)*. TC is more susceptible to microbial degradation and photodegradation compared to CC and a more aged source should be associated with a lower ratio (< 1.0) *(2,11)*.

The trans-chlordane/trans-nonachlor (TC/TN) ratio is also shown in Figure 5.6C and no seasonal trend was present. Also in more aged air masses over the Pacific Ocean and Siberia (e.g. 9-10 Jan 2005, 6-7 Feb 2005, and 12-13 May 2006) the ratio could not be calculated because the chlordanes were below the detection limit. The TC/TN ratio was significantly positively correlated (p-value, 0.006) with the TC/CC ratio, indicating that

increases in both ratios are indicative of shorter transport time from un-weathered chlordane from the Western U.S. to MBO.

Current-Use Pesticides

Figure 5.5 shows the temporal variation in the CUP concentrations. The most frequently detected CUPs, FOD%, were γ-HCH (90%) > endosulfan I (80%) and dacthal (75%) > trifluralin (36%) > chlorpyrifos (26%) > metribuzin (9%) and triallate (7%). The FOD% for the degradation products chlorpyrifos oxon and endosulfan sulfate was 6% and 30%, respectively. Metribuzin and triallate were only measured in spring 2006 samples.

The concentrations of CUPs were: dacthal (<DL to 352 pg/m^3); endosulfan I (<DL to 255 pg/m^3); endosulfan II (<DL to 33 pg/m^3); endosulfan sulfate (<DL to 4 pg/m^3); γ-HCH (<DL to 29 pg/m^3); chlorpyrifos (<DL to 6 pg/m^3); chlorpyrifos oxon (<DL to 58 pg/m^3); metribuzin (<DL to 7 pg/m^3); triallate (<DL to 36 pg/m^3); and trifluralin (< DL to 2 pg/m^3) (Figure 5.5). Concentrations of CUPs were generally low in the winter, with sporadic increases in concentration in the spring, summer, and fall likely due to current applications (Figure 5.5).

Lindane, which is primarily γ-HCH, has been used as an organochlorine insecticide in warehouses, for public health purposes, and as a seed treatment *(33)*. Sources of γ-HCH include both current uses (lindane) and historic uses (as part of technical HCH). In 2004, uses of γ-HCH as a seed treatment in Canada were banned *(36)*. Active labels, for use as a seed treatment, were in effect during the MBO sampling periods in Washington state. However, there were no active registrations in California, Oregon, British Columbia, or Alaska *(21)*. Lindane continues to be produced and used in Asia *(37)*.

The γ-HCH concentrations were significantly positively correlated (p-value < 0.05) with: HCB, α-HCH, Σchlordane, trifluralin, Σendosulfan, ΣPCBs, Σparticulate-phase PAH, Σgas-phase PAH, retene, and levoglucosan concentrations (Table 5.2). The correlations between γ-HCH concentrations and markers for trans-Pacific atmospheric transport (particulate-phase PAHs), in addition to markers for biomass combustion (retene and levoglucosan), suggest that both trans-Pacific transport and regional fires lead to enhanced γ-HCH concentrations *(7)*. The highest concentrations of γ-HCH were measured during a trans-Pacific transport event from Asia on 25-26 April 2004. The second highest concentrations of γ-HCH were measured on 9-10 August 2007, in an air mass that was influenced by fires in Western Oregon, and a moderate increase in γ-HCH was also measured during the Alaskan/Canadian fires (11-12 July 2004) *(7)*. Slightly elevated concentrations were also measured during periods when Eastern Oregon/Washington SRIFs were enhanced (23-24 April 2006, and 4-6 May 2006). The γ-HCH concentrations significantly decreased (p-value < 0.05) with increasing air mass time in Siberia and significantly increased (p-value < 0.05) with increasing air mass time in Eastern Oregon/Washington (Figure 5.7).

Dacthal (DCPA), a pre-emergent current use herbicide used as a weed control for annual grasses and broad-leaved weeds in turfs, ornamentals, vegetable and fruit crops, has a soil half life of 16-86 days *(38)*. Dacthal undergoes atmospheric transport *(12,39)*, and is used intensively in Eastern Oregon/Washington and Central California (Figure 5.2) *(40)*. Dacthal concentrations were significantly positively correlated (p-value < 0.05) with Σendosulfan concentrations only (Table 5.2). Western U.S. dacthal use areas overlap with endosulfan use areas (Figure 5.2). Enhancements in dacthal concentrations occurred

during mid to late spring (Figure 5.5), likely coinciding with application periods, and periods when Eastern Oregon/Washington SRIFs were also enhanced: 19-20 June 2004; 27-28 May 2005; 22-26 April 2006; and 4-6 May 2006 (Figures 5.2 and 5.3). Elevated dacthal concentrations were significantly positively correlated (p-value < 0.05) with increasing air mass time spent in Eastern Oregon/Washington (Figures 5.7 and 5.3).

Endosulfan is a broadly used current use insecticide and technical endosulfan is 70% endosulfan I and 30% endosulfan II *(41)*. Endosulfan I and II have been previously measured in air samples collected from rural and urban sites in British Columbia *(3)*. In addition, endosulfan is both associated with agricultural areas and used throughout the Western U.S. (Figure 5.2) and British Columbia, Canada *(25,40)*. Significant positive correlations (p-value < 0.05) existed between Σendosulfan concentrations and dacthal, γ-HCH, Σchlordane, ΣPCB, and retene concentrations (Table 5.2). Increasing concentrations were measured during the spring and summer and during periods when air masses spent considerable time in E. Oregon/Washington: 19-20 June 2004; 13-14 Mar 2005; 7-8 September 2005; 22-24 April 2006; and 4-6 May 2006 (Figures 5.5 and 5.3). Increased air mass time spent in E. Oregon/Washington was significantly positively correlated (p-value < 0.05) with increased endosulfan I concentrations (Figure 5.7).

To further investigate the sources of endosulfans to MBO, the ratio of endosulfan I concentrations to the sum of endosulfan I and II concentrations was calculated. The endosulfan I/(endosulfan I + endosulfan II) ratios were assessed in boundary layer and free tropospheric air using the median water vapor mixing ratio as a divider. No significant difference (p-value > 0.05) existed between the two groups of endosulfan ratios, with a free tropospheric average (±standard error) of 0.90 ± 0.01 and boundary

layer average (±standard error) of 0.88 ± 0.02. During spring 2004, the ratio measured in Asian air masses was similar to these ratios, with an average (±standard error) of 0.92 ± 0.01 *(8)*.

The Endosulfan I/ (Endosulfan I + Endosulfan II) ratio was fairly constant in spring, summer, and fall 2004-2006 (Figure 5.6D). Endosulfan II was not detected in winter samples and thus, a winter time ratio could not be calculated. During periods of increased air mass time over the Pacific Ocean and Siberia, endosulfan was not detected (e.g. 9-10 Jan 2005, 6-7 Feb 2005, and 12-13 May 2006) and during periods of increased air mass time in Asia and the Western U.S., the fraction was similar.

Volatization of trifluralin, a current use selective pre-emergence herbicide, after application, can be significant with loss of ~18% applied *(42)*. The majority of the use of trifluralin in the Western U.S. is in California, with some use in Washington and Oregon (Figure 5.2). Significant positive correlations (p-value < 0.05) existed between trifluralin concentrations and HCB, α-HCH, γ-HCH, Σchlordane, Σgas-phase PAH, ΣPCB, retene, and levoglucosan concentrations (Table 5.2). Enhanced trifluralin concentrations were measured during periods of impact from all designated source regions in the Western U.S.; when Western Oregon SRIFs were enhanced (21-22 Apr 2004, 25-26 Apr 2004, 10-11 May 2004, 9-10 August 2005, and 27-29 April 2006), when Eastern Oregon/Washington SRIFs were enhanced (7-8 Sept 2005), and when Central California SRIFs were enhanced (May 2005, 4-5 Apr 2006) (Figures 5.5 and 5.3). Trifluralin enhancements are indicative of regional transport and not trans-Pacific transport.

Significant positive correlations (p-value < 0.05) existed between NO concentrations and trifluralin concentrations existed the spring 2006, suggesting

trifluralin may be associated with highly populated agricultural regions in the Western U.S., such as Central California. Figure 5.3 shows the trajectories for the 4-5 Apr 2006 sample over Central California, which is both an agriculturally intensive and highly populated. Correlations between trifluralin concentrations and biomass combustion marker (retene and levoglucosan) concentrations also suggest fires are associated with increased trifluralin concentrations. The highest concentrations of trifluralin were measured on 9-10 August 2005, in an air mass influenced by fires in Western Oregon *(7)*.

Triallate and metribuzin were only measured in the spring 2006 data samples. Volatization of triallate, a pre-emergent current use herbicide *(33)*, after application is ~21% of applied triallate *(42)*. Triallate use in the Western U.S. is primarily located in Eastern Oregon/Washington (Figure 5.2) and enhanced triallate concentrations were measured in air masses with enhanced SRIFs from this region (22-25 April 2006) (Figure 5.3). These measurements are consistent with where triallate is used (Figure 5.2) and its spring time application. Metribuzin, a current use triazine herbicide *(33)*, concentrations were enhanced on 6-7 Apr 2006, 18-19 Apr 2006, and 4-6 May 2006 (Figure 5.5). Statistically significant (p-value < 0.05) decreases in concentration were associated with increasing air mass time spent in Eastern Oregon/Washington area (Figure 5.7).

Chlorpyrifos, a current use organophosphate insecticide, is one of the most frequently used pesticides in U.S. homes for roach and termite control *(43)*. It has been previously reported to be detected more frequently in urban areas than agricultural areas *(9)*. Chlorpyrifos concentrations were significantly negatively correlated (p-value < 0.05) with HCB and significantly positive correlations existed with NO concentrations. The correlation between NO and chlorpyrifos concentrations indicate increased

concentrations of chlorpyrifos are associated with highly populated regions in the Western U.S., such as Central California's. Enhanced chlorpyrifos concentrations occurred during periods of increasing air mass time in Central California (4-5 April 2006) and E. Oregon/Washington (13-14 March 2005 and 22-24 April 2006), reflecting the broad use of chlorpyrifos in the Western U.S. in urban areas as well as agricultural areas (Figures 5.5 and 5.3).

In summary, enhancements of pesticides occurred during trans-Pacific and regional transport, in addition to fire events. Enhanced HUP (hexachlorobenzene (HCB), α-hexachlorocyclohexane (α-HCH)) and γ-HCH concentrations occurred during trans-Pacific atmospheric transport. Regional atmospheric transport resulted in enhanced CUP concentrations (γ-HCH, dacthal, endosulfan, metribuzin, triallate, trifluralin, and chlorpyrifos), with episodic concentration enhancements during spring application periods. These results are in line with the estimated half lives for these pesticides, that is the pesticides with the longest half lives showed enhancements in trans-Pacific transport, and the pesticides with the shortest half lives showed enhancements in regional transport (Table 5.3). Enhanced Σchlordane, HCH, HCB, and trifuralin concentrations were associated with fires due to volatization of pesticides deposited to soils and vegetation. TC/CC and α/γ HCH ratios were significantly different in "aged" free tropospheric air masses (0.87 ± 0.05 and 5.2 ± 0.8, respectively) compared to regional boundary layer air masses (1.4 ± 0.1 and 2.9 ± 0.3, respectively) and Asian boundary layer air masses (1.2 ± 0.1 and 2.5 ± 0.2, respectively).

Acknowledgements

The authors would like to thank Dan Jaffe, Paul Hutter, Nat Bingham, Eugen Helmbrecht, James B. Dennison, Isaac Bertschi, Peter Weiss-Penzias, Phil Swartzendruber, and Jessica Murray. Mt. Bachelor Corporation, especially the lift maintenance crew. Will Hafner for the development of a Visual Basic trajectory analysis program. The research described in this paper has been funded in part by the United States Environmental Protection Agency (EPA) under the Science to Achieve Results (STAR) Graduate Fellowship Program to Toby Primbs. EPA has not officially endorsed this publication and the views expressed herein may not reflect the views of the EPA. We would also like thank National Science Foundation CAREER (ATM-0239823) for funding. This work was made possible in part by National Institute of Health (Grant # P30ES00210).

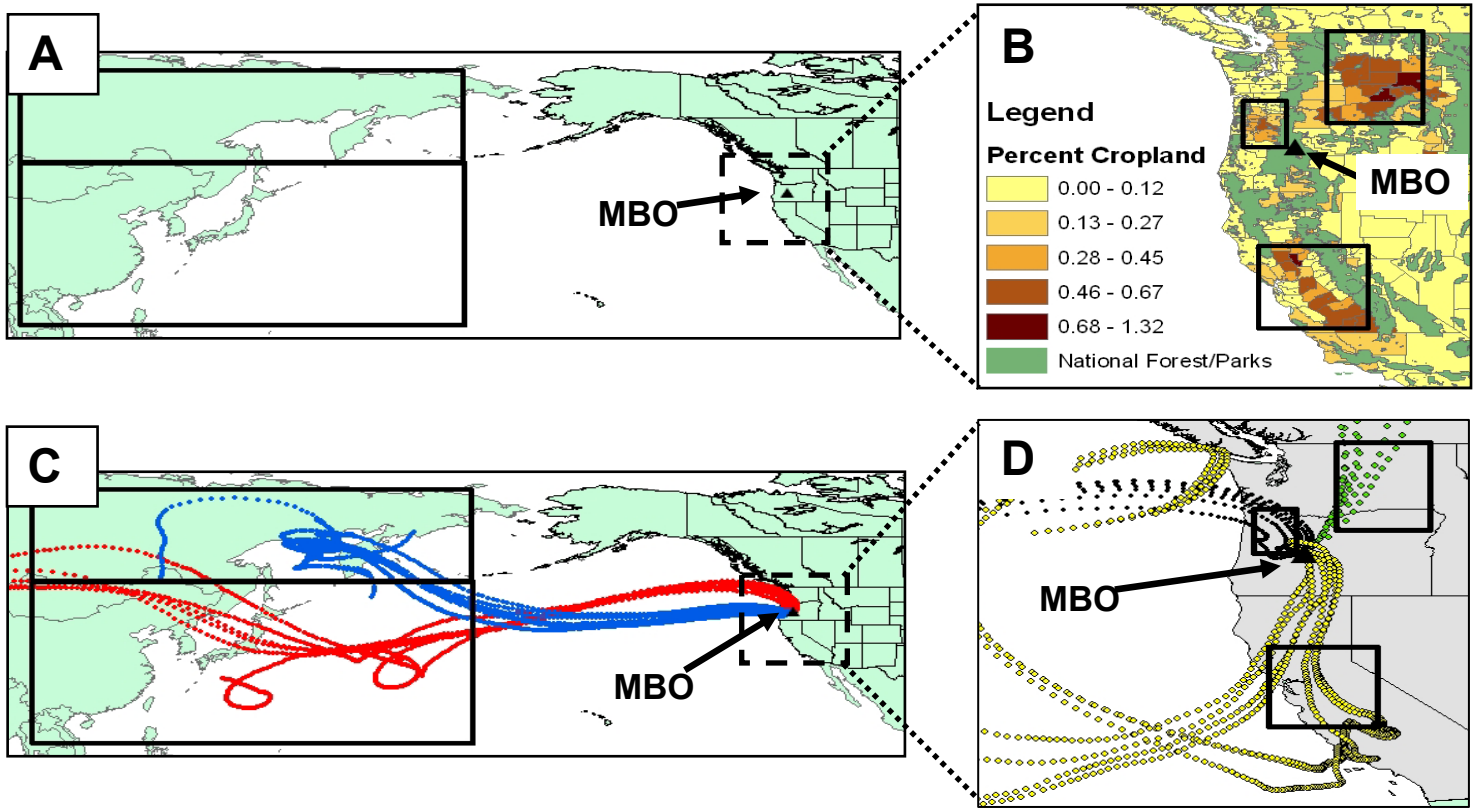

Figure 5.1: MBO, black triangle, (43.98°N 121.69°W, 2.7 km a.s.l.) is located in Oregon's Cascade Range. **A)** Asia and Siberia source regions (boxes) with respect to MBO. **B)** Zoomed in map of Western North America shows the percent cropland on the county level and in green is national parks/forests. Also shown are the Western Oregon, Eastern Oregon/Washington, and Central California source regions (boxes). **C)** Example trajectories 25-26 April 2004 (red, Asia) and 12-13 May 2006 (blue, Siberia). **D)** Zoomed in map of Western North America shows example trajectories 4-5 April 2006 (yellow, Central California), 13-14 March 2005 (green, Eastern Oregon/Washington), and 28-29 April 2006 (black, Western Oregon).

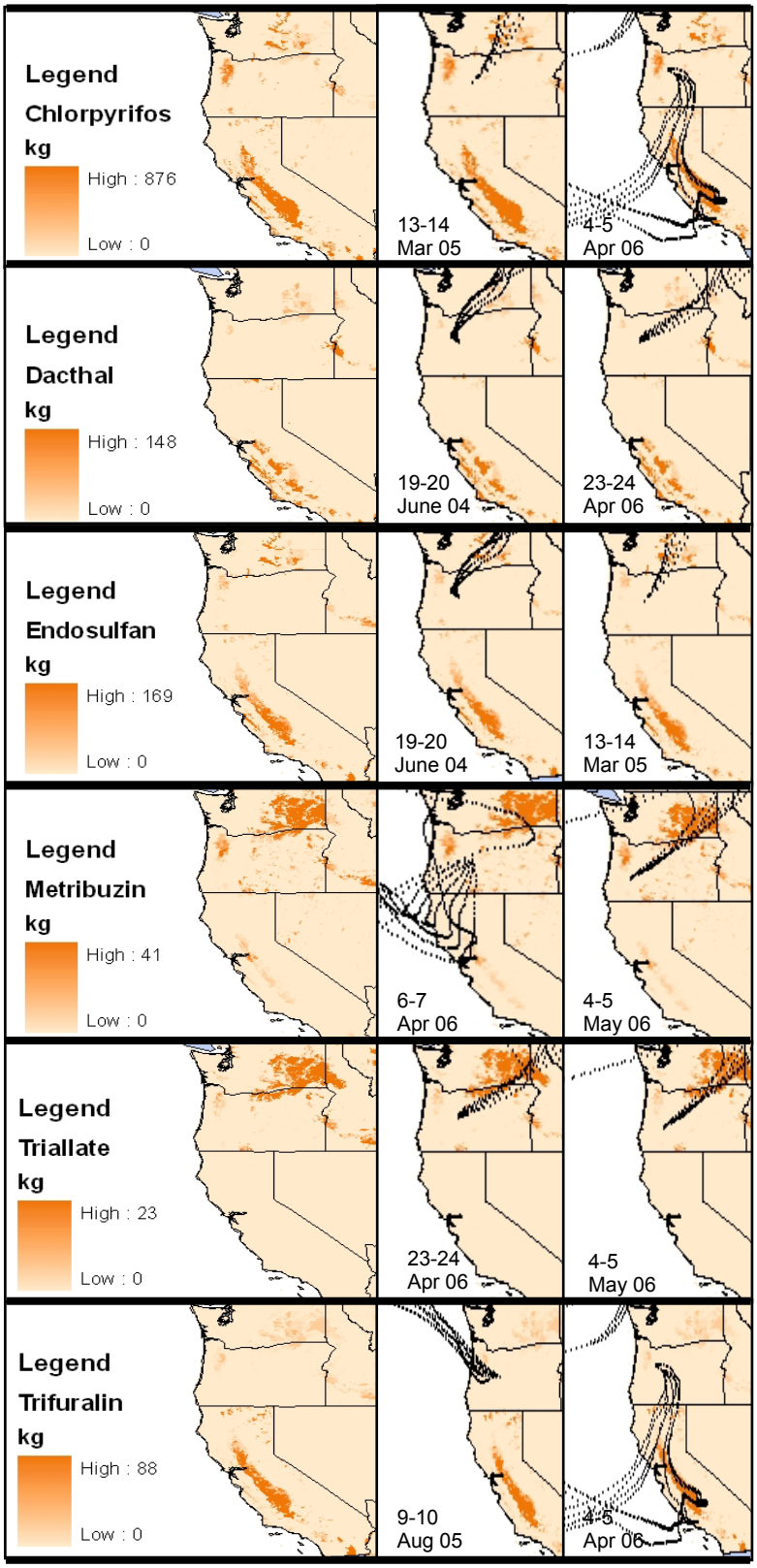
Legend
Chlorpyrifos
kg
High : 876
Low : 0
13-14
Mar 05
4-5
Apr 06
Legend
Dacthal
kg
High : 148
Low : 0
19-20
June 04
23-24
Apr 06
Legend
Endosulfan
kg
High : 169
Low : 0
19-20
June 04
13-14
Mar 05
Legend
Metribuzin
kg
High : 41
Low : 0
6-7
Apr 06
4-5
May 06
Legend
Triallate
kg
High : 23
Low : 0
23-24
Apr 06
4-5
May 06
Legend
Trifuralin
kg
High : 88
Low : 0
9-10
Aug 05
4-5
Apr 06

Figure 5.2

Figure 5.2: Agricultural pesticide 1997 usage maps in kilograms per 1° x 1° grid cell for dacthal, endosulfan, chlorpyrifos, metribuzin, triallate, and trifluralin; in addition to example trajectories of samples with enhanced concentrations overlayed on the usage *(20)*.

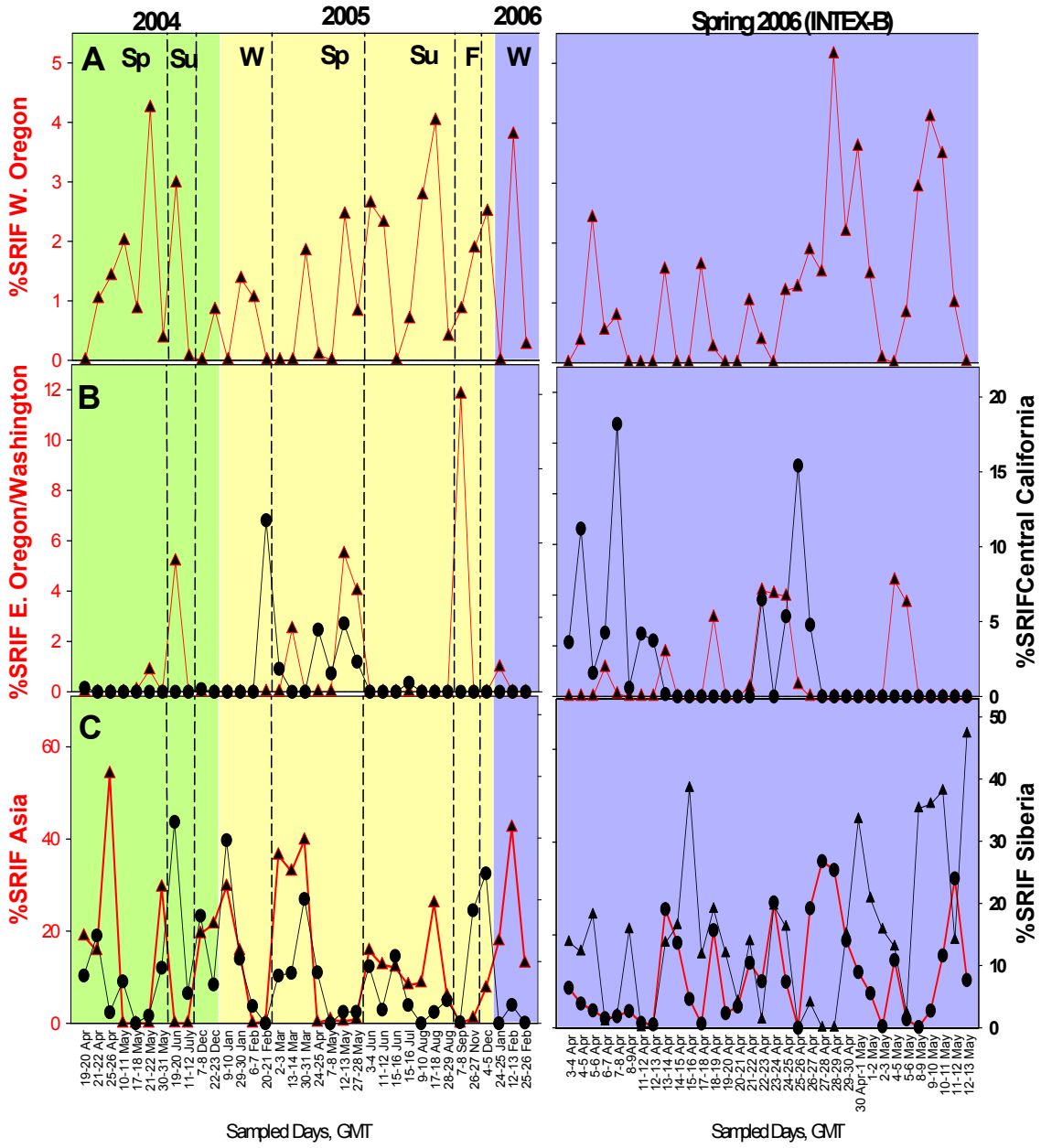

Figure 5.3: Source region impact factors for: **A)** Western Oregon (red, triangles); **B)** Eastern Oregon/Washington (red, triangles) and Central California (black, circles); **C)** Asia (red, triangles) and Siberia (black, circles). Winter (W) (Dec. Jan., Feb.), Spring (Sp) (Mar., Apr., May), Summer (Su) (June, July, Aug.), Fall (F) (Sept., Oct., Nov.) are separated by dashed lines. Background colors designate different years.

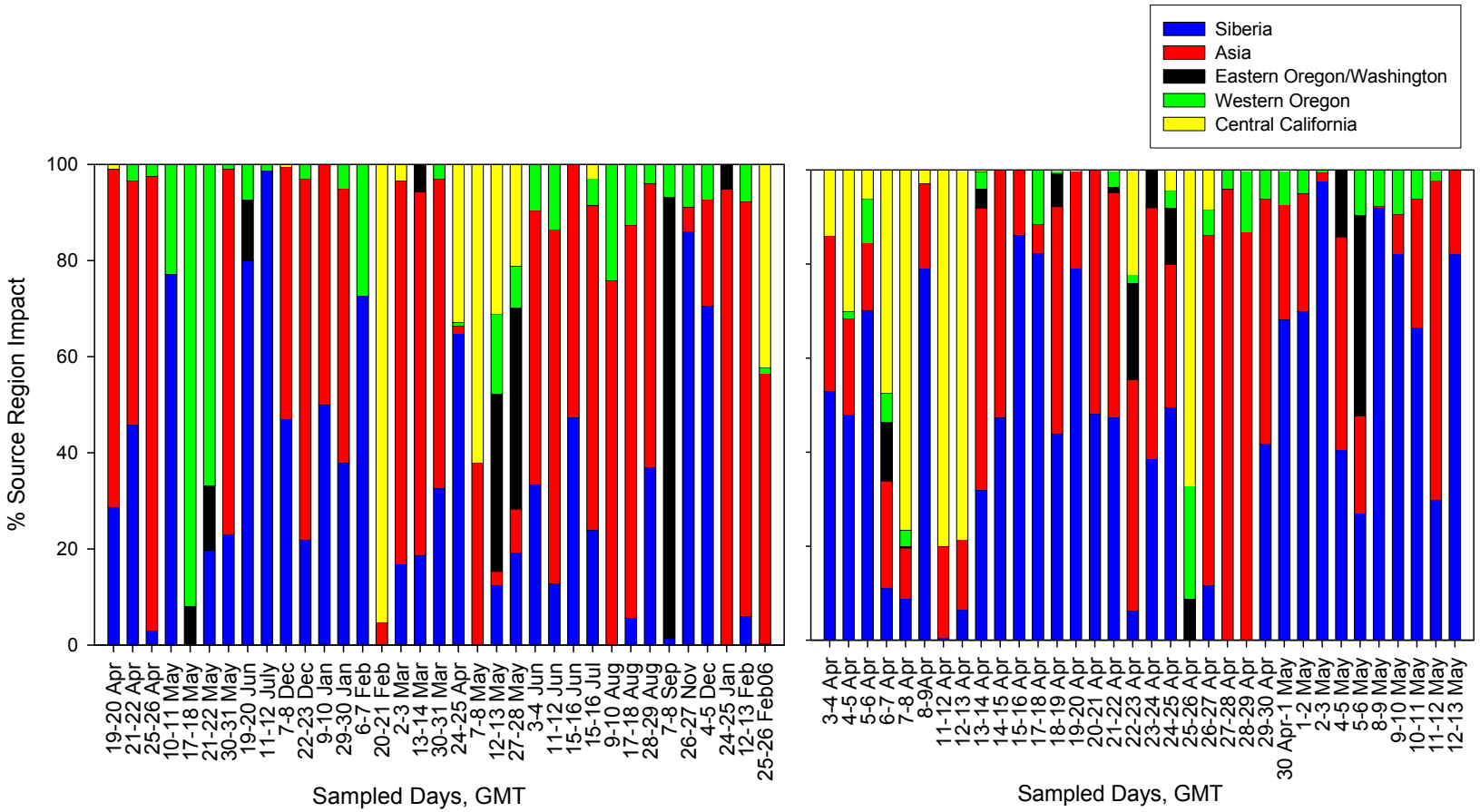

Figure 5.4: Source region impact factors for Asia, Siberia, W. Washington, W. Oregon, E. Oregon/Washington, and Central California represented as a percentage of total hourly points in all designated source regions.

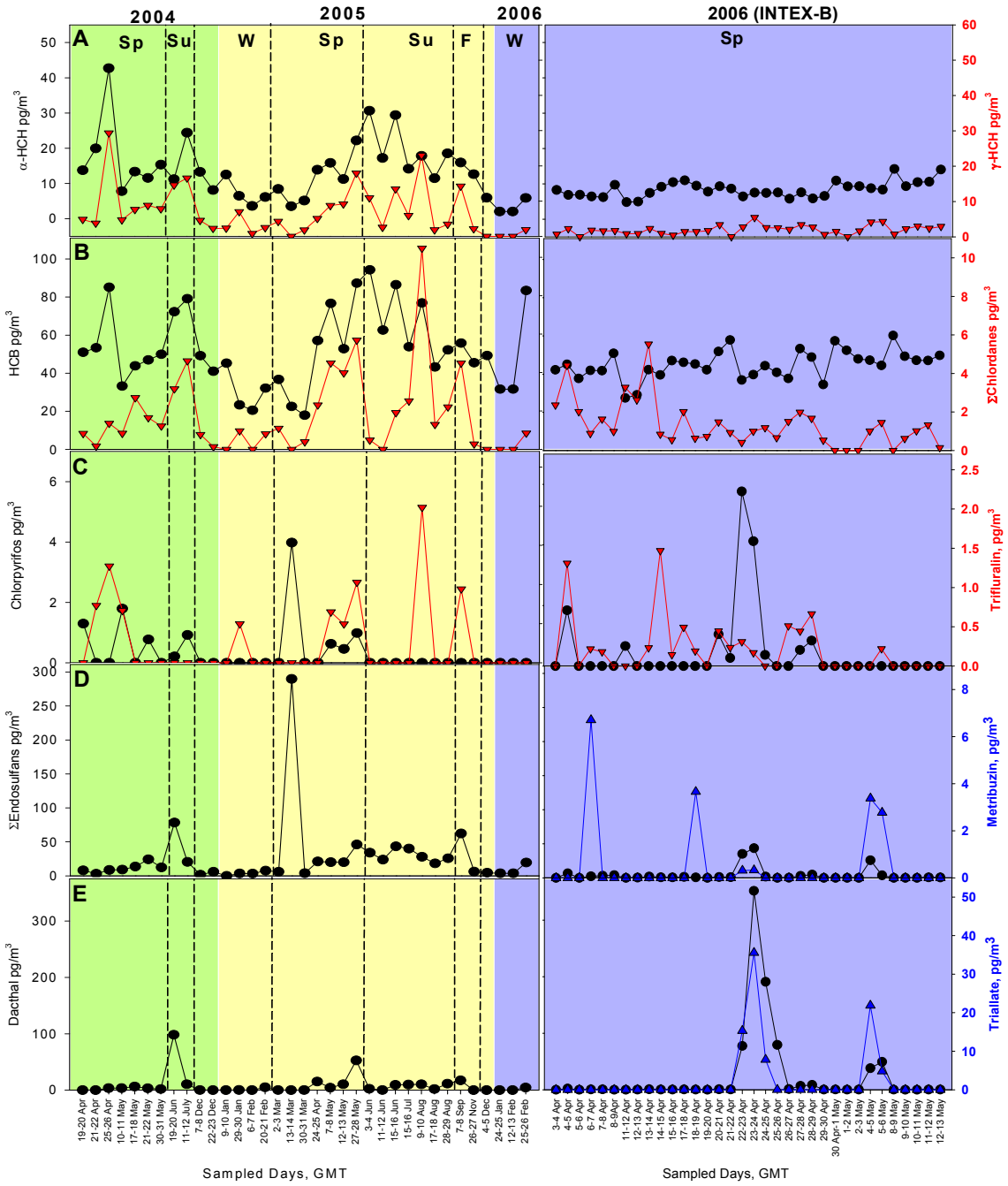

Figure 5.5: Pesticide concentrations 2004-2006: **A)** α-HCH (black, circle) and γ-HCH (red, triangle); **B)** HCB (black, circle) and Σchlordanes (red, triangle); **C)** chlorpyrifos (black, circle) and trifluralin (red, triangle); **D)** Σendosulfans (black, circle) and metribuzin (blue, triangle); and **E)** dacthal (black, circle) and triallate (blue, triangle). Metribuzin and triallate (blue) were only detected in the Spring 2006. Winter (W) (Dec. Jan., Feb.), Spring (Sp) (Mar., Apr., May), Summer (Su) (June, July, Aug.), Fall (F) (Sept., Oct., Nov.) are separated by dashed lines. Background colors designate different years.

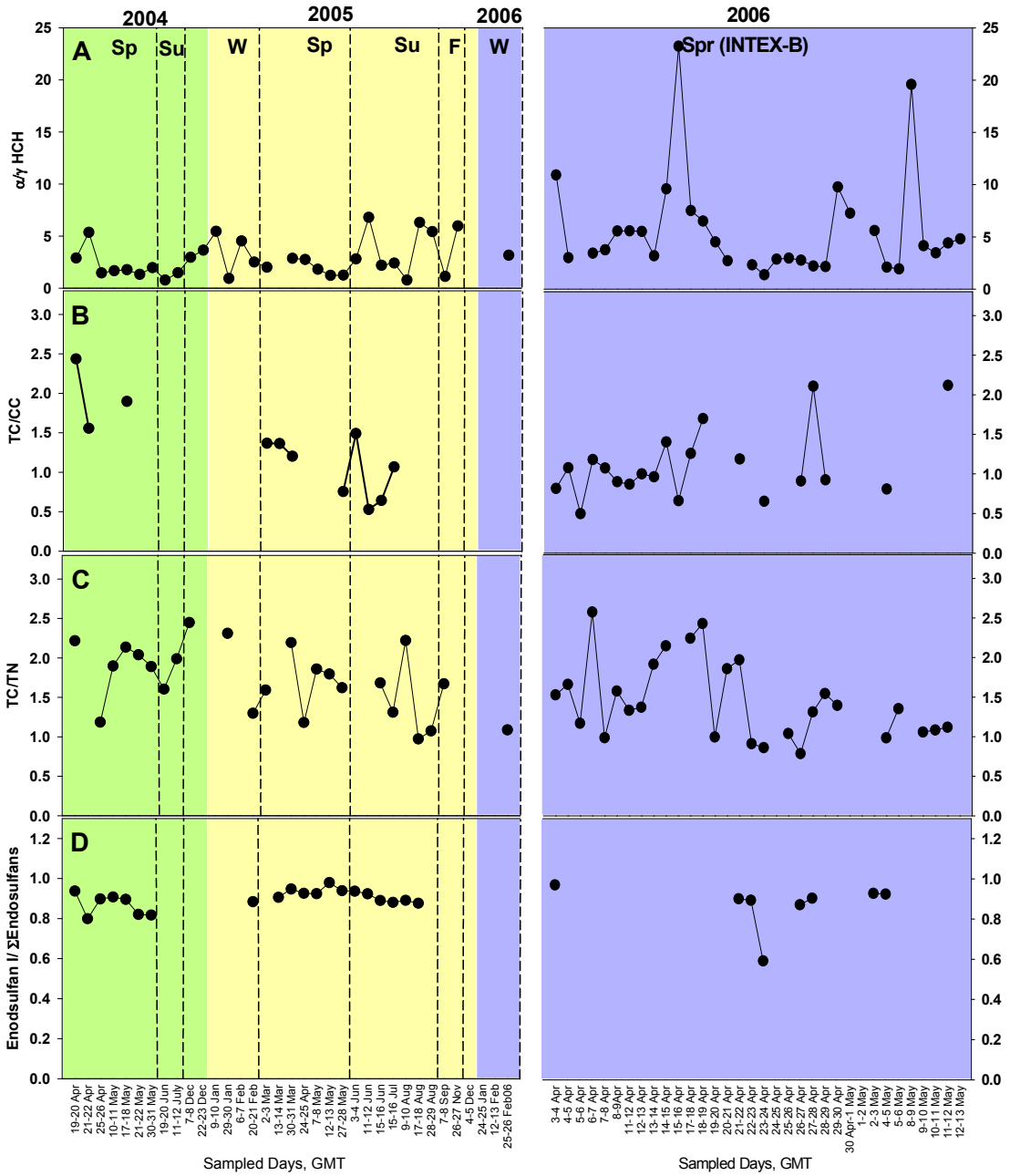

Figure 5.6: Pesticide ratios **A)** α/γ HCH, **B)** trans-chlordane/cis-chlordane (TC/CC), **C)** trans-chlordane/ trans-nonachlor TC/TN, and **D)** endosulfan I/ Σendosulfans. Winter (W) (Dec. Jan., Feb.), Spring (Sp) (Mar., Apr., May), Summer (Su) (June, July, Aug.), Fall (F) (Sept., Oct., Nov.) are separated by dashed lines. Background colors designate different years.

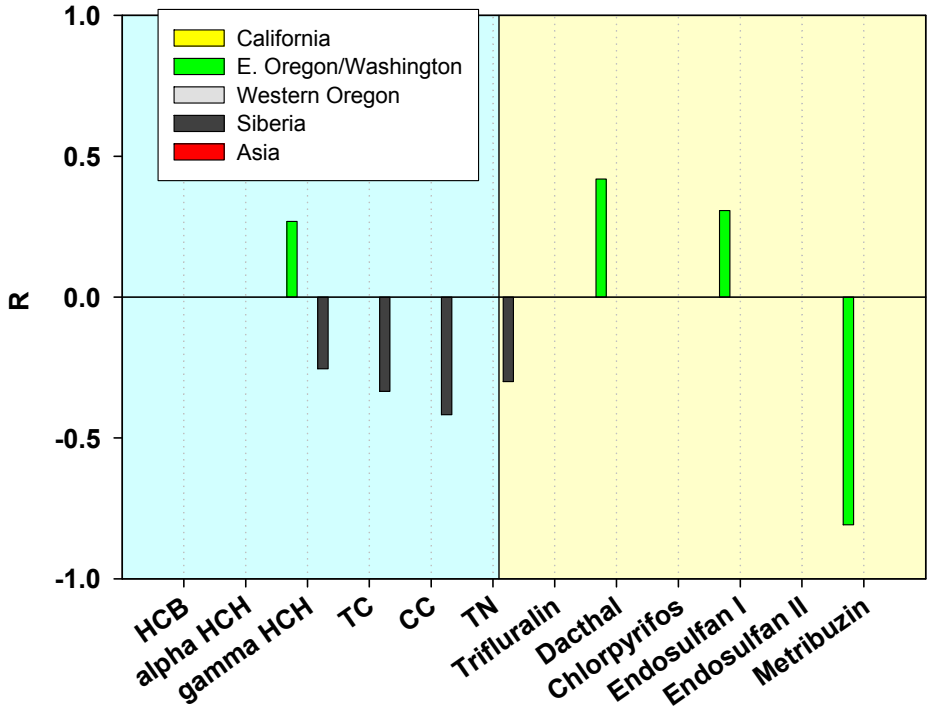

Figure 5.7: Significant (p-value < 0.05) correlation coefficient (R) of SOC concentrations with SRIFs for the source regions: E. Oregon/Washington and Siberia (p-value < 0.05) 2004-2006. SOC concentrations were not statistically significant with Asia, Central California, and Western Oregon.

Table 5.1: Slopes (±standard error), p-value, and R^2 from log pesticide concentration (pg/m^3) versus 1000/T(K).

Analyte*	MBO	p-value	R^2
HCB	-1.5 ± 0.4	0.0002	0.21
α-HCH	-1.9 ± 0.6	0.002	0.15
TC	-3.3 ± 0.8	0.0003	0.24
CC	-2.7 ± 0.9	0.004	0.28
TN	-3.1 ± 0.7	0.0001	0.30
Trifluralin	-3.3 ± 0.9	0.003	0.37
γ-HCH	-4.7 ± 1.0	< 0.0001	0.30
Dacthal	-7.9 ± 2.9	0.01	0.14
Chlorpyrifos	NS	0.2	0.10
Endosulfan I	-4.7 ± 1.7	0.009	0.14
Endosulfan II	NS	0.5	0.02
Endosulfan Sulfate	NS	0.2	0.10

*Only pesticides measured in >10% of the samples are shown, others were not significant.

Table 5.2: Significant correlation coefficients (p-value <0.05) between SOCs: Σgas-phase PAHs (Σgas-PAHs), Σparticulate-phase PAHs (Σpart-PAHs), ΣPCBs, HCB, α-HCH, γ-HCH, Σchlordanes (Σchlord), chlorpyrifos (chlorp), trifluralin (trif), endosulfans (endos), metribuzin (metr), dacthal (dac), triallate (triall), retene (ret), and levoglucosan (lev). Combustion byproduct and PCBs have been discussed in detail elsewhere *(7)*.

	Σgas-PAHs	Σpart-PAHs	ΣPCBs	HCB	α-HCH	γ-HCH	Σchlord	Chlorp	Trif	Σendos	Metr	Dac	Triall	Ret	Lev
Σgas-PAHs	*NA*		0.61	0.66	0.52	0.61	0.50		0.44					0.71	0.33
Σpart-PAHs		*NA*		0.47	0.81	0.65									
ΣPCBs	0.61		*NA*	0.43		0.65	0.80		0.62	0.51				0.65	0.63
HCB	0.66	0.47	0.43	*NA*	0.78	0.67	0.37	-0.50	0.49					0.45	
α-HCH	0.52	0.81		0.78	*NA*	0.76			0.49					0.36	
γ-HCH	0.61	0.65	0.65	0.67	0.76	*NA*	0.55		0.62	0.53				0.57	0.35
Σchlord	0.50		0.80	0.37		0.55	*NA*		0.60	0.36				0.46	0.43
Chlorp				-0.50				*NA*							
Trif	0.44		0.62	0.49	0.49	0.62	0.60		*NA*					0.50	0.69
Σendos			0.51			0.53	0.36			*NA*		0.36		0.38	
Metr											*NA*				
Dac										0.36		*NA*			
Triall													*NA*		
Ret	0.71		0.65	0.45	0.36	0.57	0.46		0.50	0.38				*NA*	0.35
Lev	0.33		0.63			0.35	0.43		0.69					0.35	*NA*

Table 5.3: Estimated pesticide half lives *(44)*.

Pesticide	Estimated Half Lives, hours
HCB	951
HCHs	1830
Chlordanes	50.6
Nonachlors	52.4
Chlorpyrifos	2.8
Trifluralin	10.7
Endosulfans	31.3
Metribuzin	14.1
Dacthal	582
Triallate	7.7

Literature Cited

(1) Jaffe, D.; Prestbo, E.; Swartzendruber, P.; Weiss-Penzias, P.; Kato, S.; Takami, A.; Hatakeyama, S.; Kajii, Y. Export of atmospheric mercury from Asia *Atmospheric Environment* **2005**, *39*, 3029-3038.

(2) Bailey, R.; Barrie, L. A.; Halsall, C. J.; Fellin, P.; Muir, D. C. G. Atmospheric organochlorine pesticides in the western Canadian Arctic: Evidence of transpacific transport *J Geophys Res-Atmos* **2000**, *105*, 11805-11811.

(3) Harner, T.; Shoeib, M.; Kozma, M.; Gobas, F. A. P. C.; Li, S. M. Hexachlorocyclohexanes and endosulfans in urban, rural, and high altitude air samples in the Fraser Valley, British Columbia: Evidence for trans-Pacific transport *Environ Sci Technol* **2005**, *39*, 724-731.

(4) Killin, R. K.; Simonich, S. L.; Jaffe, D. A.; DeForest, C. L.; Wilson, G. R. Transpacific and regional atmospheric transport of anthropogenic semivolatile organic compounds to Cheeka Peak Observatory during the spring of 2002 *J Geophys Res-Atmos* **2004**, *109*, D23S15.

(5) Weiss-Penzias, P.; Jaffe, D. A.; Swartzendruber, P.; Dennison, J. B.; Chand, D.; Hafner, W.; Prestbo, E. Observations of Asian air pollution in the free troposphere at Mount Bachelor Observatory during the spring of 2004 *J Geophys Res-Atmos* **2006**, *111*, D10304.

(6) Weiss-Penzias, P.; Jaffe, D.; Swartzendruber, P.; Hafner, W.; Chand, D.; Prestbo, E. Quantifying Asian and biomass burning sources of mercury using the Hg/CO ratio in pollution plumes observed at the Mount Bachelor observatory *Atmospheric Environment* **2007**, *41*, 4366-4379.

(7) Primbs, T.; Piekarz, A.; Wilson, G.; Schmedding, D.; Jaffe, D.; Higginbotham, C.; Field, J.; Simonich, S. Influence of Asian and Western U.S. Urban Areas and Fires on the Atmospheric Transport of PAHs, PCBs, and FTOHs in the Western U.S. *Environ Sci Technol* **Submitted Aug 2007**.

(8) Primbs, T.; Simonich, S.; Schmedding, D.; Wilson, G.; Jaffe, D.; Takami, A.; Kato, S.; Hatakeyama, S.; Kajii, Y. Atmospheric Outflow of Anthropogenic Semivolatile Organic Compounds from East Asia in Spring 2004 *Environ Sci Technol* **2007**, *41*, 3551-3558.

(9) Foreman, W. T.; Majewski, M. S.; Goolsby, D. A.; Wiebe, F. W.; Coupe, R. H. Pesticides in the atmosphere of the Mississippi River Valley, part II - air *Sci Total Environ* **2000**, *248*, 213-226.

(10) LeNoir, J. S.; McConnell, L. L.; Fellers, G. M.; Cahill, T. M.; Seiber, J. N. Summertime transport of current-use pesticides from California's Central Valley to the Sierra Nevada Mountain Range, USA *Environ Toxicol Chem* **1999**, *18*, 2715-2722.

(11) Hung, H.; Blanchard, P.; Halsall, C. J.; Bidleman, T. F.; Stern, G. A.; Fellin, P.; Muir, D. C. G.; Barrie, L. A.; Jantunen, L. M.; Helm, P. A.; Ma, J.; Konoplev, A. Temporal and spatial variabilities of atmospheric polychlorinated biphenyls (PCBs), organochlorine (OC) pesticides and polycyclic aromatic hydrocarbons (PAHs) in the Canadian Arctic: Results from a decade of monitoring *Sci Total Environ* **2005**, *342*, 119-144.

(12) Hageman, K. J.; Simonich, S. L.; Campbell, D. H.; Wilson, G. R.; Landers, D. H. Atmospheric deposition of current-use and historic-use pesticides in snow at national parks in the Western United States *Environ Sci Technol* **2006**, *40*, 3174-3180.

(13) Daly, G. L.; Wania, F. Organic Contaminants in Mountains *Environ. Sci. Technol.* **2005**, *39*, 385-398.

(14) Usenko, S.; Hageman, K. J.; Schmedding, D. W.; Wilson, G. R.; Simonich, S. L. Trace analysis of semivolatile organic compounds in large volume samples of snow, lake water, and groundwater *Environ Sci Technol* **2005**, *39*, 6006-6015.

(15) Swartzendruber, P. C.; Jaffe, D. A.; Prestbo, E. M.; Weiss-Penzias, P.; Selin, N. E.; Park, R.; Jacob, D. J.; Strode, S.; Jaegle, L. Observations of reactive gaseous mercury in the free troposphere at the Mount Bachelor Observatory *J Geophys Res-Atmos* **2006**, *111*, -.

(16) Piekarz, A.; Primbs, T.; Field, J. A.; Barofsky, D. F.; Simonich, S. Semi-volatile Fluorinated Organic Compounds in Asian and Pacific Northwestern U.S. Air Masses *Environ. Sci. Technol.* **Submitted June 2007**.

(17) Draxler, R. R.; Rolph, G. D. HYSPLIT (HYbrid Single-Particle Lagrangian Integrated Trajectory) Model access via NOAA ARL READY Website (http://www.arl.noaa.gov/ready/hysplit4.html). NOAA Air Resources Laboratory, Silver Spring, MD. **2003**.

(18) Singh, H. B.; Brune, W. H.; Crawford, J. H.; Fuelberg, H.; Jacob, D. J. The Intercontinental Chemical Transport Experiment – Phase B (INTEX-B): An update (http://cloud1.arc.nasa.gov/intex-b/) **2006**.

(19) U.S. Department of AgriculturesNational Agriculture Statistics Service, 2002. http://151.121.3.33: 8080/Census/Create_Census_US_CNTY.jsp#top.

(20) USGS *http://ca.water.usgs.gov/pnsp/pesticide_use_maps/* Sacramento, CA, 2000.

(21) OSU; EPA, U. S. *http://npic.orst.edu/state1.htm* Corvallis, OR, 2007.

(22) Rice, C. P.; Nochetto, C. B.; Zara, P. Volatilization of Trifluralin, Atrazine, Metolachlor, Chlorpyrifos, alpha-Endosulfan, and beta-Endosulfan from Freshly Tilled Soil *J Agr Food Chem* **2002**, *50*, 4009-4017.

(23) Wania, F. H., J-E.; Lei, Y.; Mackay D. Temperature Dependence of Atmospheric Concentrations of Semivolatile Organic Compounds *Environ. Sci. Technol.* **1998**, *32*, 1013-1021.

(24) Carlson, D. L.; Hites, R. A. Temperature dependence of atmospheric PCB concentrations *Environ Sci Technol* **2005**, *39*, 740-747.

(25) Pozo, K.; Harner, T.; Wania, F.; Muir, D. C. G.; Jones, K. C.; Barrie, L. A. Toward a Global Network for Persistent Organic Pollutants in Air: Results from the GAPS Study *Environ. Sci. Technol.* **2006**, *40*, 4867-4873.

(26) UNEP "Regionally Based Assessment of Persistent Toxic Substances; North America," UNEPChemicals: Chaˆtelaine, GE, Switzerland, 2002.

(27) Li, Y. F.; Cai, D. J.; Singh, A. Technical hexachlorocyclohexane use trends in China and their impact on the environment *Arch Environ Con Tox* **1998**, *35*, 688-697.

(28) Tao, S.; Xu, F. L.; Wang, X. J.; Liu, W. X.; Gong, Z. M.; Fang, J. Y.; Zhu, L. Z.; Luo, Y. M. Organochlorine pesticides in agricultural soil and vegetables from Tianjin, China *Environ Sci Technol* **2005**, *39*, 2494-2499.

(29) Eckhardt, S.; Breivik, K.; Manø, S.; Stohl, A. Record high peaks in PCB concentrations in the Arctic atmosphere due to long-range transport of biomass burning emissions *Atmospheric Chemistry and Physics Discussions* **2007**, *7*, 6229-6254.

(30) Willett, K. L.; Ulrich, E. M.; Hites, R. A. Differential Toxicity and Environmental Fates of Hexachlorocyclohexane Isomers *Environ. Sci. Technol.* **1998**, *32*, 2197-2207.

(31) Shen, L.; Wania, F.; Lei, Y. D.; Teixeira, C.; Muir, D. C. G.; Bidleman, T. F. Hexachlorocyclohexanes in the north American atmosphere *Environ Sci Technol* **2004**, *38*, 965-975.

(32) Bailey, R. E. Global hexachlorobenzene emissions *Chemosphere* **2001**, *43*, 167-182.

(33) EXTOXNET *http://extoxnet.orst.edu/pips/ghindex.html* Corvallis, OR, 2007.

(34) Mattina, M. J. I.; Iannucci-Berger, W.; Dykas, L.; Pardus, J. Impact of Long-Term Weathering, Mobility, and Land Use on Chlordane Residues in Soil *Environ. Sci. Technol.* **1999**, *33*, 2425-2431.

(35) Dearth, M. A.; Hites, R. A. Complete Analysis of Technical Chlordane Using Negative Ionization Mass Spectrometry *Environ Sci Technol* **1991**, *25*, 245-254.

(36) Canada's Pest Management Regulatory Agency, http://www.pmra-arla.gc.ca/english/pdf/rev/rev2002-02-e.pdf.

(37) UNEP "Regionally Based Assessment of Persistent Toxic Substances; Central and North East Asia," UNEPChemicals: Chaˆtelaine, GE, Switzerland, 2002.

(38) Wettasinghe, A.; Tinsley, I. J. Degradation of Dacthal and Its Metabolites in Soil *Bull. Environ. Contam. Toxicol.* **1993**, *50*, 226-231.

(39) Yao, Y.; Harner, T.; Ma, J.; Tuduri, L.; Blanchard, P. Sources and Occurrence of Dacthal in the Canadian Atmosphere *Environ. Sci. Technol.* **2007**, *41*, 688-694.

(40) Verrin, S. M.; Begg, S. J.; Ross, P. S. Pesticide use in British Columbia and the Yukon: An assessment of types, applications and risks to aquatic biota. *Can. Tech. Rep. Fish. Aquat. Sci.* **2004**, *2517: xvi + 209 p.*

(41) Burgoyne, T. W.; Hites, R. A. Effects of Temperature and Wind Direction on the Atmospheric Concentrations of alpha-Endosulfan *Environ Sci Technol* **1993**, *27*, 910-914.

(42) Smith, A. E.; Kerr, L. A.; Caldwell, B. Volatility of ethalfluralin, trifluralin, and triallate from a field following surface treatments with granular formulations *J Agr Food Chem* **1997**, *45*, 1473-1478.

(43) Davis, D. L.; Ahmed, A. K. Exposures from indoor spraying of chlorpyrifos pose greater health risks to children than currently estimated *Environ Health Persp* **1998**, *106*, 299-301.

(44) EPISuite; v3.12 ed.; U.S. EPA: Washington, DC, 2000.

CHAPTER 6. CONCLUSIONS

The outflow from Asia and the trans-Pacific atmospheric transport of both the gas and particulate phase anthropogenic semivolatile organic compounds (SOCs) was investigated. The pressurized liquid extraction (PLE) method for SOCs from air sampling media was optimized and the SOC profile was characterized in Asian air masses and trans-Pacific and regional air masses in the Western U.S. These measurements were conducted at an established air monitoring station on Okinawa, Japan in spring 2004 as well as at a remote high-elevation site in Oregon's Cascade Range, Mt. Bachelor Observatory (MBO), from spring 2004 to spring 2006.

The minimization of matrix interferences is mandatory for trace analysis of SOCs. Because the air sampling media used for trapping gas-phase SOCs are polymers, including polyurethane foam (PUF) and polystyrene divinyl benzene (XAD-2), the selection of PLE extraction solvents is essential in order to minimize matrix interferences due to co-extraction of the monomers and oligomers. Hansen solubility parameters were used to aid in the selections of PLE solvents to minimize matrix interferents.

To minimize the co-extraction of polymers, a PLE solvent composition of 75:25 hexane:acetone was chosen for the PUF and the XAD-2 copolymer was not solubilized under the PLE conditions used. The average percent PLE recoveries (and percent relative standard deviations) of 63 SOCs, including polycyclic aromatic hydrocarbons (PAHs), polychlorinated biphenyls (PCBs), and organochlorine, amide, triazine, thiocarbamate, and phosphorothioate pesticides, were 76.7 (6.2), 79.3 (8.1), and 93.4 (2.9) for the QFF, PUF, and XAD-2, respectively.

To assess the SOC profile and outflow in Asian air masses, measurements of SOCs were conducted at Hedo Station Observatory (HSO), Okinawa, Japan in spring 2004. Contributions from different source regions (China, Japan, the Koreas, Russia, and Ocean/Local) were estimated using source region impact factors (SRIFs). SRIFs were calculated using data from NOAA's HYSPLIT model and represent the percentage of time that an air parcel spent in a designated source region versus the total back trajectory time. Multivariable linear regression of SOC concentrations and SRIFs was used to determine source regions.

At HSO, elevated concentrations of hexachlorobenzene (HCB), hexachlorocyclohexanes (HCHs), DDTs, and particulate-phase polycyclic aromatic hydrocarbons (PAHs) were attributed to air masses from China. A large proportion of the variation in the current use pesticides, gas-phase PAHs, and polychlorinated biphenyl (PCB) concentrations was explained by meteorology. Chlordanes showed a technical mixture profile and similar concentrations regardless of Asian source region. The α/γ HCH and trans/cis chlordane ratios did not vary significantly with different Asian source regions and had regional averages of 2.5±1.0 and 1.2±0.3, respectively.

Particulate-phase PAH concentrations were significantly correlated (p-value<0.05) with other incomplete combustion byproduct concentrations, including elemental mercury (Hg^0), CO, NO_x*, black carbon, submicron aerosols, and SO_2. Using measured PAH, CO, and black carbon concentrations and estimated CO and black carbon emission inventories, the emission of 6 carcinogenic particulate-phase PAHs were estimated to be 1518-4179 metric tons/year for Asia and 778-1728 metric tons/year for

China, respectively. These results confirm that East Asian outflow contains significant emissions of carcinogenic particulate-phase PAHs.

To further understand the trans-Pacific atmospheric transport of SOCs, measurements were conducted at MBO from spring 2004 to spring 2006. This included measurements in spring 2006 as part of NASA's INTEX-B experiment. Because both urban areas and regional fires have the potential to result in increased PAH, PCB, and fluorotelomer alcohol (FTOH) concentrations at MBO, the SRIFs were calculated in two different ways: first, by assessing the potential impact from Western North America and Asian source regions; and, second, by assessing the potential influences from urban areas in the Western U.S.

Particulate-phase PAH concentrations at MBO increased with the percentage of air mass time in Asia and provided strong evidence that particulate-phase PAHs are emitted from Asia and undergo trans-Pacific atmospheric transport to North America. Elevated particulate-phase PAH concentrations, relative to gas-phase PAH concentrations, were identified in a Chinese emission inventory, measurements of Asian air masses at HSO, and measurements of trans-Pacific air masses at MBO. The PAH emission inventory for the Great Lakes Region of the U.S., as well as the measurements near Los Angeles, California, indicate lower relative particulate-phase PAH concentrations in U.S. air masses compared to both Asian and trans-Pacific air masses at MBO. Principal component analysis confirmed this interpretation. In addition, significant positive correlations ($p<0.05$) existed between Σparticulate-phase PAH and CO concentrations. A significant amount of the CO springtime concentrations in the Pacific Northwest have been previously attributed to Asian sources. However, significant

negative correlations ($p<0.05$) existed between Σgas-phase PAH and CO concentrations. These results provide evidence that the high proportion of particulate-phase PAHs in MBO air masses is due to Asian emissions and trans-Pacific atmospheric transport.

Gas-phase PAH and FTOH concentrations significantly increased at MBO with the percentage of air mass time in California's urban areas, while retene and PCB concentrations at MBO increased with the percentage of air mass time in Oregon and during regional fire events. In addition, Σgas-phase PAH, retene, and levoglucosan concentrations were significantly positively correlated (p-value < 0.001) with ΣPCB concentrations, suggesting increased atmospheric PCB concentrations were associated with fires due to the volatilization of stored PCBs from soil and vegetation. Using the concentrations measured at MBO and the corresponding SRIFs, the emissions of individual FTOHs from urban areas in the Western U.S. were estimated at 15 to 309 kg/year and the emissions of individual gas-phase PAHs were estimated at 217 to 4648 kg/year.

Enhanced historic use pesticide (HUP) concentrations (HCB, α-HCH, and γ-HCH) occurred during trans-Pacific atmospheric transport at MBO. Regional atmospheric transport at MBO resulted in enhanced current use pesticide (CUP) concentrations (γ-HCH, dacthal, endosulfan, metribuzin, triallate, trifluralin, and chlorpyrifos), with episodic concentration enhancements during spring application periods. Increased concentrations of γ-HCH, endosulfan I, and dacthal were significantly positively correlated (p-value < 0.05) with increased air mass time in regional agricultural areas in Eastern Oregon/Washington, U.S.

Enhanced Σchlordane, HCHs, HCB, and trifluralin concentrations were also associated with regional fires, which may be due to volatization of pesticides deposited to soils and vegetation. The highest concentrations of trifluralin and Σchlordane were measured during a regional fire event in the Western U.S. and increased Σchlordane concentrations measured in air masses influenced by fires in Alaska and Canada.

Trans-chlordane/cis-chlordane and α-HCH/γ-HCH ratios were found to be significantly aged in free tropospheric air masses that spent a significant amount of time over the Pacific Ocean and/or Siberia, compared to regional boundary layer air masses: average ratio (±standard error) of 0.87 ± 0.05 and 5.2 ± 0.8 for free tropospheric air and 1.39 ± 0.1 and 2.9 ± 0.3 for boundary layer air, respectively. These ratios may be used to identify air masses from agricultural regions in the Western U.S. and Asia (transport events ~ <10 days from Asia) from aged air masses spending increased time over the Pacific Ocean or Siberia.

Future work should include the characterization of Asian air masses over a larger time scale to assess temporal variability (i.e. seasonal variability in emissions). The significant Asian particulate-phase PAH emissions will likely continue to increase. In addition, during winter periods, PAH emissions may be elevated due to heating, and during summer periods, emissions of pesticides may increase. Due to the significant emissions of carcinogenic PAHs in Asian air masses, toxicological assays of air samples collected both in Asia and at MBO should be used to assess the potential risk of these air masses. These assays should be coupled with size fractionated particulate matter sampling to couple the results to aerosol size.

The size fraction of particulate matter samples collected in trans-Pacific and regional air samples can also provide additional information in regards to the role of aerosols in climate change. Particulate-phase PAHs are primarily associated with submicron aerosols, thus the enhanced particulate-phase PAHs further highlight the ability of submicron aerosols to undergo long-range atmospheric transport. Since the radiative properties of aerosols is related to their size and composition, combing size fractionation with a detailed chemical composition measurements of the sampled aerosols will provide additional information relating to climate change and the role of long-range transport.

MBO has been shown to be an effective site to assess both free tropospheric and regional air masses. There is a large data gap in the Western U.S. on the atmospheric profile of SOCs and a site like MBO is ideal in filling this gap. Further experiments should include the insertion of a switch to start the high volume air sampler via an external trigger, such as a change in the water vapor mixing ratio, which could more specifically target specific air masses. Furthermore, measurements on a twelve hour cycle should be made to further determine day and night time differences. Even during the summer, MBO experiences free tropospheric air during the nighttime, where upslope effects often occur during the daytime. Measurements of SOCs in snow, coupled with simultaneous air measurements, should also be made to further understand the distribution of SOCs at high elevation sites in the Western U.S.

Appendices

Appendix A: Okinawa, Japan SOC Concentrations (pg/m^3) for all of the Sampled Days, GMT.

	HCB	α-HCH	γ-HCH	o,p'-DDE	p,p'-DDE	o,p'-DDT	OC	TC	CC	TN	CN	Dield
22-23 Mar	96.69	9.66	4.17	< DL	< DL	< DL	< DL	5.52	5.40	2.73	0.46	< DL
23-24 Mar	61.58	9.77	3.87	< DL	< DL	< DL	0.34	1.32	1.64	0.93	0.17	< DL
25-26 Mar	68.26	5.94	< DL	< DL	< DL	< DL	< DL	4.87	4.66	3.57	0.55	11.47
29-30 Mar	68.22	14.98	5.42	< DL	< DL	< DL	< DL	2.27	2.05	2.50	0.40	6.70
30-31 Mar	53.09	10.95	6.70	< DL	< DL	< DL	< DL	0.66	1.04	0.40	0.11	< DL
2-3 Apr	116.91	25.94	12.31	4.43	4.69	5.01	< DL	0.96	1.18	0.50	0.13	3.03
3-4 Apr	78.53	18.25	6.96	< DL	< DL	1.89	0.91	1.54	1.60	2.01	0.25	8.03
4-5 Apr	53.21	10.73	5.90	< DL	< DL	1.44	< DL	0.45	< DL	0.36	< DL	< DL
12-13 Apr	87.54	10.47	3.19	< DL	< DL	< DL	< DL	3.59	3.94	2.78	0.42	7.45
15-16 Apr	93.06	23.06	3.85	< DL	< DL	< DL	< DL	3.37	3.65	2.68	0.40	< DL
20-21 Apr	148.49	36.22	15.61	7.36	8.85	16.44	< DL	6.87	5.44	3.55	0.52	8.76
21-22 Apr	157.32	32.89	13.84	5.55	< DL	12.00	< DL	6.02	3.99	3.14	0.35	< DL
24-25 Apr	70.72	13.29	6.46	< DL	< DL	< DL	< DL	4.92	4.05	2.97	0.40	< DL
25-26 Apr	81.37	12.99	7.37	< DL	< DL	< DL	< DL	8.17	4.50	4.95	0.33	10.69
27-28 Apr	83.82	23.40	11.09	3.74	5.67	4.66	< DL	5.95	3.84	2.84	0.30	< DL
28-29 Apr	67.82	23.38	13.75	1.82	2.73	2.05	< DL	0.80	< DL	< DL	< DL	< DL
29-30 Apr	88.49	9.88	5.20	< DL	< DL	< DL	< DL	4.33	3.35	2.04	0.20	< DL
1-2 May	84.28	8.25	3.00	< DL	< DL	< DL	< DL	6.98	4.48	3.76	0.44	< DL

	Trif	Chlorp	Metr	Hept	Dac	Endo I	Endo II	Endo SO4
22-23 Mar	17.73	94.01	< DL	< DL	2.70	15.79	4.28	< DL
23-24 Mar	7.02	9.66	< DL	< DL	< DL	8.31	1.09	< DL
25-26 Mar	33.61	32.74	0.34	< DL	1.18	19.18	1.56	< DL
29-30 Mar	9.00	9.53	< DL	< DL	< DL	16.93	1.31	< DL
30-31 Mar	5.74	4.60	< DL	< DL	< DL	12.13	0.88	< DL
2-3 Apr	5.92	2.45	0.82	< DL	< DL	16.75	1.04	< DL
3-4 Apr	7.86	8.65	< DL	< DL	< DL	5.79	0.34	< DL
4-5 Apr	1.41	2.08	< DL	< DL	0.11	7.10	1.14	0.76
12-13 Apr	16.28	24.30	25.13	< DL	1.13	17.93	1.21	< DL
15-16 Apr	1.64	1.98	< DL	< DL	< DL	37.94	1.30	0.57
20-21 Apr	13.06	21.28	< DL	< DL	0.75	30.44	2.41	< DL
21-22 Apr	12.42	13.29	< DL	< DL	0.82	25.62	1.89	1.08
24-25 Apr	10.79	7.16	< DL	40.73	0.35	42.98	3.42	1.74
25-26 Apr	6.35	6.73	24.76	59.53	0.66	37.52	3.17	1.37
27-28 Apr	3.16	6.58	< DL	17.51	0.07	24.69	2.53	1.19
28-29 Apr	0.79	1.22	< DL	3.74	0.10	14.48	< DL	0.30
29-30 Apr	7.77	3.05	27.40	32.15	< DL	14.99	0.34	< DL
1-2 May	8.14	5.27	80.59	33.12	0.68	9.70	1.01	1.80

	PCB 101	PCB 118	PCB 153	PCB 138	PCB 187	PCB 183
22-23 Mar	4.09	5.96	5.26	7.78	2.30	0.97
23-24 Mar	< DL	0.94	0.66	1.05	0.39	0.15
25-26 Mar	3.16	3.82	2.80	2.65	< DL	< DL
29-30 Mar	6.99	1.56	1.10	0.99	0.47	0.19
30-31 Mar	0.36	0.98	0.56	0.53	0.23	0.12
2-3 Apr	< DL	0.78	0.69	0.94	0.31	0.14
3-4 Apr	4.96	1.66	1.13	0.99	0.46	0.17
4-5 Apr	0.06	0.65	0.27	< DL	< DL	< DL
12-13 Apr	17.62	6.26	5.73	5.84	4.16	1.49
15-16 Apr	< DL	0.87	0.65	0.82	0.38	0.16
20-21 Apr	8.37	3.18	2.93	2.65	1.33	0.49
21-22 Apr	< DL	2.76	2.14	2.72	0.97	0.36
24-25 Apr	< DL	1.19	0.87	0.88	0.53	0.25
25-26 Apr	< DL	1.06	1.03	1.49	0.46	0.18
27-28 Apr	1.13	0.78	0.57	0.92	0.26	0.11
28-29 Apr	< DL	0.43	0.28	< DL	< DL	< DL
29-30 Apr	< DL	1.04	0.69	0.70	0.22	< DL
1-2 May	10.58	1.23	0.76	1.26	0.34	0.21

	FLO	PHE	ANT	FLA	PYR	RET
22-23 Mar	824.57	7949.13	280.26	582.94	2341.19	689.68
23-24 Mar	164.44	3371.17	244.79	236.27	1032.87	224.58
25-26 Mar	404.95	4188.12	186.30	482.02	2007.35	460.76
29-30 Mar	562.48	1005.60	< DL	141.37	450.10	142.11
30-31 Mar	1005.21	3623.38	364.58	649.03	1373.28	326.25
2-3 Apr	1130.11	2375.35	104.58	974.66	986.03	169.87
3-4 Apr	597.39	1964.16	169.61	506.65	999.19	231.83
4-5 Apr	242.89	937.96	89.74	276.78	389.93	88.09
12-13 Apr	1102.41	7254.44	291.07	485.91	2403.39	550.97
15-16 Apr	497.40	2210.32	122.15	221.34	728.86	124.86
20-21 Apr	181.96	3505.39	87.50	652.18	1916.15	443.36
21-22 Apr	553.57	2783.53	53.09	600.34	1265.18	250.19
24-25 Apr	310.87	1752.50	102.75	274.10	538.26	123.86
25-26 Apr	431.43	2153.45	53.69	285.30	987.65	165.91
27-28 Apr	740.09	876.64	< DL	335.68	371.17	83.64
28-29 Apr	280.42	1243.06	79.13	208.66	467.80	54.37
29-30 Apr	110.64	2775.94	175.57	333.58	1246.45	269.87
1-2 May	386.79	2435.27	81.07	272.91	1033.82	211.29

	BaA	CT	BbF	BkF	BeP	BaP	IcdP	DahA	BghiP	TPB	Lev
22-23 Mar	< DL	219.13	< DL	< DL	< DL	< DL	< DL	< DL	< DL	32.66	< DL
23-24 Mar	4.31	81.76	21.26	5.51	10.93	< DL	12.80	< DL	11.46	9.69	1827.12
25-26 Mar	< DL	267.73	< DL	< DL	< DL	5.04	36.73	< DL	21.41	88.35	4429.29
29-30 Mar	< DL	43.53	< DL	< DL	< DL	4.24	6.12	< DL	4.18	11.98	1930.82
30-31 Mar	34.95	204.13	238.44	50.67	126.56	11.39	156.92	23.30	138.82	11.42	2242.29
2-3 Apr	103.96	281.82	482.30	107.22	234.66	218.01	290.37	39.25	316.24	24.40	6730.96
3-4 Apr	25.50	138.02	215.08	52.40	120.32	71.13	116.45	13.92	99.93	17.49	4455.44
4-5 Apr	23.25	62.72	138.30	34.28	73.93	68.44	83.81	10.14	65.78	7.24	3348.10
12-13 Apr	< DL	174.22	< DL	< DL	< DL	< DL	< DL	< DL	< DL	43.07	1790.06
15-16 Apr	17.06	57.85	59.55	19.80	35.21	19.32	29.67	< DL	22.43	6.67	2118.49
20-21 Apr	45.94	226.48	249.59	61.57	124.47	83.07	148.79	17.83	118.90	51.33	2544.38
21-22 Apr	47.71	197.91	316.45	86.05	190.91	106.21	166.76	< DL	135.24	33.31	2381.13
24-25 Apr	21.30	67.27	89.37	31.33	53.91	< DL	42.25	< DL	36.05	11.51	3468.01
25-26 Apr	< DL	81.93	53.11	< DL	29.75	< DL	32.18	< DL	22.33	14.07	1436.16
27-28 Apr	< DL	68.81	203.36	71.03	127.65	40.95	143.46	< DL	84.98	10.94	1704.93
28-29 Apr	33.53	50.94	137.27	36.75	72.08	39.56	65.04	< DL	51.70	18.72	4523.60
29-30 Apr	< DL	78.83	16.68	3.75	18.34	< DL	5.84	< DL	5.81	10.32	2505.84
1-2 May	< DL	70.43	< DL	< DL	6.30	< DL	< DL	< DL	< DL	16.62	1272.53

Appendix B: Mt. Bachelor Observatory SOC Concentrations (pg/m^3) for all of the Sampled Days, GMT.

	HCB	α-HCH	γ-HCH	TC	CC	TN	CN	Dield
2004								
19-20 Apr	50.98	13.75	4.78	0.57	<DL	0.26	<DL	<DL
21-22 Apr	53.34	19.95	3.73	0.17	<DL	<DL	<DL	<DL
25-26 Apr	85.12	42.70	29.34	0.73	<DL	0.62	<DL	<DL
10-11 May	33.26	7.81	4.67	0.55	<DL	0.29	<DL	<DL
17-18 May	43.87	13.36	7.58	1.33	0.54	0.62	0.20	<DL
21-22 May	46.98	11.56	8.76	0.77	0.50	0.38	<DL	<DL
30-31 May	49.94	15.33	7.81	0.79	<DL	0.42	<DL	<DL
19-20 Jun	72.31	11.19	14.55	1.81	<DL	1.13	0.21	<DL
11-12 July	79.16	24.41	16.52	2.21	1.16	1.11	0.12	<DL
7-8 Dec	49.18	13.29	4.50	0.55	<DL	0.22	<DL	<DL
22-23 Dec	41.00	8.12	2.23	<DL	<DL	<DL	0.14	<DL
2005								
9-10 Jan	45.23	12.53	2.30	<DL	<DL	<DL	<DL	<DL
29-30 Jan	23.36	6.47	6.98	0.67	<DL	0.29	<DL	<DL
6-7 Feb	20.53	3.62	0.80	<DL	<DL	<DL	<DL	<DL
20-21 Feb	32.16	6.13	2.45	0.46	<DL	0.35	<DL	<DL
2-3 Mar	36.72	8.44	4.22	0.67	<DL	0.42	<DL	<DL
13-14 Mar	22.56	3.54	<DL	<DL	<DL	<DL	<DL	<DL
30-31 Mar	17.90	5.12	1.79	0.27	<DL	0.12	<DL	<DL
24-25 Apr	57.18	13.87	5.05	1.25	<DL	1.06	<DL	<DL
7-8 May	76.65	15.84	8.73	1.98	1.45	1.07	<DL	<DL
12-13 May	52.84	11.23	9.17	1.74	1.27	0.97	<DL	<DL
27-28 May	87.29	22.20	17.91	2.32	1.93	1.43	<DL	<DL
3-4 Jun	94.25	30.64	10.92	0.48	<DL	<DL	<DL	<DL
11-12 Jun	62.65	17.22	2.53	<DL	<DL	<DL	<DL	<DL
15-16 Jun	86.47	29.41	13.43	1.20	<DL	0.71	<DL	<DL
15-16 Jul	53.86	14.16	5.89	0.82	1.08	0.62	<DL	<DL
9-10 Aug	76.90	17.82	22.98	4.94	3.31	2.22	<DL	<DL
17-18 Aug	43.23	11.47	1.82	0.33	0.62	0.34	<DL	<DL
28-29 Aug	52.29	18.53	3.42	0.63	0.98	0.59	<DL	<DL
7-8 Sep	55.82	15.93	14.22	1.77	1.66	1.06	<DL	<DL
26-27 Nov	45.50	12.63	2.12	0.28	<DL	<DL	<DL	<DL
4-5 Dec	49.26	5.93	<DL	<DL	<DL	<DL	<DL	<DL

	HCB	α-HCH	γ-HCH	TC	CC	TN	CN	Dield
2006								
24-25 Jan	31.63	2.03	<DL	<DL	<DL	<DL	<DL	<DL
12-13 Feb	31.63	2.03	<DL	<DL	<DL	<DL	<DL	<DL
25-26 Feb	83.42	5.88	1.87	0.44	<DL	0.40	<DL	<DL
3-4 Apr	42.22	8.25	0.75	0.82	1.00	0.54	<DL	<DL
4-5 Apr	45.11	6.87	2.28	1.75	1.62	1.05	<DL	<DL
5-6 Apr	37.72	6.90	<DL	0.52	1.05	0.45	<DL	<DL
6-7 Apr	41.97	6.41	1.87	0.39	0.33	0.15	<DL	<DL
7-8 Apr	41.83	6.21	1.65	0.55	0.51	0.56	<DL	<DL
8-9Apr	50.91	9.71	1.75	0.36	0.40	0.23	<DL	<DL
11-12 Apr	27.53	4.81	0.86	1.13	1.30	0.85	<DL	3.18
12-13 Apr	29.10	4.97	0.90	0.96	0.96	0.70	<DL	2.52
13-14 Apr	42.33	7.41	2.32	2.16	2.24	1.13	<DL	<DL
14-15 Apr	39.54	9.15	0.95	0.39	0.28	0.18	<DL	<DL
15-16 Apr	47.09	10.48	0.45	0.22	0.33	<DL	<DL	<DL
17-18 Apr	46.16	10.99	1.46	0.90	0.71	0.40	<DL	<DL
18-19 Apr	45.30	9.46	1.45	0.32	0.19	0.13	<DL	<DL
19-20 Apr	42.28	7.79	1.72	0.36	<DL	0.36	<DL	<DL
20-21 Apr	51.88	9.30	3.43	0.96	<DL	0.52	<DL	<DL
21-22 Apr	57.86	8.64	<DL	0.40	0.33	0.20	<DL	<DL
22-23 Apr	36.94	6.43	2.77	0.20	<DL	0.22	<DL	<DL
23-24 Apr	39.69	7.50	5.45	0.27	0.41	0.31	<DL	<DL
24-25 Apr	44.40	7.44	2.59	<DL	0.88	0.30	<DL	<DL
25-26 Apr	40.89	7.53	2.54	0.34	<DL	0.32	<DL	<DL
26-27 Apr	37.72	5.78	2.09	0.42	0.46	0.53	0.10	<DL
27-28 Apr	53.34	7.58	3.42	0.89	0.42	0.68	<DL	<DL
28-29 Apr	48.91	5.85	2.72	0.61	0.66	0.40	<DL	<DL
29-30 Apr	34.54	6.55	0.67	0.31	<DL	0.22	<DL	1.91
30 Apr-1 May	57.41	10.89	1.50	<DL	<DL	<DL	<DL	<DL
1-2 May	52.46	9.26	<DL	<DL	<DL	<DL	<DL	<DL
2-3 May	47.96	9.32	1.66	<DL	<DL	<DL	<DL	<DL
4-5 May	47.33	8.74	4.17	0.31	0.38	0.31	<DL	<DL
5-6 May	44.57	8.35	4.32	0.83	<DL	0.62	<DL	<DL
8-9 May	60.23	14.21	0.73	<DL	<DL	<DL	<DL	<DL
9-10 May	49.35	9.32	2.25	0.32	<DL	0.30	<DL	<DL
10-11 May	47.25	10.45	3.01	0.53	<DL	0.49	<DL	3.58
11-12 May	47.16	10.57	2.40	0.56	0.27	0.50	<DL	2.91
12-13 May	49.80	14.05	2.92	0.15	<DL	<DL	<DL	<DL

	Trif	Triall	Metr	Dac	Chlorp-Ox	Chlorp	Endo I	Endo II	Endo SO4
2004									
19-20 Apr	<DL	<DL	<DL	<DL	<DL	1.30	8.05	<DL	<DL
21-22 Apr	0.73	<DL	<DL	<DL	<DL	<DL	3.02	<DL	<DL
25-26 Apr	1.23	<DL	<DL	3.52	<DL	<DL	8.14	0.54	<DL
10-11 May	0.67	<DL	<DL	3.45	<DL	1.79	7.31	1.84	<DL
17-18 May	<DL	<DL	<DL	6.19	<DL	<DL	11.12	1.26	1.32
21-22 May	<DL	<DL	<DL	3.28	<DL	0.77	21.50	2.18	0.58
30-31 May	<DL	<DL	<DL	1.90	<DL	<DL	10.79	1.25	0.33
19-20 Jun	<DL	<DL	<DL	98.10	<DL	0.21	61.36	13.41	3.62
11-12 July	<DL	<DL	<DL	10.44	<DL	0.92	16.75	3.73	<DL
7-8 Dec	<DL	<DL	<DL	0.08	<DL	<DL	1.59	<DL	<DL
22-23 Dec	<DL	<DL	<DL	<DL	<DL	<DL	5.27	<DL	0.63
2005									
9-10 Jan	<DL	<DL	<DL	<DL	<DL	<DL	<DL	<DL	<DL
29-30 Jan	0.50	<DL	<DL	0.29	<DL	<DL	3.51	<DL	<DL
6-7 Feb	<DL	<DL	<DL	<DL	<DL	<DL	3.38	<DL	<DL
20-21 Feb	<DL	<DL	<DL	5.02	<DL	<DL	7.64	<DL	<DL
2-3 Mar	<DL	<DL	<DL	0.02	<DL	<DL	6.00	<DL	<DL
13-14 Mar	<DL	<DL	<DL	<DL	58.29	3.98	255.34	33.44	0.94
30-31 Mar	<DL	<DL	<DL	0.03	<DL	<DL	3.86	<DL	<DL
24-25 Apr	<DL	<DL	<DL	15.19	<DL	<DL	19.12	1.99	<DL
7-8 May	0.65	<DL	<DL	4.28	<DL	0.63	19.07	1.05	<DL
12-13 May	0.50	<DL	<DL	10.31	<DL	0.46	18.05	1.44	0.54
27-28 May	1.03	<DL	<DL	52.67	<DL	0.98	41.46	3.40	1.26
3-4 Jun	<DL	<DL	<DL	2.46	<DL	<DL	32.83	0.68	0.59
11-12 Jun	<DL	<DL	<DL	0.10	<DL	<DL	22.42	1.45	<DL
15-16 Jun	<DL	<DL	<DL	9.22	<DL	<DL	39.55	2.68	1.19
15-16 Jul	<DL	<DL	<DL	9.73	<DL	<DL	35.50	2.92	1.72
9-10 Aug	1.98	<DL	<DL	10.24	<DL	<DL	23.83	2.93	1.28
17-18 Aug	<DL	<DL	<DL	1.91	<DL	<DL	15.69	2.12	0.56
28-29 Aug	<DL	<DL	<DL	11.36	<DL	<DL	21.95	2.68	1.22
7-8 Sep	0.94	<DL	<DL	17.21	<DL	<DL	53.06	7.48	1.78
26-27 Nov	<DL	<DL	<DL	<DL	<DL	<DL	6.21	<DL	<DL
4-5 Dec	<DL	<DL	<DL	<DL	<DL	<DL	4.58	<DL	<DL

	Trif	Triall	Metr	Dac	Chlorp-Ox	Chlorp	Endo I	Endo II	Endo SO4
2006									
24-25 Jan	<DL	<DL	<DL	<DL	<DL	<DL	3.79	<DL	<DL
12-13 Feb	<DL	<DL	<DL	<DL	<DL	<DL	3.79	<DL	<DL
25-26 Feb	<DL	<DL	<DL	4.44	<DL	<DL	19.27	<DL	0.34
3-4 Apr	<DL	<DL	<DL	<DL	<DL	<DL	<DL	<DL	<DL
4-5 Apr	1.31	<DL	<DL	2.09	<DL	1.84	6.29	0.20	<DL
5-6 Apr	<DL	<DL	<DL	<DL	<DL	<DL	<DL	<DL	<DL
6-7 Apr	0.22	<DL	6.70	0.60	<DL	<DL	2.25	<DL	<DL
7-8 Apr	0.18	<DL	<DL	0.68	<DL	<DL	3.06	<DL	<DL
8-9Apr	<DL	<DL	<DL	<DL	<DL	<DL	3.94	<DL	<DL
11-12 Apr	<DL	<DL	<DL	<DL	<DL	0.66	<DL	<DL	<DL
12-13 Apr	<DL	<DL	<DL	0.14	5.15	<DL	0.36	<DL	<DL
13-14 Apr	0.23	<DL	<DL	0.82	<DL	<DL	1.83	<DL	<DL
14-15 Apr	1.47	<DL	<DL	0.31	<DL	<DL	0.76	<DL	<DL
15-16 Apr	0.14	<DL	<DL	0.22	<DL	<DL	0.64	<DL	<DL
17-18 Apr	0.49	<DL	<DL	0.53	<DL	<DL	1.34	<DL	<DL
18-19 Apr	0.19	<DL	3.66	0.27	7.06	<DL	0.61	<DL	<DL
19-20 Apr	<DL	<DL	<DL	<DL	<DL	<DL	<DL	<DL	<DL
20-21 Apr	0.45	<DL	<DL	0.88	<DL	1.05	1.21	<DL	<DL
21-22 Apr	0.24	<DL	<DL	0.44	<DL	0.26	0.99	<DL	<DL
22-23 Apr	0.31	15.32	0.31	77.46	22.09	5.77	30.84	3.40	0.86
23-24 Apr	0.17	35.56	0.33	351.90	<DL	4.12	38.13	4.55	0.89
24-25 Apr	<DL	7.81	<DL	190.86	<DL	0.37	1.08	0.75	<DL
25-26 Apr	<DL	<DL	<DL	79.46	<DL	<DL	<DL	<DL	<DL
26-27 Apr	0.51	<DL	<DL	1.18	<DL	<DL	<DL	<DL	0.10
27-28 Apr	0.44	<DL	<DL	6.83	<DL	0.53	2.51	0.37	<DL
28-29 Apr	0.66	<DL	<DL	8.49	<DL	0.84	4.15	0.44	0.14
29-30 Apr	<DL	<DL	<DL	0.25	<DL	<DL	<DL	<DL	<DL
30 Apr-1 May	<DL	<DL	<DL	0.42	<DL	<DL	<DL	<DL	<DL
1-2 May	<DL	<DL	<DL	0.14	<DL	<DL	<DL	<DL	<DL
2-3 May	<DL	<DL	<DL	0.38	<DL	<DL	<DL	<DL	<DL
4-5 May	<DL	21.86	3.37	38.14	<DL	<DL	23.70	1.85	0.25
5-6 May	0.22	4.82	2.77	49.39	<DL	<DL	3.33	0.27	<DL
8-9 May	<DL	<DL	<DL	0.13	<DL	<DL	<DL	<DL	<DL
9-10 May	<DL	<DL	<DL	<DL	<DL	<DL	<DL	<DL	<DL
10-11 May	<DL	<DL	<DL	<DL	<DL	<DL	<DL	<DL	<DL
11-12 May	<DL	<DL	<DL	0.40	<DL	<DL	0.63	<DL	<DL
12-13 May	<DL	<DL	<DL	0.31	<DL	<DL	0.56	<DL	<DL

	PCB 101	PCB 118	PCB 153	PCB 138	PCB 187	PCB 183
2004						
19-20 Apr	<DL	0.54	0.15	0.55	<DL	<DL
21-22 Apr	<DL	<DL	<DL	<DL	<DL	<DL
25-26 Apr	<DL	0.56	0.27	0.57	<DL	<DL
10-11 May	<DL	1.94	1.14	3.05	0.18	<DL
17-18 May	<DL	0.73	0.52	0.59	0.22	<DL
21-22 May	<DL	0.88	0.56	1.18	0.15	0.13
30-31 May	<DL	0.63	0.27	0.72	<DL	<DL
19-20 Jun	2.87	1.05	1.03	0.99	0.33	0.11
11-12 July	<DL	2.28	1.94	2.66	0.45	0.32
7-8 Dec	<DL	0.72	0.20	0.39	<DL	<DL
22-23 Dec	<DL	0.44	0.12	0.35	0.07	0.08
2005						
9-10 Jan	<DL	0.21	<DL	<DL	<DL	<DL
29-30 Jan	<DL	0.53	0.17	0.33	<DL	<DL
6-7 Feb	<DL	<DL	<DL	<DL	<DL	<DL
20-21 Feb	<DL	0.30	0.04	0.23	<DL	<DL
2-3 Mar	<DL	<DL	<DL	<DL	<DL	<DL
13-14 Mar	<DL	<DL	<DL	<DL	<DL	<DL
30-31 Mar	<DL	<DL	<DL	<DL	<DL	<DL
24-25 Apr	<DL	<DL	0.06	<DL	<DL	<DL
7-8 May	<DL	0.90	0.55	0.93	<DL	<DL
12-13 May	6.19	0.83	0.47	0.78	0.12	<DL
27-28 May	4.80	2.38	1.33	1.95	0.25	<DL
3-4 Jun	<DL	0.77	0.20	0.57	<DL	<DL
11-12 Jun	<DL	<DL	<DL	<DL	<DL	<DL
15-16 Jun	<DL	1.18	<DL	<DL	<DL	<DL
15-16 Jul	<DL	0.52	0.29	0.52	0.02	<DL
9-10 Aug	7.99	4.24	2.63	3.09	0.38	0.15
17-18 Aug	<DL	0.49	0.43	0.76	<DL	<DL
28-29 Aug	<DL	0.41	0.08	<DL	<DL	<DL
7-8 Sep	4.59	2.35	1.24	1.54	0.15	<DL
26-27 Nov	<DL	0.28	<DL	<DL	<DL	<DL
4-5 Dec	<DL	<DL	<DL	<DL	<DL	<DL

	PCB 101	PCB 118	PCB 153	PCB 138	PCB 187	PCB 183
2006						
24-25 Jan	<DL	<DL	<DL	<DL	<DL	<DL
12-13 Feb	<DL	<DL	<DL	<DL	<DL	<DL
25-26 Feb	<DL	<DL	<DL	<DL	<DL	<DL
3-4 Apr	<DL	<DL	<DL	<DL	<DL	<DL
4-5 Apr	<DL	0.51	0.22	0.45	<DL	<DL
5-6 Apr	<DL	<DL	<DL	<DL	<DL	<DL
6-7 Apr	<DL	0.25	0.14	0.18	<DL	<DL
7-8 Apr	<DL	0.24	0.14	0.20	<DL	<DL
8-9Apr	<DL	0.33	0.15	0.26	<DL	<DL
11-12 Apr	<DL	<DL	<DL	<DL	<DL	<DL
12-13 Apr	<DL	<DL	<DL	<DL	<DL	<DL
13-14 Apr	<DL	0.34	0.19	0.27	0.07	<DL
14-15 Apr	<DL	0.32	0.13	0.24	<DL	<DL
15-16 Apr	<DL	0.45	0.20	0.41	<DL	<DL
17-18 Apr	<DL	0.32	0.25	0.25	0.15	<DL
18-19 Apr	<DL	0.20	0.13	0.14	<DL	<DL
19-20 Apr	<DL	<DL	<DL	<DL	<DL	<DL
20-21 Apr	<DL	0.60	<DL	<DL	<DL	<DL
21-22 Apr	<DL	0.30	0.19	0.36	<DL	<DL
22-23 Apr	<DL	<DL	<DL	<DL	<DL	<DL
23-24 Apr	<DL	<DL	<DL	<DL	<DL	<DL
24-25 Apr	<DL	<DL	<DL	<DL	<DL	<DL
25-26 Apr	<DL	<DL	<DL	<DL	<DL	<DL
26-27 Apr	<DL	<DL	<DL	<DL	<DL	<DL
27-28 Apr	<DL	0.59	0.53	0.57	0.47	0.04
28-29 Apr	<DL	0.54	1.06	0.85	0.84	0.28
29-30 Apr	<DL	0.14	0.10	<DL	<DL	<DL
30 Apr-1 May	<DL	<DL	<DL	<DL	<DL	<DL
1-2 May	<DL	<DL	<DL	<DL	<DL	<DL
2-3 May	<DL	<DL	<DL	<DL	<DL	<DL
4-5 May	<DL	0.19	<DL	<DL	<DL	<DL
5-6 May	<DL	0.25	0.13	0.16	<DL	<DL
8-9 May	<DL	<DL	<DL	<DL	<DL	<DL
9-10 May	<DL	<DL	<DL	<DL	<DL	<DL
10-11 May	<DL	<DL	<DL	<DL	<DL	<DL
11-12 May	<DL	0.18	<DL	<DL	<DL	<DL
12-13 May	<DL	<DL	<DL	<DL	<DL	<DL

	FLO	PHE	ANT	FLA	PYR	RET
2004						
19-20 Apr	210.34	353.08	<DL	24.58	121.48	59.14
21-22 Apr	108.50	329.65	17.89	15.39	53.90	38.82
25-26 Apr	203.49	393.26	<DL	194.41	154.59	29.51
10-11 May	261.70	1087.44	164.19	56.96	195.49	291.40
17-18 May	159.46	633.44	61.77	26.03	77.54	134.23
21-22 May	257.19	675.52	69.49	27.88	81.62	<DL
30-31 May	62.27	489.48	59.27	22.06	66.81	114.03
19-20 Jun	203.81	511.37	22.16	32.15	353.12	115.56
11-12 July	395.09	1340.94	118.72	112.56	898.96	579.55
7-8 Dec	460.35	1003.89	44.05	80.06	93.46	131.28
22-23 Dec	59.46	192.48	<DL	14.51	56.90	54.17
2005						
9-10 Jan	159.10	226.74	<DL	5.62	<DL	<DL
29-30 Jan	160.04	412.74	34.75	15.96	40.53	<DL
6-7 Feb	33.17	56.82	<DL	<DL	<DL	<DL
20-21 Feb	119.04	442.98	25.39	30.52	37.80	27.27
2-3 Mar	124.87	309.63	<DL	36.51	70.94	16.56
13-14 Mar	46.93	51.18	<DL	39.44	66.89	<DL
30-31 Mar	79.03	130.36	<DL	2.85	8.95	<DL
24-25 Apr	96.71	260.23	10.51	15.11	19.85	9.33
7-8 May	433.50	1265.03	84.83	50.97	147.42	89.68
12-13 May	342.66	807.31	34.10	29.21	96.06	70.59
27-28 May	729.44	4024.83	407.95	173.22	636.43	298.54
3-4 Jun	394.23	3463.97	458.53	117.72	602.97	136.53
11-12 Jun	88.08	314.13	19.02	30.78	54.55	<DL
15-16 Jun	418.72	2128.03	225.94	84.01	316.59	153.01
15-16 Jul	148.03	1153.89	122.68	82.17	260.50	55.97
9-10 Aug	639.85	2370.56	98.13	229.27	447.35	287.27
17-18 Aug	123.62	160.31	5.10	14.55	24.02	9.83
28-29 Aug	127.88	285.04	11.26	12.62	19.72	15.92
7-8 Sep	255.12	1002.22	56.45	111.36	269.88	228.76
26-27 Nov	125.26	149.95	<DL	7.92	10.38	8.30
4-5 Dec	57.11	107.45	<DL	1.63	<DL	<DL

	FLO	PHE	ANT	FLA	PYR	RET
2006						
24-25 Jan	27.07	135.24	9.44	6.85	22.10	<DL
12-13 Feb	127.68	322.00	<DL	39.47	84.49	3.68
25-26 Feb	93.51	191.91	7.36	33.90	29.41	27.10
3-4 Apr	55.04	80.15	<DL	10.36	1.03	<DL
4-5 Apr	224.52	626.75	69.86	31.47	87.62	32.10
5-6 Apr	65.20	43.22	<DL	2.20	<DL	<DL
6-7 Apr	119.68	266.56	12.56	12.12	19.88	17.22
7-8 Apr	128.25	472.23	56.30	21.48	68.71	24.62
8-9Apr	87.09	379.57	34.76	13.29	35.44	16.42
11-12 Apr	36.77	75.26	<DL	6.42	<DL	1.90
12-13 Apr	63.51	184.15	11.44	7.19	20.55	6.98
13-14 Apr	260.12	541.07	32.02	24.19	48.21	19.30
14-15 Apr	128.94	376.46	11.43	16.40	39.30	16.98
15-16 Apr	100.00	552.26	45.78	18.86	70.61	20.35
17-18 Apr	325.23	594.81	65.67	22.10	69.19	27.44
18-19 Apr	232.21	585.67	44.62	24.38	49.08	20.77
19-20 Apr	138.10	288.92	14.42	23.32	22.72	8.86
20-21 Apr	98.63	203.81	17.84	8.97	30.01	14.15
21-22 Apr	303.55	1169.34	143.90	58.50	218.24	53.79
22-23 Apr	82.65	67.89	<DL	13.98	13.81	47.20
23-24 Apr	62.80	91.85	<DL	26.36	23.08	17.59
24-25 Apr	137.94	198.68	<DL	19.83	10.42	<DL
25-26 Apr	198.34	488.44	<DL	84.88	51.24	<DL
26-27 Apr	15.01	82.95	<DL	18.70	13.26	<DL
27-28 Apr	446.35	2299.92	307.74	100.24	385.65	105.45
28-29 Apr	376.49	1951.03	227.80	126.44	406.54	157.12
29-30 Apr	67.65	118.49	<DL	23.10	30.71	8.17
30 Apr-1 May	208.71	468.10	31.26	17.71	37.99	12.85
1-2 May	81.15	149.34	<DL	12.22	4.18	<DL
2-3 May	61.34	113.63	<DL	12.43	16.15	5.64
4-5 May	421.37	706.80	61.98	40.77	64.07	284.23
5-6 May	133.57	411.86	39.39	31.76	57.64	25.71
8-9 May	224.93	445.93	<DL	18.96	23.67	<DL
9-10 May	134.96	221.85	<DL	22.62	20.20	<DL
10-11 May	132.77	173.20	<DL	27.47	13.27	<DL
11-12 May	104.32	337.40	33.76	15.10	39.59	9.39
12-13 May	155.13	314.60	<DL	16.90	22.02	11.60

	BaA	CT	BbF	BkF	BeP	BaP	IcdP	BghiP	Lev	TPB
2004										
19-20 Apr	<DL	4.56	<DL	<DL	<DL	<DL	<DL	<DL	<DL	<DL
21-22 Apr	<DL	0.72	<DL	<DL	<DL	<DL	<DL	<DL	446.28	2.50
25-26 Apr	14.74	56.82	156.21	37.97	88.26	66.41	82.43	69.96	3409.62	4.53
10-11 May	<DL	<DL	<DL	<DL	<DL	<DL	<DL	<DL	2810.06	25.75
17-18 May	<DL	<DL	<DL	<DL	<DL	<DL	<DL	<DL	403.23	1.78
21-22 May	<DL	<DL	<DL	<DL	<DL	<DL	<DL	4.03	1249.15	10.20
30-31 May	<DL	<DL	<DL	<DL	<DL	<DL	<DL	<DL	675.77	15.20
19-20 Jun	<DL	1.97	<DL	<DL	<DL	<DL	<DL	<DL	303.92	<DL
11-12 July	<DL	<DL	<DL	<DL	<DL	<DL	<DL	<DL	2750.50	<DL
7-8 Dec	<DL	<DL	<DL	<DL	<DL	<DL	12.22	81.79	<DL	5.97
22-23 Dec	<DL	<DL	<DL	<DL	<DL	<DL	<DL	<DL	<DL	3.02
2005										
9-10 Jan	<DL	<DL	<DL	<DL	<DL	<DL	<DL	<DL	<DL	<DL
29-30 Jan	<DL	<DL	<DL	<DL	<DL	<DL	<DL	1.94	<DL	6.65
6-7 Feb	<DL	<DL	<DL	<DL	<DL	<DL	<DL	<DL	<DL	<DL
20-21 Feb	<DL	<DL	<DL	<DL	<DL	<DL	<DL	<DL	<DL	<DL
2-3 Mar	<DL	<DL	<DL	<DL	<DL	<DL	<DL	4.33	<DL	<DL
13-14 Mar	<DL	<DL	11.00	<DL	9.82	5.68	6.32	18.55	1048.87	<DL
30-31 Mar	<DL	3.01	<DL	<DL	<DL	<DL	<DL	<DL	<DL	5.71
24-25 Apr	<DL	<DL	<DL	<DL	<DL	<DL	<DL	<DL	1651.16	<DL
7-8 May	<DL	<DL	<DL	<DL	<DL	<DL	<DL	<DL	<DL	<DL
12-13 May	<DL	1.58	<DL	<DL	<DL	<DL	<DL	1.47	1080.19	1.44
27-28 May	<DL	<DL	<DL	<DL	<DL	<DL	<DL	<DL	2290.46	<DL
3-4 Jun	<DL	7.72	<DL	<DL	<DL	<DL	<DL	<DL	1934.96	<DL
11-12 Jun	<DL	<DL	<DL	<DL	<DL	<DL	<DL	<DL	417.50	<DL
15-16 Jun	<DL	3.73	<DL	<DL	<DL	<DL	<DL	<DL	3642.37	<DL
15-16 Jul	<DL	<DL	<DL	<DL	<DL	<DL	<DL	<DL	896.23	<DL
9-10 Aug	7.25	33.36	26.42	3.36	8.70	5.67	6.26	3.18	12224.17	1.72
17-18 Aug	<DL	3.60	<DL	<DL	<DL	<DL	<DL	<DL	479.25	1.37
28-29 Aug	<DL	<DL	<DL	<DL	<DL	<DL	<DL	<DL	1620.79	<DL
7-8 Sep	<DL	<DL	<DL	<DL	<DL	<DL	<DL	0.27	1276.69	<DL
26-27 Nov	<DL	<DL	<DL	<DL	<DL	<DL	<DL	<DL	<DL	<DL
4-5 Dec	<DL	<DL	<DL	<DL	<DL	<DL	<DL	<DL	<DL	<DL

	BaA	CT	BbF	BkF	BeP	BaP	IcdP	BghiP	Lev	TPB
2006										
24-25 Jan	<DL	<DL	<DL	<DL	<DL	<DL	<DL	<DL	<DL	1.77
12-13 Feb	<DL	<DL	<DL	<DL	<DL	<DL	2.68	6.03	1072.20	<DL
25-26 Feb	<DL	<DL	<DL	<DL	<DL	<DL	<DL	<DL	<DL	<DL
3-4 Apr	<DL	<DL	<DL	<DL	<DL	<DL	<DL	1.65	<DL	<DL
4-5 Apr	<DL	<DL	<DL	<DL	<DL	<DL	<DL	<DL	417.96	<DL
5-6 Apr	<DL	<DL	<DL	<DL	<DL	<DL	<DL	<DL	326.53	<DL
6-7 Apr	<DL	2.11	4.86	<DL	2.19	1.38	2.66	0.55	1006.18	<DL
7-8 Apr	<DL	<DL	<DL	<DL	<DL	<DL	<DL	<DL	576.19	<DL
8-9Apr	<DL	<DL	<DL	<DL	<DL	<DL	<DL	<DL	<DL	<DL
11-12 Apr	<DL	<DL	<DL	<DL	<DL	<DL	<DL	<DL	224.91	<DL
12-13 Apr	<DL	<DL	<DL	<DL	<DL	<DL	<DL	<DL	<DL	<DL
13-14 Apr	<DL	<DL	<DL	<DL	<DL	<DL	<DL	<DL	<DL	<DL
14-15 Apr	<DL	<DL	<DL	<DL	<DL	<DL	<DL	<DL	<DL	<DL
15-16 Apr	<DL	<DL	<DL	<DL	<DL	<DL	<DL	2.92	<DL	<DL
17-18 Apr	<DL	<DL	<DL	<DL	<DL	<DL	<DL	<DL	<DL	<DL
18-19 Apr	<DL	<DL	<DL	<DL	<DL	<DL	<DL	0.51	2455.81	<DL
19-20 Apr	<DL	5.88	10.37	3.59	5.29	<DL	4.86	1.56	2725.42	3.99
20-21 Apr	<DL	<DL	<DL	<DL	<DL	<DL	<DL	<DL	2429.75	<DL
21-22 Apr	<DL	<DL	<DL	<DL	<DL	<DL	<DL	<DL	562.14	<DL
22-23 Apr	<DL	1.45	<DL	<DL	1.58	0.92	1.32	2.03	<DL	0.66
23-24 Apr	<DL	3.93	9.77	2.75	2.63	1.69	2.49	3.44	<DL	<DL
24-25 Apr	<DL	6.42	13.98	<DL	<DL	<DL	7.00	4.78	4011.69	<DL
25-26 Apr	6.51	20.00	35.48	9.83	23.52	14.36	14.92	13.45	7739.53	<DL
26-27 Apr	<DL	<DL	<DL	<DL	<DL	<DL	4.22	4.25	754.52	<DL
27-28 Apr	<DL	<DL	<DL	<DL	<DL	<DL	<DL	<DL	1062.04	<DL
28-29 Apr	2.53	2.30	<DL	<DL	<DL	<DL	<DL	<DL	5187.13	<DL
29-30 Apr	<DL	<DL	<DL	<DL	<DL	<DL	<DL	7.28	1514.12	<DL
30 Apr-1 May	<DL	<DL	<DL	<DL	<DL	<DL	<DL	0.87	1550.75	<DL
1-2 May	<DL	<DL	<DL	<DL	<DL	<DL	6.00	3.40	4726.26	1.26
2-3 May	<DL	<DL	<DL	<DL	<DL	<DL	<DL	2.27	2053.66	<DL
4-5 May	<DL	<DL	<DL	<DL	<DL	<DL	<DL	<DL	738.60	<DL
5-6 May	<DL	<DL	<DL	<DL	<DL	<DL	6.58	4.43	302.63	<DL
8-9 May	<DL	<DL	<DL	<DL	<DL	<DL	<DL	<DL	2697.80	<DL
9-10 May	<DL	<DL	<DL	<DL	<DL	<DL	<DL	4.08	1922.47	<DL
10-11 May	<DL	6.90	15.67	<DL	11.67	7.24	7.79	5.38	3094.34	2.50
11-12 May	<DL	<DL	<DL	<DL	<DL	<DL	<DL	<DL	2760.87	<DL
12-13 May	<DL	<DL	<DL	<DL	<DL	<DL	<DL	<DL	2536.03	<DL